

Proceedings of the  
*12<sup>th</sup> International Symposium on  
Vibrations of Continuous Systems*

*Sporthotel Panorama  
Corvara in Badia BZ - Italy  
July 28 - August 2, 2019*





## Preface

The International Symposium on Vibrations of Continuous Systems (ISVCS) is a forum for leading researchers from across the globe to meet with their colleagues and to present both old and new ideas in the field. Each participant has been encouraged either to present results of recent research or to reflect on some aspect of the vibration of continuous systems, which is particularly interesting, unexpected or unusual. This type of presentation is meant to encourage participants to draw on understanding obtained through many years of research in the field.

ISVCS focuses on the vibrations of the fundamental structural elements: strings, rods, beams, membranes, plates, shells, bodies of revolution and other solid bodies of simple geometry. Structures composed of assemblies of structural elements are also of interest, especially if such structures display interesting or unusual response.

The ISVCS started 22 years ago, at Stanley Hotel, Estes Park, Colorado, USA August 11-15, 1997. It comes every two years, the present 12th Symposium takes place on 28 July – 2 Auguts 2019 the SportHotel Panorama, Corvara in Badia, Italy. Typical days at the Symposium will consist of morning technical presentations, afternoon hikes or excursions in the local area and, in the evening, further technical discussions and social gatherings. The various outings and social gatherings provide important opportunities for relaxed and informal discussion of technical and not-so-technical topics surrounded by the natural beauty of the Italian Dolomites.

This volume of Proceedings contains 28 short summaries of the technical presentations to be made at the Symposium, as well as short biographical sketches of the participants.

The present edition is the second one without the presence of Art Leissa, founder and Honorary Chairman of ISVCS. We all miss Art. Many others senior board members are absent (J. Wauer, S. Dickinson); we hope that some of them will join again in the next Symposia.

Last but not least we remember with pain that Fred Ward Williams, a frequent attendee of past Symposia, left us unexpectedly on April 23 at the age of 89. An obituary by Prof David Kennedy and Ranjan Banerjee is made in these proceedings.

*General Chairman* Erasmo Carrera

*Editorial Chairman* Ilanko Ilanko

*Local Arrangements Chairman* Francesco Pellicano

*Publicity Chairman* Yoshihiro Narita

*Honorary Chairman* Art Leissa

## **Past Symposia**

The 1st International Symposium:

The Stanley Hotel, Estes Park, Colorado, USA

August 11-15, 1997

The 2nd International Symposium:

The Sunstar Hotel, Grindelwald, Switzerland

July 11-16, 1999

The 3rd International Symposium:

Jackson Lake Lodge, Grand Teton National Park, Wyoming, USA

July 23-27, 2001

The 4th International Symposium

Keswick, Lake District, England

July 23-27, 2003

The 5th International Symposium:

Berchtesgaden at Lake Königssee, Germany

July 25-29, 2005

The 6th International Symposium:

PlumpJack Squaw Valley Inn, Olympic Valley, California, USA

July 23-27, 2007

The 7th International Symposium:

Zakopane, Poland

July 19-25, 2009

The 8th International Symposium:

Whistler, British Columbia, Canada

July 18-22, 2011

The 9th International Symposium:

Courmayeur, Italy

July 22-26, 2013

The 10th International Symposium:

Stanley Hotel, Estes Park, Colorado, USA,

July 26-31, 2015

The 11th International Symposium:

the Royal Victoria Hotel, Llanberis, Snowdonia, Wales, UK,

July 16-21, 2017

Details of the Proceedings of the past Symposia can be found at

<http://www.isvcs.org>

# Table of Contents

## Presentation Summaries (Presenting author is shown underlined)

1. **Professor Frederic Ward Williams – Obituary**  
D. Kennedy, J.R. Banerjee page 1
  
2. **Dynamic Buckling of Thin Walled Structures Revisited**  
H. Abramovich page 5
  
3. **Longitudinal Vibration of a Conical Bar using Rayleigh-Love Theory**  
J.R. Banerjee, A. Ananthapuvirajah, S.O. Papkov page 9
  
4. **Explicit dynamic solutions of damaged beams**  
F. Cannizzaro, N. Impollonia, S. Caddemi, I. Caliò page 13
  
5. **Preliminary Assessments on the Development of Refined Shell Models for Free Vibrations via Machine Learning**  
E. Carrera, M. Petrolo page 17
  
6. **Tunable 1D linear acoustic diodes: A design based on soft functionally graded phononic crystals**  
Y. Chen, B. Wu, Y. Su, W.Q. Chen page 21
  
7. **Detection of Structural Damage Based on Perturbed Local Equilibrium**  
L. Cheng page 25
  
8. **Solutions of Vibration Problems with Boundary Excitation by the Fourier Method and their Application to Optimal Boundary Control**  
P. Cupiał page 27
  
9. **Modelling of Planar Dynamics of Inflated Membrane Structures**  
A. DasGupta page 31
  
10. **Application of Machine Learning Methods to Structural Similitudes**  
A. Casaburo, G. Petrone, F. Franco, S. De Rosa page 35

- 11. Structural and acoustic response of sandwich plates by means of sublaminar models with variable kinematics**  
L. Dozio, R. Vescovini, M. D'Ottavio page 39
- 12. New Analytical Solutions for Vibrations of Shallow Shells**  
M. Eisenberger, L.A. Godoy page 43
- 13. Total Lagrangian Large Amplitude Beam Vibrations and the Limits of Poisson and von Karman**  
P.R. Heyliger page 47
- 14. Vibration optimization of variable-stiffness composites fabricated by tailored fiber placement machine and electrodeposition molding**  
S. Honda, K. Katagiri, K. Sasaki page 51
- 15. Separating the effect of crack severity and location in a skeletal structure with a single crack**  
S. Ilanko, Y. Mochida, J. De Los Rios, D. Kennedy page 55
- 16. From semi-analytical to Finite Element integrated low-dimensional models for nonlinear dynamic analysis of composite cylindrical shells**  
E. Jansen, T. Rahman page 59
- 17. Natural Frequency Degradations in Cracked Plates**  
Y. Luo, D. Kennedy, C.A. Featherston page 63
- 18. Wave propagation analysis within multilayer media by using the dynamic stiffness method**  
X. Liu page 67
- 19. Sensitivity Analysis of Eigenproblems and Application to Wave Propagation in Timber**  
B. Mace, A. Cicirello, M.J. Kingan, Y. Yang page 71
- 20. Analysis on Nonlinear Forced Vibrations of a Thin Shell-panel Including Clamped Edges**  
S. Maruyama, K. Nagai, D. Kumagai, T. Okawara page 75

- 21. Vibration analysis of multi-cracked plates with a roving body using the Rayleigh-Ritz Method**  
Y. Mochida, S. Ilanko page 79
- 22. Some Topics on In-plane Vibration of Laminated Rectangular Plates: Analysis, Optimization and Combination**  
Y. Narita, N. Innamì page 83
- 23. Vibration around non-trivial equilibrium of highly flexible composite thin-walled structures and plates**  
A. Pagani, E. Carrera page 87
- 24. Complex Dynamics of Shells under Different Thermal Conditions**  
F. Pellicano, A. Zippo, G. Iarriccio, M. Barbieri page 91
- 25. On the analysis of 1D impacting rods of arbitrary cross section and with arbitrary material parameters**  
J. Burgert, W. Seemann page 95
- 26. On the Stability of Parametrically Excited Continuous Gyroscopic Systems**  
A. De Felice, S. Sorrentino page 99
- 27. Free Vibrations of Curved Periodic Beams and Combinations**  
S. Ding, J. Wu, C. Bian, Y. Zhang, L. Xie, J. Wang page 103
- 28. pinned-pinned beam with and without a distributed foundation: A simple exact relationship between their eigenvalues**  
W.P. Howson, A. Watson page 107
- 29. Accurate Free Vibration Analysis of Rectangular Mindlin Plates with Arbitrary Boundary Conditions by the Superposition Method**  
S. Yu, X. Yin page 111

## **Biosketches of participants page**

Haim Abramovich.....	page 115
Ranjan Banerjee.....	page 116
Salvatore Caddemi.....	page 117
Ivo Calì.....	page 118
Francesco Cannizzaro.....	page 119
Erasmus Carrera.....	page 120
Weiqiu Chen.....	page 121
Li Cheng.....	page 122
Piotr Cupiał.....	page 123
Anirvan DasGupta.....	page 124
Sergio De Rosa.....	page 125
Lorenzo Dozio.....	page 126
Moshe Eisenberger.....	page 127
Peter Hagedorn.....	page 128
Paul R. Heyliger.....	page 129
Shinya Honda.....	page 130
Sinniah Ilanko.....	page 131
Eelco Jansen.....	page 132
David Kennedy.....	page 133
Xiang Liu.....	page 134
Brian Mace.....	page 135
Shinichi Maruyama.....	page 136
Yusuke Mochida.....	page 137
Narita Yoshihiro.....	page 138
Alfonso Pagani.....	page 139
Francesco Pellicano.....	page 140
Wolfgang Seemann.....	page 141
Silvio Sorrentino.....	page 142
Ji Wang.....	page 143
Andrew Watson.....	page 144
Xuewen Yin.....	page 145
Shudong Yu.....	page 146



## Obituary

### Professor Frederic Ward Williams 1940-2019



Fred Williams was the son of Sir Frederic Calland Williams, creator of the first electronic stored-program digital computer. After obtaining a First Class degree at Cambridge Fred studied for a PhD at Bristol supervised by Sir Alfred Pugsley, whose old school, hands-off approach aided Fred's development as an independent researcher.

Fred then spent 3 years teaching at a university in Nigeria, where he and his new wife Anne were terrifyingly caught up in some civil unrest. Safely back in the UK he joined Professor Bill Wittrick at Birmingham, applying his civil engineering expertise to the buckling and vibration of aircraft structures. In Fred's words, he "quickly experienced a sense of privilege, respect and even awe... Bill's courtesy and consideration were unflinching. An abiding memory is the way he would identify and remove one's areas of ignorance ... in a way which was direct but never crushing. .. Bill, like the best of master craftsmen, passed on by example and training the very highest standards of scholarly integrity, enthusiasm and thoroughness." Words that perfectly describe Fred himself.

Fred recalls an occasion when "Wittrick and I worked intensively together all day, including lunch, to meet the need of one of his research students. An algorithm grew out of the discussion, to the surprise of both of us, as the result of numerous thoughts (some of which were helpful and some of which proved to be misleading). A key thought occurred over lunch but almost faded before it could be fully developed in the afternoon. Without doubt, this algorithm was the most comprehensive joint discovery of which I have first hand experience and memories of that day are still clear about twenty years later."

In 1975 Fred became the youngest professor in Cardiff, where he remained for the rest of his career. But not before he had written a computer program VIPASA with the Wittrick-Williams algorithm at its heart.

At a conference he met Dr Mel Anderson from NASA Langley Research Center, who went on to incorporate VIPASA into a design program which became widely used in the US aerospace industry. Mel came to the UK with his family for a year to work with Fred on a new analysis code VICON. They also developed 3D frame software which was used in the design of the space shuttle. With funding from British Aerospace and NASA, Fred's team at Cardiff further consolidated the software into a design code VICONOPT which is still used in the aerospace industry.

In 1988 Fred met Professor Zhong Wanxie from Dalian University of Technology. So began a passion that continued throughout his career. He visited China every year, sometimes for several months, and also established the Cardiff Advanced Chinese Engineering Centre, hosting scores of visitors including senior professors with whom we have collaborated ever since. Fred was intrigued by the Chinese version of a well-known proverb, and posted a notice on his office door saying “Failure is killing only two birds with one stone”. Sadly he was asked to remove it on the occasion of a royal visit.

As head of Cardiff’s Division of Structural Engineering, Fred’s recipe for success was “Quality, Income, Papers”. He led by example, publishing over 400 papers and carrying his research into his teaching, particularly his final year module on plate theory.

Fred is remembered with respect and affection by generations of research students, many of whom have advanced to successful careers in academia or industry. Always firm but fair, explaining and encouraging. One student recalls enthusiastically trying to explain something but making a fundamental mistake, upon which Fred called out “STOP!” If your meeting with Fred was in the late afternoon you knew it would have to continue until the problem was solved. I would often return home late having been “Fredded”.

But Fred could never be just a colleague. To all of us and our families he became a friend, generous in his hospitality, keen to share his love of travelling and the great outdoors. He contributed enthusiastically to the success of ISVCS and organised the 2003 event at his beloved Keswick.

In 2000 Fred took up a prestigious 3 year appointment at City University of Hong Kong, also continuing our collaboration with universities in mainland China. I remember arriving in Beijing on an overnight flight and finding Fred waiting for me in the hotel lobby with equations to solve. The Wittrick-Williams algorithm featured in a textbook by Tsinghua’s Professor Yuan Si and became widely known in China.

Returning to Cardiff Fred worked part-time, then was appointed Emeritus Professor, winding down to enjoy a well earned retirement. His last visit to China was in 2013 when Dalian appointed him a Guest Professor.

Fred leaves a legacy of expertise in structural mechanics, and his work will surely continue through those of us who have had the privilege of learning from him. I have received condolences from over 70 of his colleagues and students in some 20 different countries.

In January Fred wrote to some of his closest friends, “I thank you from the bottom of my heart for all your friendship has meant to me and wish you well for the future.” We thank Fred for teaching and inspiring us and for letting us share in his wonderful life.

David Kennedy

### **Fred Williams: A friend, mentor and an indomitable spirit in my life**

In November 1978 I had just finished my PhD Viva at Cranfield. The same evening, I had a phone call from Professor Fred Williams which was a turning point in my career and life. I was thinking of packing my luggage and leaving the United Kingdom for good. I remember the telephone conversation vividly even to this day. Fred asked me on the phone very directly, “Will you be interested in a post-doctoral research in Cardiff?” I knew very little about Fred at that time, but I was told that he was one of the youngest and brightest professors in the country. My telephone conversation with Fred was amazing. I thought that this professor, whom I had never met, could really be my mentor and guru to fulfil my ambitions in life. How can a person be so precise when he talks? He was open, honest, clear and importantly very straightforward and exactly to the point. He said that if I was interested, he would invite me to come to Cardiff for an interview for the post-doc job.

That interview was an unforgettable experience. The most transformative period of my life began to emerge. It took me only a few seconds to realise that Fred was an incredibly intelligent man. His towering and charismatic personality impressed me enormously. He structured my interview in an extremely clever and well-thought-out manner. During the conversation, prior to the formal interview, he was in fact X-raying me. The formal interview took only fifteen minutes. I was offered the job of Research Associate and I was Fred's very first post-doc. My instinct told me that my future would be totally secure in his hands. I had an overwhelming feeling within me that I had to respect this man.

I joined Fred in Cardiff on 1 February 1979 and worked with him for six years on large (1km size) space structures, in close collaboration with NASA Langley Research Center. The Ranjan Banerjee that you see today was in the making. The magic of Fred worked wonders. His planning and thinking were immaculate. He knew how to inspire a person and how to get the best out of a person. He planned, he thought, and he always had a contingency plan in case something went wrong. He was such a structured person, always analytical in his approach, always precise. According to Fred, a researcher should be as objective as possible. In his presence I was determined to succeed.

I have many special memories of Fred which I have no space to include here. Fred was a highly principled person and he always stuck to his principles. From a personal perspective, the screw of my academic life turned because of Fred. He had so much influence on me and on my thinking. There is no drama, no poetry, no melodrama in this statement. He rekindled my hopes and aspiration even after I left him to join City University in 1985. He had the right ideas and a true sense of values. When I met him first, he weighed me up in just five minutes. He was a real and genuine visionary and certainly a meticulous man. He monitored and observed my progress all along and my success was uninterrupted because of him. I am still consolidating the knowledge that I acquired from him. I achieved more than I could have ever imagined. This has been possible because of Fred and I am very proud to have worked with him.

When I met Fred a couple of months before his death, he was in a sparkling mood, as sharp as ever. I treasure those moments. He has given me everything I asked for, more than I bargained for. I am very sad to see him depart and it truly breaks my heart. We will carry forward his ideas.

In summary, Fred has been to me a memory of the past, running into the present and flowing on into the ocean of the future.

Ranjan Banerjee



## Dynamic Buckling of Thin Walled Structures Revisited

H. Abramovich

Faculty of Aerospace Engineering, Technion, I.I.T., 32000 Haifa, Israel  
[haim@technion.ac.il](mailto:haim@technion.ac.il)

### Abstract

The topic of applying an axially time dependent load onto a column, thus inducing lateral vibrations and eventually causing the buckling of the column was studied for many years. Sometimes this is called vibration buckling, as proposed by Lindberg [1]. As it is described in his fundamental report [1], the axial oscillating load might lead to unacceptable large vibrations amplitudes at a critical combination of the frequency and amplitude of the axial load and the inherent damping of the column. This behavior is presented in Fig. 1a, where an oscillating axial load induces bending moments that cause lateral vibrations of the column. As described in [1] the column will laterally vibrate at large amplitude when the loading frequency will be twice the natural lateral bending frequency of the column. The term used by Lindberg, *vibration buckling* presents some kind of similarity to vibration resonance. However, in the case of vibration resonance the applied load is in the same direction as the motion, namely in our case lateral to the column, and the resonance will occur when the loading frequency equals the natural frequency of the column. This type of vibration buckling was called by Lindberg as: *dynamic stability of vibrations induced by oscillating parametric loading*. This type of resonance is also called in the literature as *parametric resonance* (see [2] and [3]).

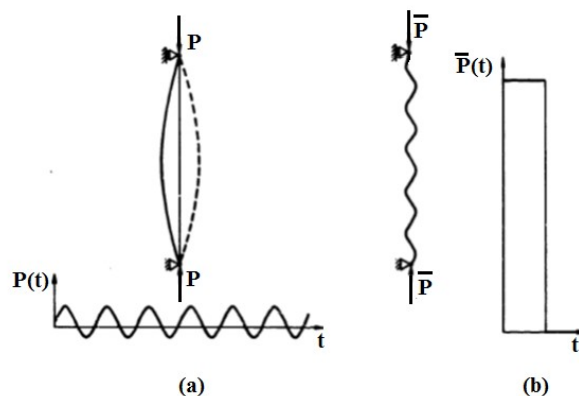


Fig. 1 (a) Buckling under parametric resonance, (b) Pulse type buckling

Another type of vibration type is sometimes also called pulse buckling, where the structure will be deformed to unacceptably large amplitudes as a result of a transient response of the structure to the dynamic axially applied load [1]. One should note that the sudden applied load might cause a permanent deformation due to plastic response of the column, a snap to a larger postbuckling deformation or simply a return to its undeformed state. This is pictured in Fig. 1b where the response of the column to a sudden short time axial load is shown.

One should note that buckling will occur when an unacceptably large deformation or stress is encountered by the column. The column can withstand a large axial load before reaching the buckling condition provided the load duration is short enough. Under an intense, short duration

axial load, the column would buckle into a very high-order mode as shown in Fig 1b. Lindberg [1] claims that pulse buckling falls under the following mathematical definition: *dynamic response of structural systems induced by time-varying parametric loading*. Throughout the present abstract, the pulse buckling will be equivalent to dynamic buckling.

The dynamic buckling of structures has been widely addressed in the literature. It started with the famous paper by Budiansky and Roth [4], thru Hegglin's report on dynamic buckling of columns [5] and continued with Budiansky & Hutchinson [6] and Hutchinson & Budiansky [7] in the mid-sixties.

One of the most intriguing and challenging thing is to define a criterion to clearly define the critical load causing the structure to buckle under the subjected pulse loading. As presented by Kubiak [8] and also by Ari Gur [9], [10],[11] a new quantity is introduced called DLF (Dynamic Load Factor) to enable the use of the dynamic buckling criteria. It is defined as

$$DLF \equiv \frac{\text{Pulse Buckling Amplitude}}{\text{Static Buckling Amplitude}} \equiv \frac{(P_{cr})_{dyn.}}{(P_{cr})_{static}} \quad (1)$$

According to Kubiak [8] the most popular criterion had been proposed by Volmir [12] for plates subjected to in-plane pulse loading. As quoted in [8], Volmir proposed the following criterion:

*“Dynamic critical load corresponds to the amplitude of pulse load (of constant duration) at which the maximum plate deflection is equal to some constant value k (k - half or one plate thickness)”*.

Another, very widely used criterion, has been formulated and proposed by Budiansky & Hutchinson [4],[6],[7] . Originally, the criterion was formulated for shell type structures but was used also for columns and plates. The criterion claims that:” *Dynamic stability loss occurs when the maximum deflection grows rapidly with the small variation of the load amplitude”*.

This criterion is schematically presented in Fig. 2b, where  $R(\lambda, t)$  is the response of the simply non-linear model assumed in [6] and presented also in Fig. 2a, and  $\lambda$  is the nondimensional applied dynamic pulse type compressive load. Figure 2c, presents the application of the criterion for the axisymmetric dynamic buckling of clamped shallow spherical shells as presented in [4].

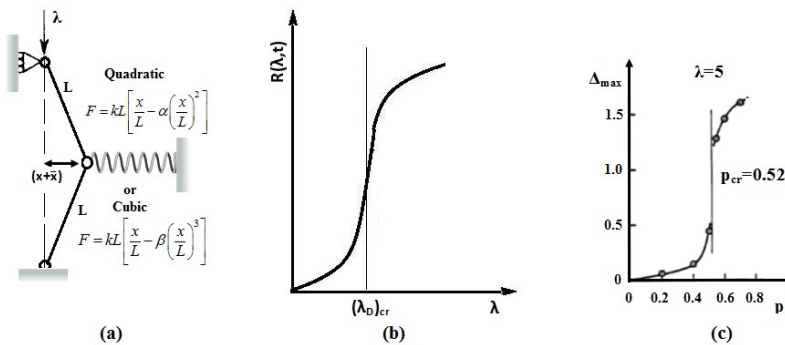


Fig. 2 (a) The non-linear model ([6]), (b) The Budiansky & Hutchinson (B&H) schematic criterion (from [6]), (c) The application of the B&H criterion to axisymmetric dynamic buckling of clamped shallow spherical shells ([4])

The dynamic buckling of columns, plates and shells is revisited, reviewing the main issues of the method, and presenting experimental and numerical calculations performed at the Technion (see Fig. 3) and results of other studies available in the literature.

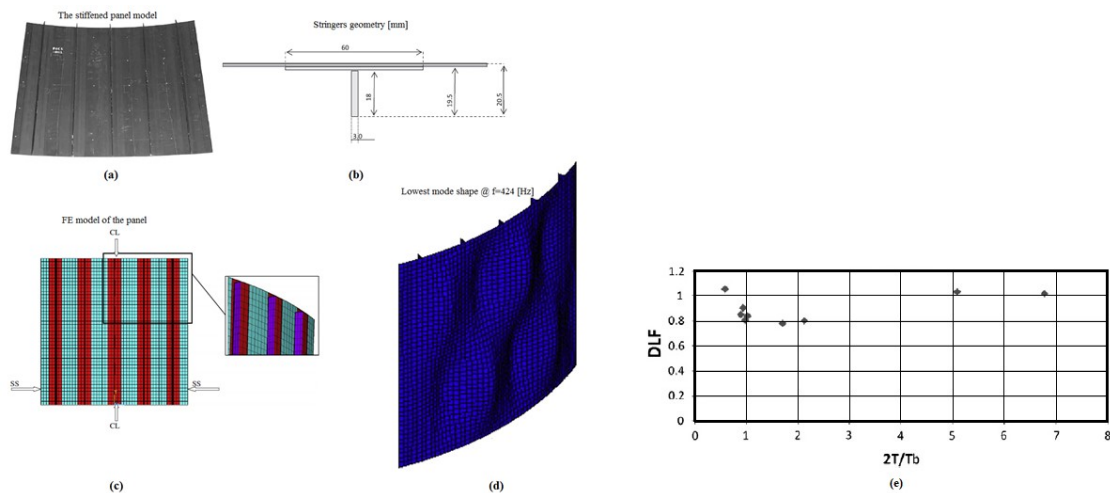


Fig. 3 Dynamic buckling investigation of a curved laminated composite stringer stiffened panel [13] : (a) The stringered panel model, (b) Geometric dimensions of the stringer, (c) The FE model, (d) The lowest mode shape of the stringered panel @  $f=424$  [Hz] (e) Variation of DLF with the nondimensional load duration –experimental results

## References

1. Lindberg, H.E., Dynamic pulse buckling-theory and experiment, SRI International , DNA 6503H, Handbook, 333 Ravenswood Avenue, Menlo Park, California 94025, USA, 1983.
2. Simitises, G.J., *Dynamic stability of suddenly loaded structures*, Springer Verlag, 1990, New York, USA, 290p.
3. Chung, M., Lee, H.J., Kang, Y.C., Lim, W.-B., Kim, J. H., Cho, J.Y., Byun, W. Kim, S.J. and Park, S.-H., Experimental study on dynamic buckling phenomena for super cavitating underwater vehicle, *International Journal of Naval Architecture and Ocean Engineering*, Vol. 4, 2012, pp. 183-198, <http://dx.doi.org/10.2478/IJNAOE-2013-0089>.
4. Budiansky, B. and Roth, R.S., Axisymmetric dynamic buckling of clamped shallow spherical shells, *Collected Papers on Instability of Shell Structures*, NASA TN-D-1510, 761 p., 1962, pp. 597-606.
5. Hegglin, B., Dynamic buckling of columns, SUDAER No. 129, June 1962, Department of Aeronautics & Astronautics, Stanford University, Stanford, California, USA, 55p.
6. Budiansky, B. and Hutchinson, J. W., Dynamic buckling of imperfection sensitive structures", *Proceedings of the 11<sup>th</sup> International Congress of Applied Mechanics*, pp. 636–651, Berlin, 1964. H. Götler, ed., Springer-Verlag, 1966.
7. Hutchinson, W. J and Budiansky, B., Dynamic buckling estimates, *AIAA Journal*, Vol. 4, No. 3, 1966, pp. 525-530.
8. Kubiak, T., Dynamic buckling of thin-walled composite plates with varying widthwise material properties, *International Journal of Solids and Structures*, Vol. 42 ,2005, pp. 5555–5567.
9. Ari-Gur, J., Weller T. and Singer J., Experimental and theoretical studies of columns under axial impact, *International Journal of Solids and Structures*, Vol. 18, No. 7, 1982, pp. 619-641.
10. Ari-Gur, J., and Hunt, D. H., Effects of anisotropy on the pulse response of composite panels, *Composite Engineering ( now Composites Part B)*, Vol. 1, No. 5, 1991, pp. 309 -317.
11. Ari-Gur, J., and Simonetta, R., Dynamic pulse buckling of rectangular composite plates, *Composites Part B*, Vol. 28, 1997, pp. 301 -308.
12. Volmir, S.A., *Nonlinear dynamics of plates and shells*, Science, 1972, Moscow, USSR.
13. Abramovich, H. and Less, H., Dynamic buckling of a laminated composite stringer-stiffened cylindrical panel", *Composite Part B*, Vol. 43, Issue 5, July 2012, pp. 2348-2358.



## Longitudinal Vibration of a Conical Bar using Rayleigh-Love Theory

**J.R. Banerjee\*, A. Ananthapuvirajah\*, S.O. Papkov\*\***

\* Department of Mechanical Engineering  
and Aeronautics  
City, University of London  
London EC1V OHB, UK  
[J.R.Banerjee@city.ac.uk](mailto:J.R.Banerjee@city.ac.uk)  
[A.Ananthapuvirajah.1@city.ac.uk](mailto:A.Ananthapuvirajah.1@city.ac.uk)

\*\* Department of Mathematics  
Sevastopol State University  
Universitetskaya Str.33,  
Sevastopol 299053  
[Stanislav.papkov@gmail.com](mailto:Stanislav.papkov@gmail.com)

### Summary

The classical theory of free longitudinal vibration of a bar is essentially based on its axial deformation when describing its free vibratory motion. Thus, the theory does not account for the lateral contraction of the bar arising from the Poisson's ratio effects. It was Lord Rayleigh [1] who first recognised the significance of lateral deformation on the free longitudinal vibration of a bar and advanced the classical theory. Many years later, Love [2] shed further lights on Rayleigh's theory and the bar model which includes the effects of lateral strain in the formulation of the free longitudinal vibration is now known as Rayleigh-Love bar [3-4]. The research on the free longitudinal vibration of Rayleigh-Love bars is mostly confined to uniform (prismatic) bars although there have been a few attempts to study non-uniform Rayleigh-Love bars [5-6] which have applications in the design of foundation because conical bars are often used as idealised structures [7-8]. This paper provides considerable insights into the free longitudinal vibration behaviour of conical Rayleigh-Love bars by recasting the governing differential equation in the form of Legendre's equation [9] for which the solution exists in series form.

In a rectangular Cartesian coordinate system, Figure 1 shows a linearly tapered bar of solid circular cross-section with the  $X$ -axis coinciding with the axis of the bar. The bar tapers downwards and the diameter  $d(x)$ , area  $A(x)$  and the polar second moment of area  $I(x)$  of the cross-section at a distance  $x$  from the left hand end  $g$  (which is considered to be the origin) varies linearly so that

$$d(x) = d_g \left(1 - c \frac{x}{L}\right), \quad A(x) = A_g \left(1 - c \frac{x}{L}\right)^2, \quad I(x) = I_g \left(1 - c \frac{x}{L}\right)^4 \quad (1)$$

where  $c$  is the taper ratio,  $L$  is the length,  $d_g$ ,  $A_g$  and  $I_g$  are respectively, the diameter, area and the polar second moment of area at the left hand end  $g$  of the bar.

Clearly, the diameter at the right hand end  $h$  is given by  $d_h = d_g(1 - c)$  so that the taper ratio  $c$  must lie within the range  $0 \leq c \leq 1$ . Thus,  $c = 0$  represents a uniform bar whereas when  $c = 1$ , the bar tapers to a point which is the limiting case that cannot be achieved in practice.

Incorporating the Rayleigh-Love theory [1,2], the expressions for kinetic ( $T$ ) and potential ( $V$ ) energies of the conical bar of Figure 1 are given by

$$T = \frac{1}{2} \int_0^L \{\rho A(x) \dot{u}^2 + \rho v^2 I(x) (\dot{u}')^2\} dx; \quad V = \frac{1}{2} \int_0^L EA(x) (u')^2 dx \quad (2)$$

where  $u$  is the displacement of a point on the axis of the bar at a distance  $x$  from the left hand end,  $\rho$  is the density,  $E$  is the Young's modulus and  $v$  is the Poisson's ratio of the bar material. An overdot and a prime represent differentiation with respect to time  $t$  and  $x$ , respectively. Hamilton's principle is now applied to derive the governing differential equation of the conical bar of Figure 1 in free vibration.

Hamilton's principle states

$$\delta \int_{t_1}^{t_2} (T - V) dt = 0 \quad (3)$$

where  $T$  and  $V$  are the kinetic and potential energies,  $\delta$  is the variational operator and  $t_1$  and  $t_2$  are the time intervals of the dynamic trajectory.

Substituting  $T$  and  $V$  from Equation (2) into Equation (3), making use of the variational operator  $\delta$ , substituting Equation (1) and finally performing integrations per parts, the governing differential equation and the expression for the axial force are obtained as follows

$$\text{Governing Differential Equation: } \xi^2 u'' + 2\xi u' + C_1 \xi^4 \dot{u}'' + 4C_1 \xi^3 \dot{u}' - C_2 \xi^2 \ddot{u} = 0 \quad (4)$$

$$\text{where } \xi = \left(1 - c \frac{x}{L}\right); \quad C_1 = \frac{\rho I_g v^2}{EA_g}; \quad C_2 = \frac{\rho L^2}{Ec^2} \quad (5)$$

and a prime now denotes differentiation with respect to  $\xi$ .

$$\text{Axial Force: } F(\xi) = \frac{EA_g c}{L} \xi^2 [u' + C_1 \xi^2 \dot{u}'] \quad (6)$$

For harmonic oscillation,  $u = Ue^{i\omega t}$  and hence Equation (4) becomes

$$\xi(1 - \bar{C}_1 \xi^2)U''(\xi) + 2(1 - 2\bar{C}_1 \xi^2)U'(\xi) + \bar{C}_2 \xi U(\xi) = 0 \quad (7)$$

where  $\bar{C}_1 = C_1 \omega^2$  and  $\bar{C}_2 = C_2 \omega^2$ , which are non-dimensional quantities.

By seeking solution in the form  $U = W(\xi\sqrt{\bar{C}_1})/\xi$ , Equation (7) can be expressed in the form of Legendre's differential equation as follows

$$(1 - \zeta^2)W''(\zeta) - 2\zeta W'(\zeta) + \mu(\mu + 1)W(\zeta) = 0 \quad (8)$$

where

$$\zeta = \xi\sqrt{\bar{C}_1}; \quad \mu = -\frac{1}{2} + \sqrt{\frac{9}{4} + \frac{\bar{C}_2}{\bar{C}_1}} \quad (9)$$

The solution of the Legendre's equation can now be obtained in series form which can be found in many advanced mathematics texts, see for example Ref [9]. In this way,  $W(\zeta)$  can be expressed in terms of two series, say functions  $\Phi(\zeta)$  and  $\Psi(\zeta)$ , connected by two arbitrary constants  $A_1$  and  $A_2$ . Thus

$$W(\zeta) = A_1 \Phi(\zeta) + A_2 \Psi(\zeta) \quad (10)$$

The expression for axial force in Equation (6) in terms of the new variable  $\zeta$  now becomes

$$F(\zeta) = \frac{EA_g c}{L} \zeta^2 (1 - \zeta^2) \{A_1 \Phi'(\zeta) + A_2 \Psi'(\zeta)\} \quad (11)$$

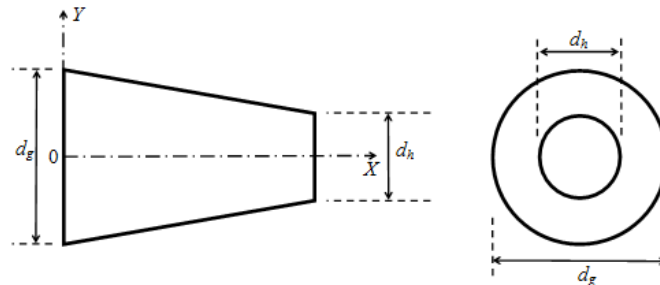


**Figure 1.** Coordinate system and notation for a solid conical bar.

For a given boundary conditions of the conical bar shown in Figure 1, the constants  $A_1$  and  $A_2$  of Equations (10) and (11) can be eliminated to obtain the frequency equation yielding the natural frequencies and the associated mode shapes of the bar. For illustrative purposes, results are given for a

cantilever conical bar for which the thick end  $g$  of Figure 1 is considered to be built-in. Clearly, at  $x = 0$ , i.e.,  $\xi = 1$  and  $\zeta = \sqrt{c_1}$ , see Equations (5) and (9), the displacement  $W(\zeta)$  of Equation (10) will be zero whereas at the free end, at  $x = L$ , i.e.,  $\xi = 1 - c$  and  $\zeta = (1 - c)\sqrt{c_1}$ , see Equations (5) and (9),  $F(\zeta)$  of Equation (11) will be zero. Hence there will be two equations and two unknown constants  $A_1$  and  $A_2$  from which the frequency equation can be derived by eliminating  $A_1$  and  $A_2$ .

Using the above theory, the natural frequencies and mode shapes of a cantilever conical beam are computed for the taper ratio  $c = 0.5$  and  $0.75$ , respectively. The results are shown in Table 1 in non-dimensional form for four different values of the length to radius ratio ( $L/r$ ) of the bar alongside the results obtained using the classical theory which ignores the lateral inertia and for which the  $L/r$  ratio is irrelevant. Clearly, for smaller values of  $L/r$  ratios, differences in natural frequencies between the current theory and classical theory are apparent, particularly for the higher order ones. For  $c = 0.5$  and  $L/r = 2$ , the difference in the first five natural frequencies are 0.34, 6.8, 19, 36 and 58%, respectively.

**Table 1.** Non Dimensional Natural frequency for various taper ratio.

Taper ratio ( $c$ )	Frequency number ( $i$ )	Non-Dimensional natural frequency $\lambda_i = \omega_i \sqrt{\frac{\rho}{EL^2}}$				
		Rayleigh-Love theory				Classical theory
		$L/r$				
		2	4	6	8	
0.5	1	1.162	1.165	1.165	1.165	1.166
	2	4.312	4.527	4.569	4.584	4.605
	3	6.552	7.426	7.623	7.695	7.792
	4	8.045	9.994	10.497	10.690	10.953
	5	8.925	12.195	13.167	13.556	14.105
0.75	1	0.844	0.845	0.845	0.845	0.845
	2	4.323	4.491	4.523	4.534	4.550
	3	6.740	7.478	7.631	7.686	7.760
	4	8.376	10.172	10.579	10.729	10.930
	5	9.274	12.533	13.354	13.665	14.088

Figure 2 shows the first five non-dimensional natural frequencies and mode shapes for the conical bar with cantilever boundary condition when the taper ratio  $c = 0.5$  and  $L/r = 4$  using both the Rayleigh-Love theory and the classical theory. Note that the natural frequencies shown in the parenthesis correspond to the classical theory. Although the mode shapes for the first three natural frequencies have not changed appreciably when applying the Rayleigh-Love theory as opposed to the classical theory, the fourth and fifth mode shapes have undergone some changes as can be seen in Figure 2. However, for higher order natural frequencies and lower values of  $L/r$  ratios, the changes are expected to be much more pronounced. The investigation is focused on the free longitudinal vibration of conical bars in the high frequency range with lower values of  $L/r$  ratios for which an accurate natural frequency computation is an essential requirement when carrying out energy flow analysis in structure. The classical theory may be deficient in this respect.

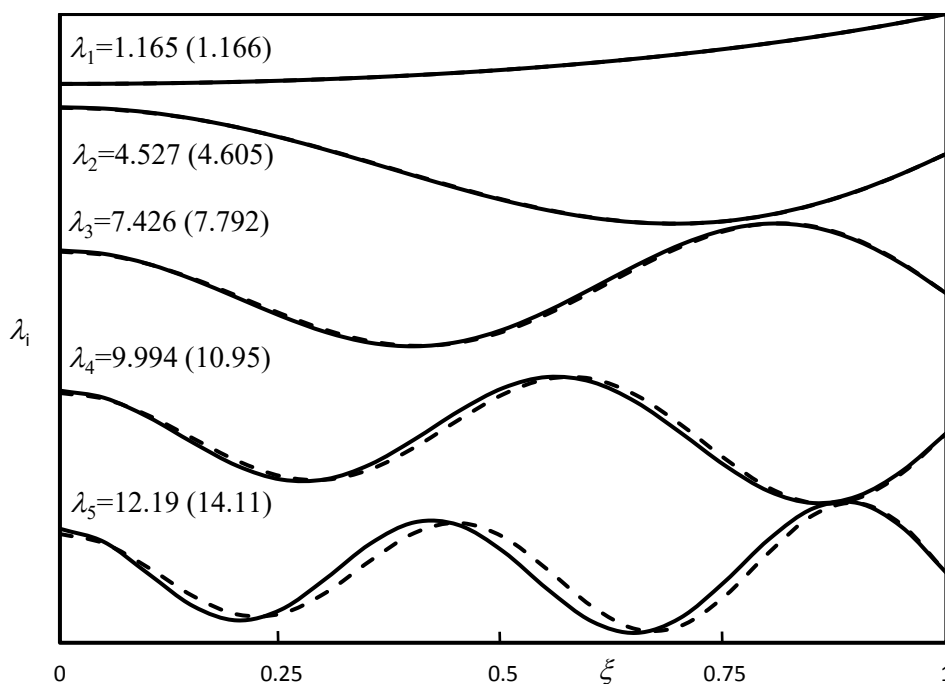


**Figure 2.** Mode shapes of a conical bar. ——— Rayleigh-Love theory ----- classical theory.

## References

- [1] Rayleigh Lord.: The Theory of Sound. Vol. 1-2, Cambridge University Press, 2011.
- [2] Love, AEH.: A Treatise on the Mathematical Theory of Elasticity. 4th ed, Cambridge University Press, 1997.
- [3] Fedotov, I.; Gai, Y.; Polyanin, A.; Shatalov, M.: Analysis for an N-stepped Rayleigh Bar with Sections of Complex Geometry. Applied Mathematical Modelling, Vol.32, pp. 1-11, 2008.
- [4] Banerjee, J.R.; Ananthapuvirajah, A.: An Exact Dynamic Stiffness Matrix for a Beam Incorporating Rayleigh–Love and Timoshenko Theories. International Journal of Mechanical Sciences, Vol.150, pp. 337-347, 2018.
- [5] Fedotov, I.A.; Polyanin, A.D.; Shatalov, M.Yu.: Theory of Free and Forced Vibrations of a Rigid Rod Based on the Rayleigh Model. Doklady Physics, Vol. 52, No 11, pp. 607-612, 2007.
- [6] Shatalov, M.; Schiesser, W.; Polyanin, A.; Fedotov, I.: Rayleigh-Love model of longitudinal vibrations of conical and exponential rods: exact solutions and numerical simulation by the method of lines. ICSV18 – 18th International Congress on Sound and Vibration, 2011.
- [7] Meek, J.W.; Wolf, J.P.: Cone Models for Homogeneous Soil. International Journal of Geotech Engineering, Vol. 118, pp. 667-685, 1992.
- [8] Meek, J.W.; Wolf, J.P.: Cone Models for Rigid Rock. International Journal of Geotech Engineering, Vol. 118, pp. 686-703, 1992.
- [9] Riley, K.F.; Hobson, M.P.; Bence S.J.: Mathematical Methods for Physics and Engineering. Cambridge University Press, 1997.

## Explicit dynamic solutions of damaged beams

**Francesco Cannizzaro**\*, **Nicola Impollonia**\*, **Salvatore Caddemi**\*, **Ivo Calio**\*

\* Department of Civil Engineering and Architecture  
University of Catania  
Via Santa Sofia 64, 95125 Catania, Italy  
francesco.cannizzaro@dica.unict.it  
nicola.impollonia@unict.it  
salvatore.caddemi@unict.it  
icalio@dica.unict.it

### Summary

Exact solutions are the best possible way for solving a large variety of dynamic problems for continuous systems. Within this scope, recent advances have been made in the field of damaged structures. In particular, for discontinuous beams, generalised functions have been widely applied as an effective modelling strategy for numerous problems in structural engineering [1]. According to this approach, a concentrated damage can be conveniently treated as a concentrated stiffness reduction mathematically modelled with a Dirac's delta in the governing equation. A similar strategy is based on considering the unknown bending moments at the right hand side of the governing equation as, for example, adopted in the governing equation of the free vibration of a multi-cracked Euler-Bernoulli beam in presence of an additional concentrated mass [2]. Here, without considering the presence of a concentrated mass, the following governing equation of a a multi-cracked Euler-Bernoulli beam is considered:

$$u^{IV}(\xi, t) + \frac{mL^4}{E_o I_o} \delta(\xi, t) = \sum_{i=1}^n \lambda_i u''(\xi_i, t) \delta''(\xi - \xi_i). \quad (1)$$

being  $u(\xi, t)$  the normalised deflection function,  $\xi$  the normalised spatial abscissa,  $m$  the distributed mass,  $L$  the length of the beam,  $E_o I_o$  the flexural stiffness, in presence of multiple cracks located at the abscissae  $\xi_i$ ,  $i=1, \dots, n$  with dimensionless crack compliances  $\lambda_i = E_o I_o / K_i L$  (where  $K_i$  is the stiffness of the rotational spring equivalent to the crack) which can be collected in the vector  $\lambda = [\lambda_1, \lambda_2, \dots, \lambda_i, \dots, \lambda_n]$ .

Once the governing equation is properly integrated with the necessary expedients to treat the generalised terms, the main advantage of such an approach is avoiding the enforcement of continuity conditions at the cracked sections (irrespectively of their number). The enforcement of the end conditions only is required leading to a more effective computational strategy. Within this method, exact solutions have been proposed for a significant amount of problems (see for example the statics of multi-cracked circular arches [3] or the dynamic behaviour of axially loaded multi-cracked frames [4]).

It is remarkable to note that the above mentioned approach presented in [2] avoids enforcing continuity conditions at the cracked sections and provides exact solution for the mode shapes. However, it can also be noted that the latter approach implies the numerical solution of the characteristic equation to obtain the eigenfrequencies. In some cases the Wittrick & Williams algorithm is employed to compute the natural frequencies and the relevant mode shapes of a structure with the desired accuracy [4]. Numerical solutions of eigen problems can be sometimes cumbersome and difficult to handle. For the latter reasons, it would be desirable for problems associated to copious computations (e.g. re-analyses, sensitivity assessments, inverse

problems and forced vibrations) to have at disposal explicit expressions of the modal parameters aiming at fast and simple solutions. Therefore, explicit solutions are enticing tools to solve dynamic problems in alternative to cumbersome numerical procedures even when devoted to pursue exact solutions.

Within the study of forced vibrations of multi-cracked beams, the Sherman-Morrison formula (which was applied with reference to static interval analysis in [5]) is here employed to approximately express the main modal parameters. Precisely, the dependency of the  $p$ -th frequency parameter  $\alpha_p^4(\lambda)$ , the generalised modal mass  $M_p(\lambda)$  and the load term  $Q_p(t; \lambda)$  on the crack intensities, by enforcing the correspondence between explicit approximate and exact parameters for  $2n+1$  damage configurations, is explicitly formulated.

In Figure 1 a comparison between approximate and exact solutions of these modal parameters is reported for the single cracked beam shown in Figure 1a (with  $q_o = 1$ ), demonstrating how the considered approximation is in good agreement with the exact parameters. The reported modal parameters are normalized by those relative to a reference damage intensity ( $\lambda = 0.2$ ).

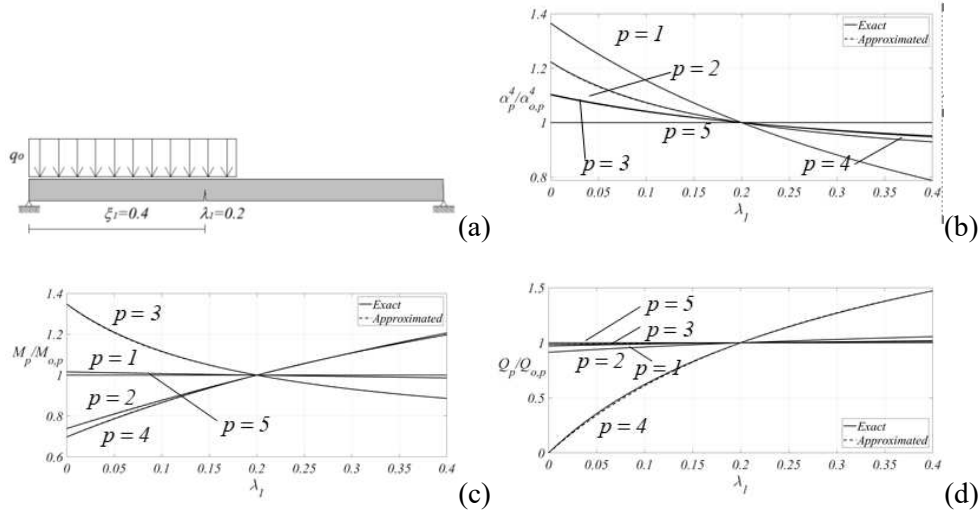


**Figure 1.** Comparison between exact and approximated modal properties vs crack intensity for the beam in (a): (b) frequency parameter, (c) generalized modal mass and (d) load term.

The explicit and accurate expressions proposed for the modal parameters are then employed, via modal superposition analysis, to infer explicit solutions of the response of a damaged beam subjected to forced vibrations. The latter explicit formulation allows a full sensitivity analysis of the response to the damage intensities including, among others, the evaluation of bounds of the response. The accuracy of the response sensitivity to the damage, obtained by the proposed explicit approach, has been assessed by means of a comparison with the exact solution procedure applied to each damage configuration. In Figure 2 the bounds of the response associated to a time history computed with this approach (blue lines) are compared to the exact results for the beam reported in Figure 1 (considering the characteristics  $L=5$  m,  $E=2.1 \cdot 10^{11}$  N/m<sup>2</sup>,  $I=8.33 \cdot 10^{-6}$  m<sup>4</sup>,  $m=75$  kg/m) and subjected to a pulsating load ( $\omega = 5$  rad / s) associated to a re-analysis according to a scanning exact procedure (grey band). The computational burden associated to the approximated approach is significantly lower with respect to the re-analysis and the agreement with the exact approach is ensured.

A further possible application of the presented approach, when the transient contribution is neglected, is the evaluation of the frequency-response of a damaged beam (with the same physical characterization of the previous application) subjected to a pulsating concentrated load

( $P_o = 1$ ,  $\omega = 5 \text{ rad/s}$ ) at the midspan, Figure 3a. The results relative to the undamped and reported in Figure 3b. The results are reported in terms of steady-state transversal displacement of the midpoint normalized by the corresponding response of the beam when subjected to the static load versus the normalized frequency parameter of the pulsating load  $\eta = \alpha_\omega^2 / \alpha_{o,1}^2$ . The results show how the proposed approximated explicit approach is able to bind the envelope obtained with the re-analysis for the whole considered range of the load frequency, also when the response is unbounded.

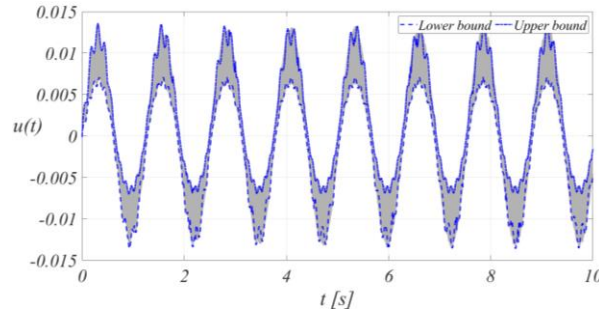


**Figure 2.** Interval time-domain response for the beam reported in Figure 1a: comparison between the exact results associated to a re-analysis (grey band) and response bounds obtained with the proposed approach.

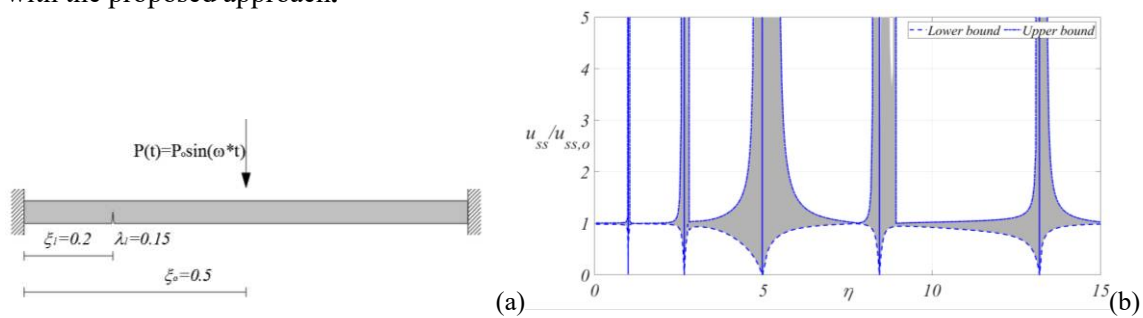


**Figure 3.** Frequency-response interval spectrum for the undamped beam in (a): (b) normalized response bounds obtained with the proposed approach.

## References

- [1] Caddemi, S.; Calì, I.; Cannizzaro, F.: Closed-form solutions for stepped Timoshenko beams with internal singularities and along-axis external supports. *Archive of Applied Mechanics* Vol. 83, No. 4, pp. 559-577, 2013; ISSN: 0939-1533, doi: 10.1007/s00419-012-0704-7.
- [2] Cannizzaro, F.; De Los Rios, J.; Caddemi, S.; Calì, I.; Ilanko, S.: On the use of a roving body with rotary inertia to locate cracks in beams. *Journal of Sound and Vibration*, Vol. 425, pp. 275-300, 2018; <https://doi.org/10.1016/j.jsv.2018.03.020>.
- [3] Cannizzaro, F.; Greco, A.; Caddemi, S.; Calì, I.: Closed form solutions of a multi-cracked circular arch under static loads. *International Journal of Solids and Structures*, Vol. 11, pp. 191-200, 2017; doi: 10.1016/j.ijsolstr.2017.05.026.
- [4] Caddemi, S., Calì, I., Cannizzaro, F.: The Dynamic Stiffness Matrix (DSM) of axially loaded multi-cracked frames. *Mechanics Research Communications*, Vol. 24, pp. 90-97, 2017; doi: <https://doi.org/10.1016/j.mechrescom.2017.06.012>.
- [5] Impollonia, N.: A method to derive approximate explicit solutions for structural mechanics problems. *International Journal of Solids and Structures*, Vol. 43, pp. 7082-7098, 2006.



## Preliminary Assessments on the Development of Refined Shell Models for Free Vibrations via Machine Learning

**Erasmus Carrera, Marco Petrolo**

Department of Mechanical and Aerospace Engineering  
 Politecnico di Torino  
 Corso Duca degli Abruzzi 24, 10129 Torino, Italy  
 [erasmo.carrera, marco.petrolo]@polito.it

### Summary

This work presents a new framework to build refined shell models for structural dynamics applications. Shell structural theories are well-established formulations for the analysis of thin-walled structures [1]. The adoption of refined models with enriched displacement field is of interest for composite structures to detect various effects including shear deformability and transverse stretching [2]. One of the methodologies to refine structural models is the Axiomatic/Asymptotic Method (AAM) [3] exploiting the hierarchical capabilities of the Carrera Unified Formulation (CUF) [4] to evaluate the influence of each generalized unknown on the solution as design parameters change. The AAM leads to Best Theory Diagrams [5] in which, for a given accuracy level, the minimum number of required unknowns is available. The easiest way to obtain a BTM is to evaluate the accuracy of each combination of unknowns of a given full model. For instance, a fourth-order equivalent-single-layer model (ED4) has 15 variables leading to  $2^{15}$  reduced models. One of them is in Eq. 1 in which nine out of 15 unknowns are active, see Fig. 1 for the reference frame. This paper presents a new methodology to build the BTM with far less computational overhead as

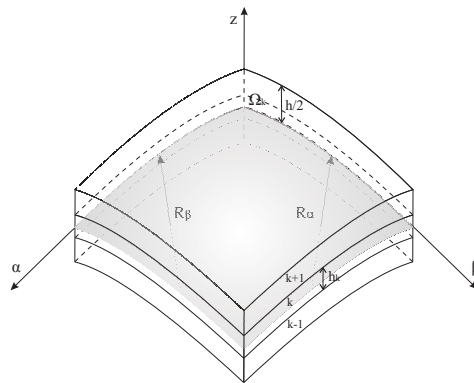


Figure 1: Shell reference frame.

follows:

1. CUF generates the FEM arrays for the eigenvalue problem on the basis of an ED4 and its reduced models,  $(\mathbf{k}_{\tau si j}^k - \omega^2 \mathbf{m}_{\tau si j}^k) \mathbf{u}_{\tau i}^k = 0$ . Each analysis generates results concerning natural frequencies and modal shapes.
2. The results from each analysis become the input to train an Artificial Neural Network (ANN).
3. ANN generates outputs for all the  $2^{15}$  models and for varying design parameters.

ANN is well-known for its universal approximation capabilities [6]. A typical ANN configuration has a multilayer feed-forward artificial neural network. Each layer has a finite number of neurons. This paper adopts Levenberg-Marquardt training functions and a single layer. The coding of inputs and targets is the following:

- An input is a vector with 15 elements. Each element is either '1' or '0' to indicate an active or inactive generalized displacement unknown, respectively.
- Each input has an associated output composed by a vector containing the normalized first five frequencies and the MAC matrix components. Normalization of frequency uses the reference values of the full fourth-order model.

As an example, the following equation shows the coded input of a generic shell model:

$$\begin{aligned} u_x &= u_{x_1} + z u_{x_2} + z^4 u_{x_5} \\ u_y &= u_{y_1} + z u_{y_2} + z^3 u_{y_4} \\ u_z &= u_{z_1} + z u_{z_2} + z^2 u_{z_3} \end{aligned} \Rightarrow [111111001010100] \quad (1)$$

The numerical example deals with a simply-supported square laminated shell previously analyzed in [7]. The shell has  $a = b$ ,  $R_\alpha = R_\beta = R$ , and  $a/h = 10$ . The material properties are  $E_1/E_2 = 25$ ,  $G_{12}/E_2 = G_{13}/E_2 = 0.5$ ,  $G_{13}/E_2 = 0.2$ ,  $\nu = 0.25$ . The stacking sequence is 0/90/0 with layers of same thickness. The finite element model of a quarter of shell has a  $4 \times 4$  mesh as this discretization provides sufficiently accurate results. Table 1 shows the ED4 reference values adopted to train the ANN and a comparison with a fourth-order layer-wise model.

Table 1: Reference values for the first frequency,  $\omega \sqrt{\frac{\rho a^4}{h^2 E_T}}$ .

	R/a = 2	R/a = 5	R/a = 10	Plate
LD4 [7]	12.773	11.685	11.515	11.457
ED4	13.008	11.972	11.811	11.756

Figure 2 shows the accuracies of all the  $2^{15}$  models concerning the first natural frequency and the BTD. The FEM solution considered all  $2^{15}$  analyses whereas the ANN used 2000 analyses and ten neurons. Table 2 shows the BTD models. Each triangle indicates a generalized variable and its color indicates the status of the variable, i.e., 'black' stands for an active variable and 'white' for inactive. For instance, the best shell model with nine DOF is the following:

$$\begin{aligned} u_x &= u_{x_1} + z u_{x_2} + z^3 u_{x_4} \\ u_y &= u_{y_1} + z u_{y_2} + z^3 u_{y_4} \\ u_z &= u_{z_1} + z u_{z_2} + z^2 u_{z_3} \end{aligned} \quad (2)$$

As shown in Table 2, constant, linear and cubic unknown variables have a more significant role.

The results show that

- The ANN framework is a valid tool to create BTD with reduced computational costs.
- For the problem considered, The importance of third-order terms in the displacement field is evident.
- The future developments must address the possibility to build BTD via ANN for various design parameters. Such a development may potentially decrease the computational overhead even more significantly than in the current numerical examples.

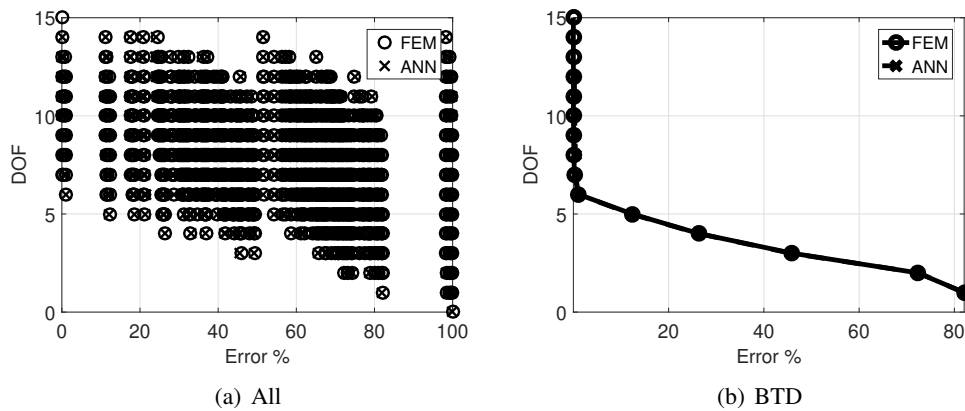


Figure 2: Verification of the ANN trained with 2000 inputs against FEM  $2^{15}$  FEM results.

Table 2: BTD models

DOF	$u_{x1}$	$u_{y1}$	$u_{z1}$	$u_{x2}$	$u_{y2}$	$u_{z2}$	$u_{x3}$	$u_{y3}$	$u_{z3}$	$u_{x4}$	$u_{y4}$	$u_{z4}$	$u_{x5}$	$u_{y5}$	$u_{z5}$
15	▲	▲	▲	▲	▲	▲	▲	▲	▲	▲	▲	▲	▲	▲	▲
14	▲	▲	▲	▲	▲	▲	△	▲	▲	▲	▲	▲	▲	▲	▲
13	▲	▲	▲	▲	▲	▲	△	▲	▲	▲	▲	▲	△	▲	△
12	▲	▲	▲	▲	▲	▲	△	▲	▲	▲	▲	▲	△	▲	△
11	▲	▲	▲	▲	▲	▲	△	▲	▲	▲	▲	▲	△	▲	△
10	▲	▲	▲	▲	▲	▲	△	▲	▲	▲	▲	▲	△	△	△
9	▲	▲	▲	▲	▲	▲	△	△	▲	▲	▲	▲	△	△	△
8	▲	▲	▲	▲	▲	▲	△	△	△	▲	▲	▲	△	△	△
7	▲	▲	▲	▲	▲	▲	△	△	△	▲	△	△	△	△	△
6	▲	▲	▲	▲	▲	▲	△	△	△	▲	△	△	△	△	△
5	▲	▲	▲	▲	▲	△	△	△	△	△	△	△	△	△	△

## References

- [1] Leissa, A.W.: Vibration of Shells. NASA-SP-288, LC-77-186367, 1973.
- [2] Carrera, E.: Developments, ideas and evaluations based upon the Reissner's mixed variational theorem in the modeling of multilayered plates and shells. Applied Mechanics Review, Vol. 54, pp. 301–329, 2001.
- [3] Carrera, E.; Petrolo M.: Guidelines and recommendation to construct theories for metallic and composite plates. AIAA Journal, Vol. 48, No. 12, pp. 2852–2866, 2010.
- [4] Carrera, E.; Cinefra, M.; Petrolo M.; Zappino, E.: Finite Element Analysis of Structures Through Unified Formulation. John Wiley & Sons, Chichester, 2014.
- [5] Petrolo M.; Carrera, E.: Best Theory Diagrams for multilayered structures via shell finite elements. Advanced Modeling and Simulation in Engineering Sciences, In Press.
- [6] Hagan, M.T.; Demuth, H.B.; Beale, M.H.; De Jesús, O.: Neural Network Design. Martin Hagan, 2014.
- [7] Cinefra, M.: Free-vibration analysis of laminated shells via refined MITC9 elements. Mechanics of Advanced Materials and Structures, Vol. 23, No. 9, pp. 937–947, 2016.



## Tunable 1D linear acoustic diodes: A design based on soft functionally graded phononic crystals

Yingjie Chen\*, Bin Wu\*, Yipin Su\*, Wei Qiu Chen<sup>#</sup>

\* Department of Engineering  
Mechanics  
Zhejiang University  
No. 38, Zheda Road, 310027  
Hangzhou, China  
11624006@zju.edu.cn

<sup>#</sup> Key Laboratory of Soft Machines  
and Smart Devices of Zhejiang  
Province  
Zhejiang University  
No. 38, Zheda Road, 310027  
Hangzhou, China  
chenwq@zju.edu.cn

### Summary

Phononic crystals (PCs) have been a hot research topic since the concept was proposed nearly 30 years ago [1]. The particularity of PCs relies on the band gap in its frequency spectrum within which the waves can not propagate through the structure. The band gap in PCs is formed by the Bragg scattering due to the structural periodicity. Another mechanism, i.e. the local resonance, to form the band gap was later found by Liu et al. [2]. Materials with local resonant units are known as metamaterials (MMs). PCs are now also included as a particular type of MMs.

MMs have been widely explored to design novel functional devices. In the design of acoustic diodes (ADs), which allow waves to propagate only in one-direction but not inversely, there are two main approaches. One is to use nonlinear media to change the frequency of the incoming wave [3], and the other exploits the wave diffraction phenomena to alter the wave number of the incoming wave [4]. But these two approaches are inapplicable to one-dimensional, linear ADs.

A new approach has been developed by the authors to realize one-dimensional ADs in the completely linear regime [5]. The design makes use of the free vibration characteristics of the AD which is practically of finite size as well as of the functionally graded property that is introduced particularly. The key is to make one resonant frequency of the structure locate in the band gap, and this frequency is further splitted into two peaks corresponding to the cases that the wave propagates in different directions. Then the wave with its frequency identical with one peak can propagate from the left to the right for instance, but cannot get through the structure in the opposite direction, and vice versa.

This study focuses on the design of tunable one-dimensional linear ADs based on our previous work. The tunability is realized by making use of soft materials which can withstand reversible large deformation under mechanical loads. The design is shown in Figure 1 below. It consists of 12 A-phases and 11 B-phases. The material parameters of both A-phases and B-phases may vary along the longitudinal direction so as to exhibit a functionally graded property. Either phase is soft and hyperelastic, characterized by a compressible Gent model with the following form of the energy density function  $\Omega$ :

$$\Omega = -\frac{\mu}{2} J_m \ln \left( 1 - \frac{I_1 - 3}{J_m} \right) - \mu \ln J + \left( \frac{\Lambda}{2} - \frac{\mu}{J_m} \right) (J - 1)^2. \quad (1)$$

Here  $\mu$  and  $\Lambda$  are the shear modulus and the first Lamé's parameter of the material in the undeformed configuration, respectively,  $I_1 = \lambda_1^2 + \lambda_2^2 + \lambda_3^2$  represents the first invariant, and  $J$  is the volume change ratio. There is a relation among the first Lamé's parameter, Poisson's ratio  $\nu$ , and shear modulus as  $\Lambda = 2\mu\nu / (1 - 2\nu)$ .  $J_m$ , usually known as the Gent constant, is the dimensionless stiffening parameter of the material. When  $J_m \rightarrow \infty$ , the above Gent model degenerates to the neo-Hookean model. It is noted that although the material is nonlinear, we only consider the linear waves (and hence linear ADs) superimposed on a finite deformation.

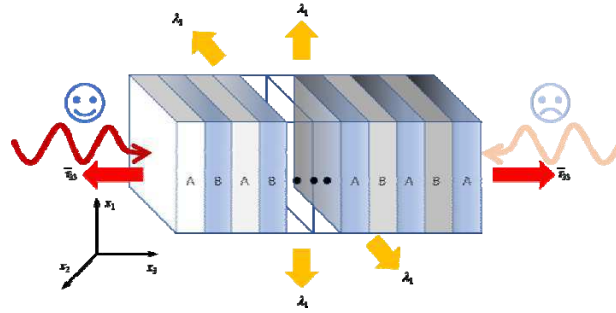


**Figure 1.** A graded AD subject to lateral bi-axial stretch and longitudinal pre-stress. When we consider the case that the wave propagates from the left to the right, a dynamic displacement of unit amplitude is imposed on the left end, and vice versa.

The graded AD can be subject to lateral bi-axial stretch  $\lambda_1$  and longitudinal pre-stress  $\bar{\tau}_{33}$  as shown in Figure 1. These mechanical loads will alter the geometry of the AD and the effective material properties of either phase, and hence can change the propagation behavior of the superimposed infinitesimal linear elastic waves. In this study, the finite pre-deformation analysis is carried out based on the fully nonlinear theory of hyperelasticity, while the wave analysis relies on the linear perturbation of the original nonlinear governing equations. Since the material is functionally graded, the approximate laminate technique [6] is employed here, along with the state-space formulations, to achieve an efficient and accurate wave analysis.

For numerical illustration, we suppose that the normalized shear modulus of the  $p$ -phase varies in the form of  $\bar{\mu}_p(x_3) = K_p(x_3 - D/2) + \tilde{\mu}_p$  in the undeformed configuration, where  $K_p$  denotes the grading degree of material  $p$ ,  $\tilde{\mu}_p$  is the normalized shear modulus at  $x_3 = D/2$ , and  $D = 12h_A + 11h_B$  is the total length of the AD, with  $h_A$  and  $h_B$  being the thicknesses of the layers A and B respectively. In the calculation, we take the normalized densities as  $\tilde{\rho}_{0A} = \tilde{\rho}_{0B} = 1$ , normalized shear moduli as  $\tilde{\mu}_A = 2, \tilde{\mu}_B = 1$ , thicknesses as  $h_A = h_B = 0.5$ , Poisson's ratios as  $\nu_A = \nu_B = 1/3$ , and Gent constants as  $J_{mA} = J_{mB} = 10$ . The normalization is taken with respect to the silicon rubber Zhermarck Elite Double 32 [7].

We here fix  $\lambda_1 = 1$  and examine the effect of pre-stress on the transmission (defined as the logarithm of the displacement ratio between the output and input ends) spectrum of the finite graded AD. To display the influences of material grading degrees on wave propagation under mechanical biasing fields, we take  $K_A = 0.02, K_B = 0.02$  to enhance the asymmetry of the finite structure. We show the transmission spectra in Figure 2 around the first band gap under the normalized pre-stresses  $\tilde{\tau}_{33}^0 = 0, 4, 8$ , and 12, respectively.  $\tilde{\omega}_L$  and  $\tilde{\omega}_R$  indicated in the figure

denote the resonant frequencies of waves propagating along opposite directions. It is found from Figure 2 that when the pre-stress equals 8 the band gap of the PC will be closed. Also, the resonant frequency peaks outside the band gap are seldom affected by the grading degree of the material. However, we can see from Figures 2(a), 2(b), and 2(d) that the grading of material properties induces the separation of the resonant frequency peaks in the band gap and asymmetric transmission behaviors in opposite propagation directions are gained. Additionally,  $\tilde{\omega}_L$  and  $\tilde{\omega}_R$  vary along with the band gap when the pre-stress changes. Thus we can conclude that the two-way filtering of the finite graded AD can be effectively tuned by the pre-stress.

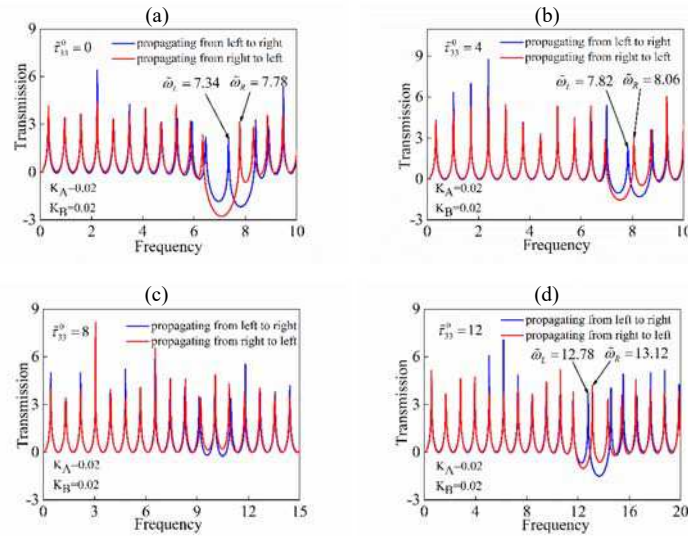


**Figure 2.** Transmission spectra under different pre-stresses ( $K_A = 0.02, K_B = 0.02$ ).

## References

- [1] Kushwaha, M.S.; Halevi, P.; Dobrzynski, L.; Djafarirouhani, B.: Acoustic Band Structure of Periodic Elastic Composites. *Physical Review Letters*, Vol. 71, No. 13, pp. 2022-2025, 1993.
- [2] Liu, Z.; Zhang, X.X.; Mao, Y.W.; Zhu, Z.Z.; Yang, Z.Y.; Chan, C.T.; Sheng, P.: Locally Resonant Sonic Materials. *Science*, Vol. 289, No. 5485, pp. 1734-1736, 2000.
- [3] Liang, B.; Yuan, B.; Cheng, J.C.: Acoustic Diode: Rectification of Acoustic Energy Flux in One-Dimensional Systems. *Physical Review Letters*, Vol. 103, No. 10, p. 104301, 2009.
- [4] Li, X.F.; Ni, X.; Feng, L.; Lu, M.H.; He, C.; Chen, Y.F.: Tunable unidirectional sound propagation through a sonic-crystal-based acoustic diode. *Physical Review Letters*, Vol. 106, No. 8, p. 084301, 2011.
- [5] Chen, Y.J.; Huang, Y.; Lü, C.F.; Chen, W.Q.: A Two-Way Unidirectional Narrow-Band Acoustic Filter Realized by a Graded Phononic Crystal. *Journal of Applied Mechanics*, Vol. 84, No. 9, p. 091003, 2017.
- [6] Chen, W.Q.; Ding, H.J.: On Free Vibration of a Functionally Graded Piezoelectric Rectangular Plate. *Acta Mechanica*, Vol. 153, No. 3-4, pp. 207-216, 2004.
- [7] Galich, P.I.; Fang, N.X.; Boyce, M.C.; Rudykh, S.: Elastic Wave Propagation in Finitely Deformed Layered Materials. *Journal of the Mechanics and Physics of Solids*, Vol. 98, pp. 390-410, 2017.



## Detection of Structural Damage Based on Perturbed Local Equilibrium

Li Cheng

Department of Mechanical Engineering,  
The Hong Kong Polytechnic University,  
Hong Hom, Kowloon, Hong Kong  
e-mail: li.cheng@polyu.edu.hk,

### Summary

Detection of structural damage is an important and technically challenging problem. As a consequence of manufacturing defect, improper use, service wear, fatigue or even sabotage, engineering assets (*e.g.*, land/water/air/space vehicles, civil infrastructure and heavy equipment) experience continuous accumulation of damage over their lifespan. The damage, in whatever form it manifests, can considerably jeopardize the structural integrity and system functionality, potentially leading to catastrophic failure without timely detection. With safety being the paramount priority for all engineering assets, reliability, integrity and durability criteria must be strictly met. To meet this requirement, a large variety of nondestructive evaluation (NDE) methods have been developed in the past. Most of these well-defined techniques can fulfill offline detection of local damage in small-scale structural fragments. In practice, however, it is highly imperative to develop continuous and automated damage evaluation techniques conducive to implementation of online damage characterization. Such a consensus has entailed intensive research and development activities on damage identification and structural health monitoring (SHM) in the past two decades.

In this talk, a vibration-based damage identification method, referred to as Pseudo-Excitation (PE) technique, is reviewed. Envisaging the existing deficiencies of the conventional vibration-based damage detection method in terms of insensitivity to small damage, and driven by recent breakthroughs in advanced signal processing and measurement technology, a novel inverse damage identification technique was developed, by canvassing locally perturbed dynamic equilibrium characteristics of a structural component (exemplified by beam and plate elements) governed by high-order spatial derivatives. The basic philosophy behind is that an intact structure locally satisfies a certain type of dynamic equilibrium based on certain physical laws such as the local equation of motion. Upon occurrence of damage, the dynamic equilibrium of the intact structural is locally perturbed, resulting in a residual term in the dynamic equation, equivalent to a virtual pseudo-excitation, which can be used to pinpoint the damage occurrence.

Different versions of the approach, relying on the integral utilization of multi-types of structural vibration signals, are formulated. By exploring the local equilibrium of the structure, both “*strong*” and “*weak*” versions of PE technique are derived. Taking a beam component as an example, the strong formulation directly explores the structural equilibrium based on the dense displacement measurement, with a damage index DI defined as :

$$DI(x) = EI \frac{d^4 w(x)}{dx^4} - \rho S \omega^2 w(x) \quad (1)$$

Its weak counterpart introduces a weighting function  $\eta(x)$  and a windowed integration as

$$\overline{\text{DI}} = \int_{x_c - \tau/2}^{x_c + \tau/2} [\text{DI}(x) \cdot \eta(x - x_c)] dx \quad (2)$$

Through a proper choice of  $\eta(x)$  and integration by part, various forms of DI expressions can be generated and used to avoid direct higher-order derivatives of structural vibration signals. This, by the same token, allows the use of different measured vibration signals (e.g., vibration displacements, rotations and dynamic strains, etc.). Such a merit gives rise to the possibility of integrating multi-types of vibration signals to achieve improved detection accuracy whilst increasing the robustness of the approach against measurement uncertainties and reducing the number of measurement points. As an example, damage detection of beam-like and plate-like structures using both laser-vibrometer and Micro Piezoelectric Fiber sensor array will be demonstrated. A typical detection result is shown in Fig.2, in which multiple damage (debonding of a metal-concrete joint) is detected.

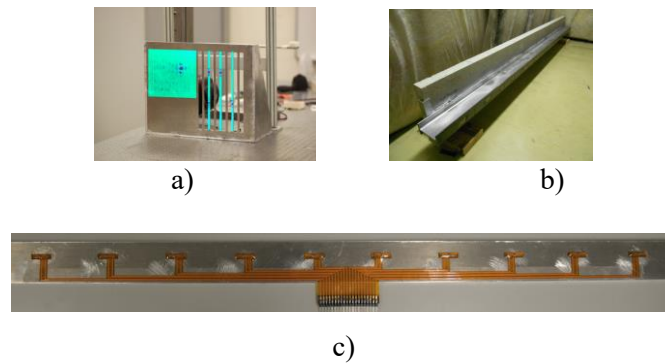


**Figure 1.** Examples of damaged structures. a). Corrosion damage in a plate-beam assembly ; b). Debonding of a metal-concrete joint; c). Metal-core piezoelectric fiber-based smart layer.

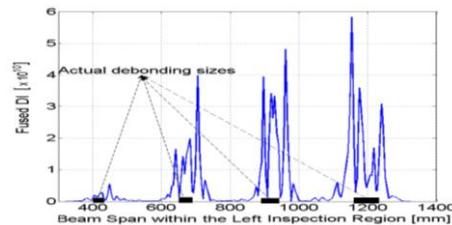


**Figure 2.** A typical detection result on a beam with multiple damage (debonding of a metal-concrete joint). DI from the strong formulation using displacement data covered from a Laser-vibro-meter measurement.

## References

- [1] Xu, H., Su, Z., Cheng, L. and Guyader, J.L.: A Pseudo-Excitation Approach for Structural Damage Identification: From “Strong” to “Weak” Modality, *Journal of Sound and Vibration*, 337, 181-198, 2015.
- [2] Zhang, C., Cheng, L., Qiu, J.H and Wang, H.Y.: Damage Detection Based on Sparse Virtual Element Boundary Measurement Using Metal-Core Piezoelectric Fiber, *Structural Health Monitoring: An International Journal*, 17(1), 15-23, 2018.
- [3] Zhang, C., Cheng, L., Qiu, J.H., Ji, H.L. and Ji, J.Y.: Structural Damage Detections Based on a General Vibration Model Identification Approach. *Mechanical Systems and Signal Processing*, Under review, 2018.

## Solutions of Vibration Problems with Boundary Excitation by the Fourier Method and their Application to Optimal Boundary Control

Piotr Cupiał

Faculty of Mechanical Engineering and Robotics  
AGH University of Science and Technology  
Al. Mickiewicza 30, 30-059 Kraków, Poland  
[pcupial@agh.edu.pl](mailto:pcupial@agh.edu.pl)

### Summary

The Fourier method of separation of variables is a standard approach used to solve forced vibration problems of linear continuous bodies, when a force is applied inside the body. Vibration problems in which a force (stress) or displacement are prescribed on the boundary are also of much interest. Such problems arise in a natural way, e.g., in the determination of the forced vibration of piezoelectric continua, when electrical potential is applied to electrodes placed on the surface of a piezoelectric body. Some of the methods discussed below are now also being implemented to study the vibration of piezoelectric 3-D bodies subject to excitation by electrostatic potential applied to the boundary.

When problems with boundary excitation are solved using the Fourier method, the satisfaction of the boundary condition is not straightforward, since the solution is obtained in terms of the modal shapes of the corresponding homogenous problem. This talk will review several methods that can be used to analyse vibration problems with time-varying boundary conditions, with emphasis on the character of the convergence of solution. The solution approaches include: a method by which a problem with non-homogenous boundary conditions is transformed, by a proper change of the dependent variable, to one with homogenous boundary conditions; the use of the Laplace transform technique; Green function approach; and the use of the theory of generalized functions (distributions). The mode superposition method can also be applied to other one-dimensional problems and to more complex geometries, including two- and three-dimensional bodies. This is not true of the travelling wave solution method, which can be used e.g. for bars. One interesting application of the series solutions is in the field of optimal control of continuous systems. A solution method will be presented, which allows the calculation of the optimal boundary control force, which brings a bar with the prescribed initial conditions or/and subjected to given transient excitation to rest at a given time  $T$ .

To illustrate different approaches, longitudinal vibration of an elastic bar with one end fixed and a time-varying force applied to its right end is considered. The problem is described by the governing equation with the prescribed initial and boundary conditions:

$$\begin{aligned} \frac{\partial^2 u}{\partial t^2} - a^2 \frac{\partial^2 u}{\partial x^2} &= 0, \quad a = \sqrt{\frac{E}{\rho}} \\ u(x,0) &= 0, \quad \frac{\partial u}{\partial t}(x,0) = 0, \quad u(0,t) = 0, \quad \frac{\partial u(l,t)}{\partial x} = \frac{P(t)}{EA} = \alpha(t) \end{aligned} \quad (1)$$

The initial conditions and the distributed forces pose no solution problems, and they have been taken to be equal to zero. In Eq. (1),  $P(t)$  is a force applied to the bar right end.

### I. Transforming the problem by a change of the dependent variable

One sets:  $u(x,t) = z(x,t) + x\alpha(t)$ , and problem (1) with a non-homogenous boundary condition is transformed to that with a homogenous one:

$$\begin{aligned} \frac{\partial^2 z}{\partial t^2} - a^2 \frac{\partial^2 z}{\partial x^2} &= -x\ddot{\alpha}(t) \\ z(x,0) &= -x\alpha(0), \quad \frac{\partial z}{\partial t}(x,0) = -x\dot{\alpha}(0), \quad z(0,t) = \frac{\partial z(l,t)}{\partial x} = 0 \end{aligned} \quad (2)$$

Assuming that the applied force is a smooth enough function of time, problem (2) can be solved in a standard way. Of the four methods discussed this approach is the only one, for which the boundary condition at the bar right end is satisfied if one sets  $x = l$ .

### II. The Laplace transform method

One takes the Laplace transform with respect to time of (1), so that the following expression for the Laplace transform of the solution is obtained:

$$\bar{u}(x,p) = \frac{\bar{P}(p)l \sinh(px/a)}{EA(pl/a) \cosh(pl/a)} \quad (3)$$

To find the time response, one uses the inverse Laplace transform formula together with the residue theorem of complex analysis. The residues are calculated at the poles (zeros of the denominator of (3)), which are equal to:  $p = 0$ ;  $p_k = \frac{a}{2l}(2k+1)\pi i$ ,  $k = 0, \pm 1, \pm 2, \dots$  ( $i$  stands for the imaginary unit). Thus, the response to a force  $P(t)$  acting on the right end of the bar is:

$$u(x,t) = \frac{4a}{\pi EA} \sum_{n=1}^{\infty} \frac{(-1)^{n-1}}{2n-1} \sin\left(\frac{2n-1}{2} \frac{\pi x}{l}\right) \int_0^t P(\tau) \sin\left[\frac{(2n-1)\pi a}{2l}(t-\tau)\right] d\tau \quad (4)$$

The Laplace transform of the longitudinal force in the bar is  $\bar{N}(x,p) = EA d\bar{u}(x,p)/dx$ , where  $\bar{u}(x,p)$  is given by Eq. (3). Assuming a force  $P(t) = P_0 H(t)$ , where  $H(t)$  is the Heaviside function, the longitudinal force in the bar is equal to:

$$N(x,t) = \frac{4P_0}{\pi} \sum_{n=1}^{\infty} \frac{(-1)^{n-1}}{2n-1} \cos\left(\frac{2n-1}{2} \frac{\pi x}{l}\right) \left[1 - \cos\frac{(2n-1)\pi at}{2l}\right] \quad (5)$$

Expression (5) can also be obtained by taking the derivative of series (4), showing that differentiating the series term by term is justified in this case. Series (5), being expressed in terms of the vibration modes of a fixed-free bar, is equal to zero for  $x = l$ . The boundary condition is satisfied in the limit as  $x$  tends to  $l$ , and there is a discontinuity at  $x = l$ .

### III. The use of Green functions

It is known from potential theory, heat conduction and the analysis of the wave equation, that the Green function of a homogenous problem can be used to calculate the response to the prescribed boundary conditions. In the present case, when a force is applied to the right end of the bar, use is made of the time-dependent Green function of a bar with the left end fixed and the right end free, the explicit expression of which is given by the series:

$$G(x, \xi, t) = \frac{4a}{\pi EA} \sum_{n=1}^{\infty} \frac{\sin\left(\frac{2n-1}{2} \frac{\pi x}{l}\right) \sin\left(\frac{2n-1}{2} \frac{\pi \xi}{l}\right)}{2n-1} \sin(\omega_n t), \quad \omega_n = \frac{(2n-1)\pi a}{2l} \quad (6)$$

Making use of this Green function, the solution of the non-homogenous problem can be calculated using the formula:

$$u(x, t) = EA \int_0^t \frac{\partial u(x, \tau)}{\partial x} \Big|_{x=l} G(x, l, t - \tau) d\tau = \int_0^t P(\tau) G(x, l, t - \tau) d\tau \quad (7)$$

This solution coincides with (4).

### IV. The use of generalized functions (distributions)

It is possible to treat the force acting on the right end of the bar as a distributed force, expressed by the Dirac delta-function. If one then calculates the Fourier solution of the forced vibration problem, expanding the solution by the mode shapes of a fixed-free rod, result (4) is obtained once again. A more rigorous and more general method making use of the theory of distributions will be presented during the Symposium, which can handle a wide range of problems, including one-dimensional problems with prescribed force or displacement excitation, equations with several independent variables, as well as problems described by a set of differential equations with non-homogenous boundary conditions.

It will be shown that in the direct vicinity of the right end the force in the bar obtained by the first solution method has a better behaviour than that obtained by the remaining methods, which effects the number of terms needed to obtain accurate results in this region. On the other hand, only solutions II, III and IV are applicable to the approach that will be used to calculate the optimal control force.

### References

- [1] Butkovskiy A.G.: Theory of Optimal Control of Distributed Parameter Systems, American Elsevier, 1969.
- [2] Cupial P.: On time-optimal vibration control of one-dimensional distributed-parameter systems. Machine Dynamics Problems, Vol. 29, No. 2, 5-22, 2005.
- [3] Friedman B.: Principles and Techniques of Applied Mathematics. Dover, 1990.
- [4] Stakgold I.: Green's Functions and Boundary Value Problems. Wiley. 1979.



# Modelling of Planar Dynamics of Inflated Membrane Structures

Anirvan DasGupta

Department of Mechanical Engineering, and Center for Theoretical Studies  
 IIT Kharagpur, 721302, India  
 anirvan.dasgupta@gmail.com

## Summary

Inflatable structures have received considerable attention in the recent past due to their advantages of light weight, quick and self-deployability, and compact storage. Such structures are typically found in terrestrial and space applications [1]. However, the membrane material is usually very thin and has material nonlinearity. Further, large deformations of the membrane make the problem geometrically nonlinear as well. Some initial references on the large deformation analysis are available in [2, 3, 4]. In this work, however, we focus our attention on a simple axisymmetric inflated beam. We aim at obtaining a one-dimensional theory for such inflated structures, and studying the modes of vibrations about an equilibrium configuration.

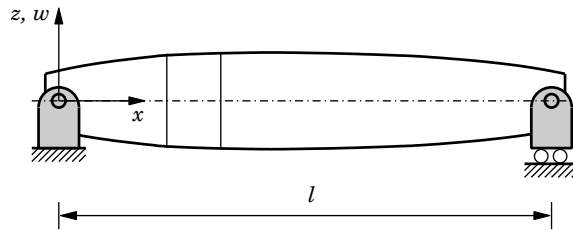


Figure 1: Schematic diagram of an inflated axisymmetric beam

We consider an axisymmetric inflated beam, as shown in Fig. 1. The beam is assumed to be inflated starting from an initial tube of uniform radius. The ends of the beam are assumed to be closed by light discs that maintain a constant end-radius, and are simply-supported. We assume that the structure executes oscillatory motion about its equilibrium straight configuration. The existence of a neutral plane, and negligible damping and pressure variations are assumed. The structural time period is assumed to be much larger than the acoustic time period. The membrane material is considered to be a homogeneous and isotropic hyperelastic solid.

Consider the deflection of a small element of the beam, as shown in Fig. 2. The surface of the beam is parametrized by  $(\theta, z)$ , where  $\theta$  is the angular coordinate, and  $z$  is the axial coordinate. Upon deflection, the cross-section may not remain orthogonal to the neutral fiber, whose deflection is represented by the field variable  $w(z, t)$ . This implies that the element will undergo both flexure and shear. To model this simply, we introduce an unknown complementary shearing factor  $\alpha$  in the kinematics of rotation of the cross-section. Further, the cross-section of the beam will also deform and ovalize, which is captured by introducing two more field variables  $u(z, t)$  and  $v(z, t)$ . We combine all these effects in our kinematics of deformation of the beam element as follows. The parametrization of beam surface in the undeflected configuration may be written as

$$x^1 = a(z) \cos \theta, \quad x^2 = a(z) \sin \theta, \quad x^3 = z \quad (1)$$

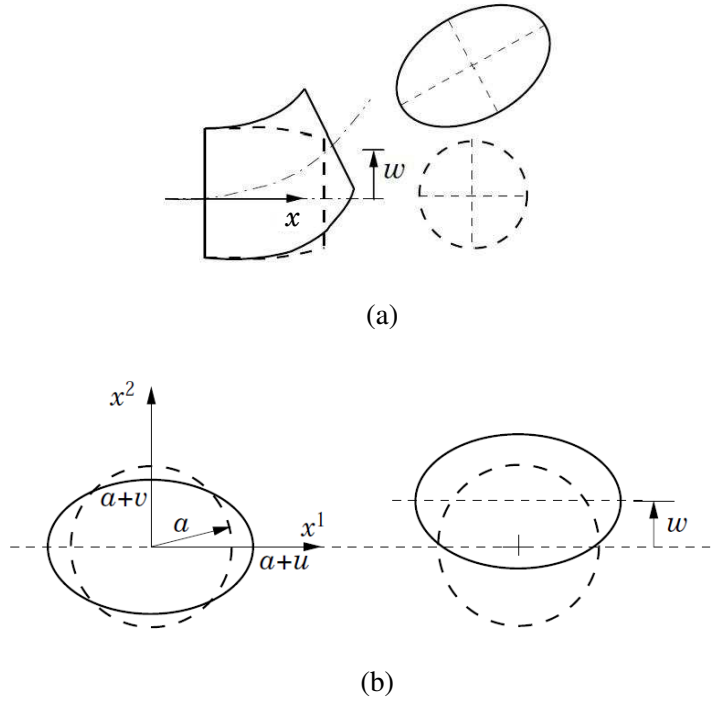


Figure 2: Deformation of (a) a beam element, and (b) a beam cross-section

where  $a(z)$  is the radius of the beam. In the deflected configuration, the parametrization is expressed as

$$\tilde{x}^1 = [a + u] \cos \theta, \quad \tilde{x}^2 = w + [a + v] \sin \theta, \quad \tilde{x}^3 = z - \alpha[a + v] \sin \theta \quad w_{,z} \quad (2)$$

where  $w_{,z} = \partial w / \partial z$ .

Using these parametrizations, one can now determine the induced metric tensors  $g_{ij}$  and  $\tilde{g}_{ij}$  in the undeflected and deflected configurations, respectively. The material strain energy function of an incompressible hyperelastic membrane can then be written as

$$V_m = \int_0^l \int_0^{2\pi} [C_1(I_1 - 3) + C_2(I_2 - 3)] h \sqrt{g} d\theta dz \quad (3)$$

where  $C_1$  and  $C_2$  are material constants,  $I_1 = g^{ij} \tilde{g}_{ij} + \lambda_3^2$ ,  $I_2 = \tilde{g}^{ij} g_{ij} + 1/\lambda_3^2$  (summation convention used),  $h$  is the thickness of the membrane in the undeformed state, and  $\lambda_3^2 = g/\tilde{g}$  (obtained from the incompressibility condition). The potential energy of the gas is given by  $V_p = \int_{\Omega} p d\Omega$ , where  $p$  is the gauge pressure of the gas, and  $d\Omega$  is the volume element. We convert this volume integral into an area integral using the Gauss divergence theorem, and write the total potential energy function as  $V = V_m - V_p$ . The kinetic energy of the beam is written as

$$T = \frac{1}{2} \int_0^l \int_0^{2\pi} \rho [(\dot{\tilde{x}}^1)^2 + (\dot{\tilde{x}}^2)^2 + (\dot{\tilde{x}}^3)^2] h \sqrt{g} d\theta dr \quad (4)$$

where  $\rho$  is the density of the membrane material. Finally, we form the Lagrangian of the structure as  $\mathcal{L} = T - V$ , and write the action as  $S = \int_{t_1}^{t_2} \mathcal{L} dt$ . Using the Hamilton's principle, one can derive the partial differential equations of motion of the beam. However, we use the Ritz method to discretize the equations of motion, and perform the discrete modal analysis.

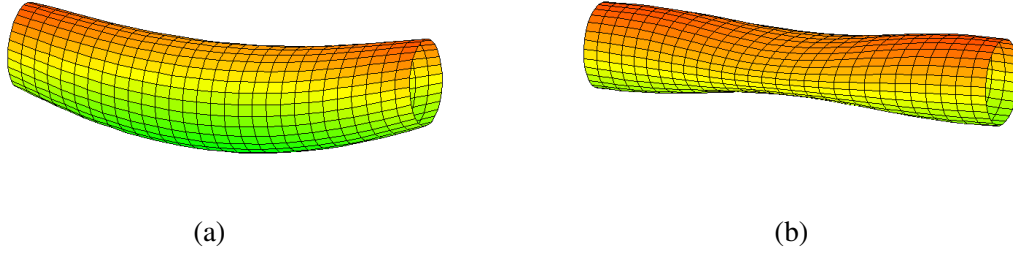


Figure 3: (a) Sinusoidal, and (b) varicose modes of vibration of an inflated beam

We consider a simply-supported beam of length  $l$  with the following geometric boundary conditions  $u(0,t) = u(l,t) = 0$ ,  $v(0,t) = v(l,t) = 0$ , and  $w(0,t) = w(l,t) = 0$ . The horizontal diameters of the two end-discs are assumed to be fixed. The Ritz expansion is assumed to be of the form

$$u(z,t) = \sum_{n=1}^N a_n(t) \sin \frac{n\pi z}{l}, \quad v(z,t) = \sum_{n=1}^N b_n(t) \sin \frac{n\pi z}{l}, \quad w(z,t) = \sum_{n=1}^N c_n(t) \sin \frac{n\pi z}{l}$$

where  $a_n(t)$ ,  $b_n(t)$  and  $c_n(t)$  are the modal coordinates. Substituting these expansions in the action and using the Hamilton's principle yields

$$\begin{aligned} \delta \int_{t_1}^{t_2} \mathcal{L}(\mathbf{a}, \mathbf{b}, \mathbf{c}, \dot{\mathbf{a}}, \dot{\mathbf{b}}, \dot{\mathbf{c}}, p, \alpha) dt &= 0 \\ \Rightarrow \mathbf{M}(\alpha) \ddot{\mathbf{Y}} + \mathbf{K}(p, \alpha) \mathbf{Y} &= \mathbf{0} \end{aligned} \quad (5)$$

where  $\mathbf{Y} = [\mathbf{a}^T, \mathbf{b}^T, \mathbf{c}^T]^T$  is the vector of the modal coordinates, and  $\mathbf{M}$  and  $\mathbf{K}$  are, respectively, the modal mass and stiffness matrices.

We perform the discrete modal analysis of (6) for a specific pressure  $p$ . At this stage, the complementary shearing factor  $\alpha$  is determined by minimizing the eigenfrequencies. The results obtained for a simply supported inflated beam indicate two kinds of modes, namely the sinusoidal mode and the varicose mode, as shown in Fig. 3. In a similar manner, by appropriate choice of shape functions, one can also study other boundary conditions.

**Acknowledgement:** This work was initiated when the author was visiting Professor Peter Hagedorn at Darmstadt with a Research Fellowship from the Alexander von Humboldt Foundation.

## References

- [1] Jenkins, C.H.M. (Ed.): Gossamer Spacecraft: Membrane and Inflatable Structures Technology for Space Applications. Vol. 191, AIAA, Reston, Virginia, 2001.
- [2] Green, A.E.; Adkins, J.E.: Large Elastic Deformation. Oxford University Press, London, 1970.
- [3] Ogden, R.W.: Non-linear Elastic Deformations. Ellis-Horwood, Chichester, 1984.
- [4] Green, A.E.; Zerna, W.: Theoretical Elasticity. Dover, New York, 1992.



## Application of Machine Learning Methods to Structural Similitudes

Alessandro Casaburo, Giuseppe Petrone, Francesco Franco, Sergio De Rosa

Pasta-Lab

Department of Industrial Engineering - Aerospace Section

Università degli Studi di Napoli Federico II

Via Claudio 21, 80125, Napoli, Italy

[alessandro.casaburo, giuseppe.petrone, francesco.franco, sergio.derosa]@unina.it

### Summary

Machine learning methods allow to find patterns and regularities in data: the available data is conveyed in a *training set*, used by an *algorithm* which modulates the adjustable parameters of a model; these are supposed to rule the system behavior. Such modulation is called *learning* and it provides to a computational device the capability of improving its performance on the task without being explicitly programmed. A trained algorithm should be able to *generalize*, i.e. to provide a correct output when interrogated with an input that does not belong to the training set. An algorithm unable to generalize is said to overfit.

An example of machine learning application in vibroacoustic field is given by Sharp et al. [1]; they classify unknown railway vibration signals to derive exposure-human response relationships. Recently, Wang et al. [2] have combined Finite Element Method (FEM) and Artificial Neural Networks (ANN) to predict the behavior of human auditory system. These works show how the choice of the right characteristic to train with a machine learning algorithm strongly affects the results, because each case study depends on its own set of features. Data selection (range, quality etc.) and feature choice are fundamental steps when using machine learning.

Therefore, pattern recognition techniques show to be very helpful. Learning from data, they are able to exploit the information in order to perform predictions in an automatic way. Such prediction capabilities may help to maximize the amount of information obtainable from any kind of test minimizing, at the same time, the number of simulations. This is helpful especially when testing experimentally systems in similitude. In fact, it is unfeasible to produce a full set of structures, from a financial and a temporal point of view; furthermore, it is useless to produce test articles too large or too small because they could be not easily analyzed during an experimental phase.

Nonetheless, the predictions of analytical and numerical tests must be necessarily validated, thus experimental tests are fundamental when designing a new product. Unfortunately, experiments are money and time consuming; in addition, some experimental uncertainties can lead to repeated test-sessions. For these reasons, it is useful to test a scaled (up or down) version (called *model*) of the full-scale structure (called *prototype*) to overcome many of the cited problems. However, the model exhibits a response different from the prototype, thus it is needed a tool that would allow to design the model and, by testing it, to reconstruct the response of the prototype. Similitude theory provides such tools, the similitude methods, which provide the *similitude conditions* that, if satisfied, allow to derive a set of univocal scaling laws linking the system response to the input parameters (geometrical, material, excitation etc.). When this happens, a *replica* is obtained and the prototype response is perfectly predicted. If, at least, one of the conditions is no more satisfied, then an *avatar* is obtained: avatars lack of univocal scaling laws and the prototype behavior is hard to be reconstructed with acceptable errors.

Literature provides many similitude methods. The most important is the dimensional analysis, based on the definition of dimensionless groups by means of Buckingham's  $\Pi$  Theorem, and it has been used for the first time in structural engineering by Wissmann [3]. Simitzes and Rezaeepazhand [4] use Similitude Theory Applied to Governing Equations (STAGE), a method which introduces the scale factors directly into the governing equations of the system, to analyse laminated plates under different loading conditions. De Rosa and Franco [5] investigate the possibility to reduce the computational costs by means of similitude with Asymptotical Scaled Modal Analysis (ASMA), that reduces the extension of the parameters not involved into energy transfer. Successively, they propose a new method, Similitude and Asymptotic Models for Structural-Acoustic Research Applications (SAMSARA), based on the generalization of modal approach which allows to involve the modal parameters into the scaling process [6]. However, other relevant methods exist and a comprehensive review is provided by Casaburo et al. [7].

In this work, machine learning is applied, for the first time, to similitude theory in order to investigate its prediction capabilities in determining the natural frequencies and the scaling characteristics of a structure. Particular attention is given to avatars, that are the most interesting models because, for many reasons (for example boundary conditions, common uncertainties), they are more probable than the proportional-side ones. Furthermore, they may rise during manufacturing processes because of errors or limits of the process itself. Therefore, avatar understanding is fundamental but the lack of univocal scaling laws limit the control on their responses. To overcome such problem, the generalization capabilities of ANNs have been investigated. ANNs, loosely inspired to human brain, are machine learning methods useful to reproduce nonlinear functions; their architecture is characterized by computational units, called *neurons*, organized in layers: the output of one layer is the input to the successive one.

To test these capabilities, a simply supported aluminium plate, having length, width and thickness equal to  $a = 2$  m,  $b = 1$  m,  $t = 0.002$  m, and its models have been considered. According to SAMSARA, the similitude condition is  $r_a = r_b$  (from here, the model is also called *proportional sides*), that leads to the univocal scaling law

$$r_f = \frac{r_t}{r_a^2} = \frac{r_t}{r_b^2} \quad (1)$$

When the condition is not fulfilled ( $r_a \neq r_b$ ), the relation between input and output parameters is no more univocal and neither of the scaling laws derived is able to reconstruct the prototype response in all the frequency range with an acceptable accuracy.

Results have been carried out using the first five natural frequencies as inputs and the scale factors of length and width as outputs. To characterize the neural network (number of training examples, number of layers and neurons), a trade-off among an acceptable error, overfitting avoidance and computational time has been performed by means of a trial-and-error approach. Levenberg-Marquardt algorithm is used for training and it is coupled with Bayesian regularization to have a better control on overfitting [8]. The network used has four hidden layers (5–10–15–5 neurons) and is trained on 3662 examples. They are randomly sampled from a set made of models having length and width scale factors ranging from 0.5 to 4, with steps of 0.05. After the training, the network performance is tested on 8 models: 2 proportional sides (PS) and 6 avatars (A). It has to be remarked that for the proportional sides the models exactly reproduce the prototype. Fig. 1 shows the ANN performance by comparing the analytical scale factors (x-axis) with the predicted ones (y-axis) of the above-mentioned 8 test models. The bisector (blue line) represents the locus of points along which the analytical and predicted results are equal.

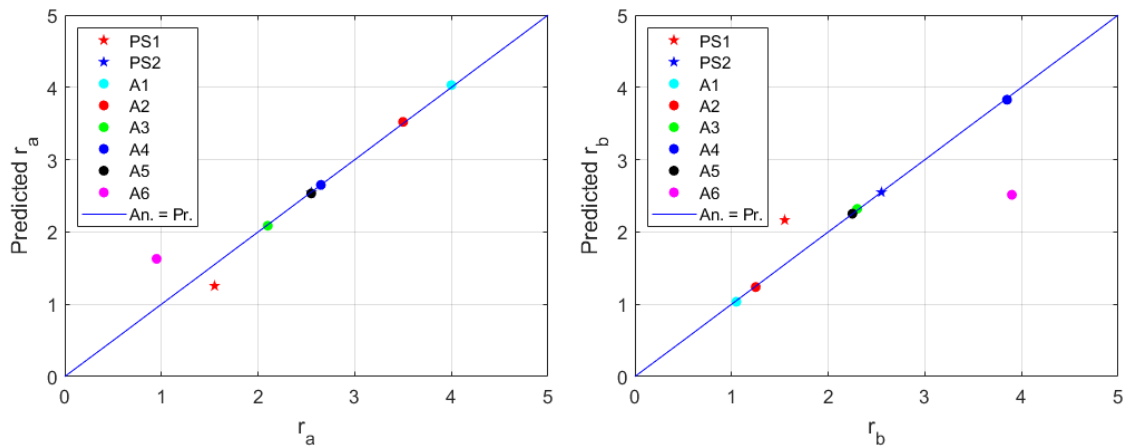


Figure 1: predicted VS analytical scaling factors: (left) length, (right) width.

The ANN performance is, generally, good. In fact, the predictions of many test models lie on the bisector, which is an index of good generalization. Two models lie far from the bisector: PS1 and A6, showing that in both cases it is still possible to have poor correlation between analytical and predicted results. Such discrepancies are measured by the mean square error (MSE), that in this case is approximately 0.23, coherent with the results. These outcomes demonstrate the usefulness of machine learning methods and motivate the efforts to identify more suitable techniques that would allow to obtain better results and, at the same time, to gain a greater control over the method.

## References

- [1] Sharp, C.; Woodcock, J.; Peris, E.; Sica, G.; Moorhouse, A.; Waddington, D.: Analysis of railway vibration signals using supervised machine learning for the development of exposure-response relationships, *Proceedings of Meetings on Acoustics*, vol. 13, 2013.
- [2] Wang, Y. S.; Guo, H.; Feng, T. P.; Ju, J.; Wang, X. L.: Acoustic behavior prediction for low-frequency sound quality based on finite element method and artificial neural network, *Applied Acoustics*, vol. 122, pp. 62 – 71, 2017.
- [3] Wissmann, J. W.: Dynamic stability of space vehicles-Structural dynamics model testing, National Aeronautics and Space Administration, NASA CR-1195, 1968.
- [4] Simites, G. J.; Rezaeepazhand, J.: Structural similitude for laminated structures, *Composite Engineering*, vol. 3, no. 7–8, pp. 751–765, 1993.
- [5] De Rosa, S.; Franco, F.: A scaling procedure for the response of an isolated system with high modal overlap factor, *Mechanical System and Signal Processing* vol. 22, pp. 1549–1565, 2008.
- [6] De Rosa, S.; Franco, F.; Li, X.; Polito, T.: A similitude for structural acoustic enclosures, *Mechanical System and Signal Processing* vol.30, pp. 330–342, 2012.
- [7] Casaburo, A.; Petrone, G.; Franco, F.; De Rosa, S.: A Review of Similitude Methods for Structural Engineering, *Applied Mechanics Reviews*, submitted in 2018, in review.
- [8] MacKay, D. J. C.: Bayesian interpolation, *Neural Computation*, vol. 4, no. 3, pp. 415–447, 1992.



## Structural and acoustic response of sandwich plates by means of sublaminar models with variable kinematics

Lorenzo Dozio<sup>\*</sup>, Riccardo Vescovini<sup>\*</sup>, Michele D'Ottavio<sup>†</sup>

<sup>\*</sup> Department of Aerospace Science and Technology  
Politecnico di Milano  
via La Masa, 34, 20156 Milano, Italy  
[lorenzo.dozio, riccardo.vescovini]@polimi.it

<sup>†</sup> LEME, UPL  
Université Paris Nanterre  
50 rue de Sèvres, 92410 Ville d'Avray, France  
michele.d\_ottavio@parisnanterre.fr

### Summary

**Introduction.** Due to their high strength to weight ratio, sandwich panels are adopted as structural members in several engineering applications, such as space launchers and ship hulls. They can be considered a particular case of composite structures, featuring a fundamental pattern of two stiff and thin outer sheets, the skins, enclosing a relatively thick and compliant layer, the core. As opposed to the case of thin-walled panels, a complicating effect of sandwich panels is due to the strong mismatch of geometric and constitutive properties along the thickness, which induces sharp gradients across the thickness direction. For this reason, specific *ad-hoc* structural models are typically required to obtain accurate and reliable predictions of their dynamic behavior. The evaluation of the acoustic performance of sandwich panels can be also crucial in some applications. Indeed, interior noise quality and speech intelligibility has become increasingly important in modern light and fast transportation vehicles, where novel arrangements are designed through the adoption of sandwich configurations to achieve high structural efficiency. In particular, various solutions have been studying in the aerospace industry with the aim of improving the cabin acoustic comfort, especially for VIP aircrafts and helicopters. A common way to reduce the noise radiated by a vibrating fuselage panel is to add viscoelastic materials. The most efficient solution is the so-called constrained-layer damping treatment, where a viscoelastic layer is inserted between the vibrating structure and a constraining rigid layer, thus leading to a sandwich configuration. Another effective approach for noise reduction is to adopt inner fuselage panels, called trim panels, specifically designed for optimizing the acoustic absorption or the transmission loss (TL). Trim panels have typically a classical sandwich multilayer structure with stiff facesheets and a thick low-density core.

**Motivation.** In both previous approaches, the material and thickness of core and skins of the sandwich panel, the number of layers of external sheets, the topology of the core and the total and relative thickness are, among others, important design parameters affecting the acoustic performances of the structural component. The acoustic design can be further complicated by the adoption of less-conventional and innovative configurations involving multiple cores. Since an extensive experimental campaign is lengthy and costly, suitable numerical simulations can be carried out to guide the design process, i.e., to evaluate the effect of the main parameters and to study the nature and arrangement of layers. However, accurate 2-D modeling of multilayered sandwich panels for vibration and acoustic analysis is challenging, mostly due to their highly heterogeneous

anisotropic constitution in the thickness direction and the wide frequency range of interest. In particular, it can be difficult to identify sufficiently simple yet reliable theoretical models without unnecessary complexity.

**Mathematical formulation.** In this work, a powerful and effective numerical tool for the acoustic analysis of composite panels of finite extent having classical and complex advanced sandwich configurations is presented [1]. Main feature of the proposed formulation is the versatile kinematic representation of the displacement field along the thickness direction, consisting in the representation of the plate by means of sublaminates, i.e. arbitrary groups of adjacent plies composing the panel. Each sublaminate is associated with an independent and arbitrary kinematic description, either equivalent single-layer or layerwise, so that the use of refined high-order theories can be tailored to specific thickness subregions. Accordingly, each component of the 3-D displacement field in the generic ply  $p$  of the sublaminate  $k$  is postulated in a layerwise (LW) manner as follows:

$$u_{\circ}(x, y, z_p, t) = F_{\alpha_{u_{\circ}}}(z_p) u_{\circ \alpha_{u_{\circ}}}^{p,k}(x, y, t) \quad \alpha_{u_{\circ}} = 0, \dots, N_{u_{\circ}}^k \quad (\circ = x, y, z) \quad (1)$$

where  $z_p$  is the local ply-specific thickness coordinate,  $F_{\alpha_{u_{\circ}}}(z_p)$  are thickness functions,  $u_{\circ \alpha_{u_{\circ}}}^{p,k}$  is the kinematic coordinate of the adopted 2-D approximation,  $N_{u_{\circ}}^k$  is the order of expansion taken as a free parameter, and the summation is implied for repeated theory's indexes  $\alpha_{u_{\circ}}$ . It is noted that equivalent single-layer (ESL) sublaminate model can be recovered by setting  $z_p$  equal to the sublaminate-specific thickness coordinate  $z_k$ . The thickness functions are taken as a proper combination of Legendre polynomials so that the continuity between adjacent plies or sublaminates is easily imposed. The equilibrium equations are derived through the Principle of Virtual Displacements (PVD). Once a specific plate theory is postulated through Eq. (1), the corresponding displacement approximation is substituted into the PVD equation so that the original 3-D problem is transformed into a 2-D problem in the  $x - y$  plane. The resulting variational form contains 2-D generalized kinematic coordinates, which are further expressed through a Ritz expansion as follows:

$$u_{\circ \alpha_{u_{\circ}}}^{p,k}(x, y, t) = N_{u_{\circ}i}(x, y) u_{\circ \alpha_{u_{\circ}i}}^{p,k}(t) \quad i = 1, \dots, M \quad (\circ = x, y, z) \quad (2)$$

where  $N_{u_{\circ}i}(x, y)$  form a complete set of admissible functions, which are taken as the product of Legendre polynomials and proper boundary functions after defining the problem in the computational domain  $(\xi, \eta)$ , with  $\xi, \eta \in [-1, 1]$ . After substituting Eq. (1) and Eq. (2) into the PVD, the discretized weak form of the dynamic equilibrium equations can be expressed in compact form by means of self-repeating building blocks, denoted as fundamental kernels of the formulation, which are invariant with respect to the number of sublaminates, the typology of the local kinematic description (ESL or LW) and the orders of expansion of each local displacement quantity. Accordingly, the proposed approach allows for the hierarchical generation of plate models with different 2-D kinematic descriptions from the same unified mathematical framework. The expansion and assembly procedure involves four main steps. The first step deals with the expansion of the kernels according to the summation related to the order of the kinematic description postulated in each sublaminate. The second step is the assembly of the ply-contributions in each sublaminate involving a cycling over the index  $p$ . All sublaminate contributions are subsequently stacked along the thickness coordinate to account for the continuity of the generic displacement variable at the interfaces between adjacent layers. The sublaminate contributions of different layers are always assembled in a LW manner. The assembly of the sublaminates contributions involves the cycling over the index  $k$ . The final step deals with expansion corresponding to the summation related to the Ritz series approximation of the kinematic quantities. Once the final set of equations governing the structural problem is obtained, the acoustic performance of the panel can be evaluated. In particular TL simulations are performed by assuming the plate in an infinite rigid baffle with a negligible air loading and imposing a diffuse field on one side of the panel through a set of incident

plane waves of same amplitude and different incidence angle  $(\theta, \phi)$ . The incident pressure field on the top side of the panel can be expressed as  $p = 2e^{-jk \sin \theta (x \cos \phi + y \sin \phi)}$  where  $k = \omega/c_0$  is the wavenumber. For each incident wave, the incidence transmission coefficient is computed as

$$\tau(\omega, \theta, \phi) = \frac{2\rho_0 c_0 P(\omega, \theta, \phi)}{S \cos \theta} \quad (3)$$

where  $S$  is the panel area and the radiated sound power is evaluated in terms of elementary radiators [2]. Finally, the diffuse transmission loss is computed as  $TL(\omega) = -10 \log(\tau_d(\omega))$ , where  $\tau_d$  is the diffuse transmission coefficient derived by integrating the response of all incident plane waves over the incident angle and weighting them with the solid angle to account for the directional distribution.

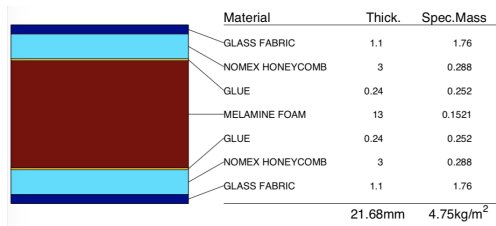


Figure 1: Stacking sequence of a sandwich acoustic trim panel.

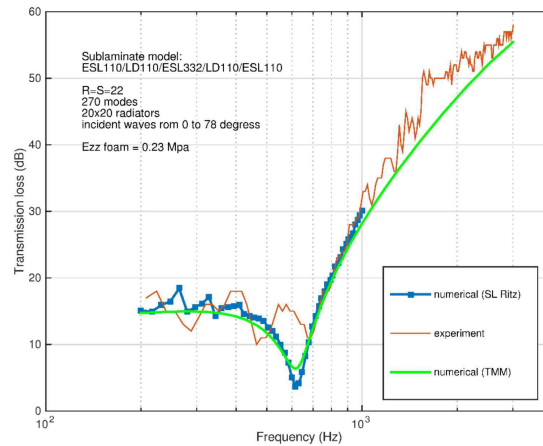


Figure 2: Diffuse transmission loss: comparison between numerical predictions and experimental data.

**Illustrative example.** Some vibration and TL results on different sandwich plates will be presented and discussed at the Symposium, including also comparison with experimental data, to show the effectiveness of the proposed approach. An illustrative example is here reported in Figure 1, which shows the stacking sequence of an acoustic trim panel of size  $0.90 \times 0.90 \text{ m}^2$ , thickness 21.7 mm, with clamped boundary conditions and composed of melamine foam placed between Nomex honeycombs and external fiberglass layers. The simulation of the TL and the experimental measurements are compared in Fig. 2. The numerical model is built by properly subdividing the plate into five sublaminates having first-order kinematics in the outer stiffer thickness regions and a higher-order normal and shear deformation theory in the internal soft layer. The high TL is assured thanks to a dilatation effect of the foam from medium frequencies and the static bending stiffness of the honeycombs. The peculiar behavior of a double wall resonance around 600-700 Hz is observed and well predicted by the simulation using a model suitably tuned to give an optimal balance between accuracy and computational cost.

## References

- [1] D'Ottavio, M.; Dozio, L.; Vescovini, R.; Polit, O.: Bending analysis of composite laminated and sandwich structures using sublaminates variable-kinematic Ritz models. *Composite Structures*, Vol. 155, pp. 45–62, 2016.
- [2] Fahy, F.J.; Gardonio, P.: *Sound and Structural Vibration*. Elsevier, 2007.



## New Analytical Solutions for Vibrations of Shallow Shells

Moshe Eisenberger<sup>\*</sup>, Luis A. Godoy<sup>#</sup>,

<sup>\*</sup> Faculty of Civil and Environmental  
 Engineering  
 Technion – Israel Inst. of Technology  
 Technion City, Haifa, Israel  
[cvmosh@technion.ac.il](mailto:cvmosh@technion.ac.il)

<sup>#</sup> Instituto de Estudios Avanzados en  
 Ingeniería y Tecnología  
 , IDIT CONICET/Universidad  
 Nacional de Córdoba, Córdoba,  
 Argentina  
[luis.godoy@unc.edu.ar](mailto:luis.godoy@unc.edu.ar)

### Summary

Three new analytical solutions for vibrations of shallow shells with two principal constant curvatures are presented in this work. The new solutions address different cases of in-plane and out-of-plane boundary conditions, and provide an interesting insight into the dynamics of such shells. The formulation is here applied to cylindrical, spherical, elliptical paraboloidal, and hyperbolic paraboloidal shallow shells, as illustrated in Figure 1. Previous works in this field have not addressed the present boundary conditions in analytical form.

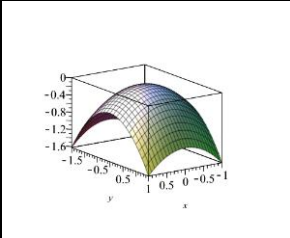
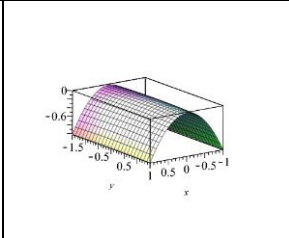
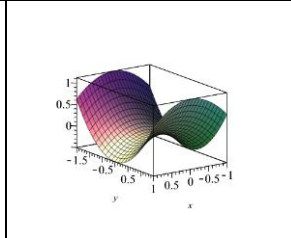
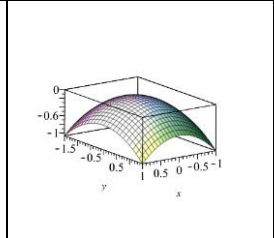
<i>Spherical</i>	<i>Cylindrical</i>	<i>Hyperbolic</i>	<i>Paraboloidal</i>
$R_x = R_y = 100$	$R_x = 100; R_y = 10000$	$R_x = 100; R_y = -150$	$R_x = 100; R_y = 200$
			

Figure 1: Sample shallow shells with two principle constant curvatures

The linearized equations of motion for the harmonic linear vibrations of shallow shells are three coupled differential equations with three unknowns,  $u(x,y)$ ,  $v(x,y)$ , and  $w(x,y)$ , and are given as [1,2]

$$\frac{\partial^2 u}{\partial x^2} + \frac{(1-\nu)}{2} \frac{\partial^2 u}{\partial y^2} + \frac{(1+\nu)}{2} \frac{\partial^2 v}{\partial x \partial y} - \left( \frac{1}{R_x} + \frac{\nu}{R_y} \right) \frac{\partial w}{\partial x} = - \frac{\rho(1-\nu^2)}{E} \frac{\partial^2 u}{\partial t^2} \quad (1)$$

$$\frac{(1+\nu)}{2} \frac{\partial^2 u}{\partial x \partial y} + \frac{\partial^2 v}{\partial y^2} + \frac{(1-\nu)}{2} \frac{\partial^2 v}{\partial x^2} - \left( \frac{\nu}{R_x} + \frac{1}{R_y} \right) \frac{\partial w}{\partial y} = - \frac{\rho(1-\nu^2)}{E} \frac{\partial^2 v}{\partial t^2} \quad (2)$$

$$\left( \frac{1}{R_x} + \frac{\nu}{R_y} \right) \frac{\partial u}{\partial x} + \left( \frac{\nu}{R_x} + \frac{1}{R_y} \right) \frac{\partial v}{\partial y} - \left( \frac{1}{R_x^2} + \frac{2\nu}{R_x R_y} + \frac{1}{R_y^2} \right) w - \frac{h^2}{12} \nabla^4 w = - \frac{\rho(1-\nu^2)}{E} \frac{\partial^2 w}{\partial t^2} \quad (3)$$

where the origin of the coordinate system is placed at the apex in each case. These equations are solved analytically for four cases of boundary conditions as given below and illustrated in Figure 2.

$$\text{Case 1} \quad \left\{ \begin{array}{l} v(\pm a/2, y) = w(\pm a/2, y) = w_{,xx}(\pm a/2, y) = 0, \\ u(\pm b/2, x) = w(\pm b/2, x) = w_{,yy}(\pm b/2, x) = 0, \end{array} \right. \quad (4)$$

$$\text{Case 2} \quad \left\{ \begin{array}{l} v(\pm a/2, y) = w(\pm a/2, y) = w_{,xx}(\pm a/2, y) = 0, \\ v(\pm b/2, x) = w_{,y}(\pm b/2, x) = w_{,yyy}(\pm b/2, x) = 0, \end{array} \right. \quad (5)$$

$$\text{Case 3} \quad \left\{ \begin{array}{l} u(\pm a/2, y) = w_{,x}(\pm a/2, y) = w_{,xxx}(\pm a/2, y) = 0, \\ v(\pm b/2, x) = w_{,y}(\pm b/2, x) = w_{,yyy}(\pm b/2, x) = 0, \end{array} \right. \quad (6)$$

$$\text{Case 4} \quad \left\{ \begin{array}{l} u(\pm a/2, y) = w_{,x}(\pm a/2, y) = w_{,xxx}(\pm a/2, y) = 0, \\ u(\pm b/2, x) = w(\pm b/2, x) = w_{,yy}(\pm b/2, x) = 0, \end{array} \right. \quad (7)$$

	Case 1	Case 2	Case 3	Case 4
In-Plane				
Out-of-Plane	SS  SS	G  G	G  G	SS  SS

The analytical solutions that satisfy exactly the differential equations and all the boundary conditions for the four cases are given in Table 1 below.

Table 1: Analytical solutions for the four cases investigated

	Case 1	Case 2	Case 3	Case 4
u	$\sin\left(\frac{\pi \eta x}{2}\right) \cos\left(\frac{\pi \mu y}{2}\right)$	$\sin\left(\frac{\pi \eta x}{2}\right) \sin\left(\frac{\pi \mu y}{2}\right)$	$\cos\left(\frac{\pi \eta x}{2}\right) \sin\left(\frac{\pi \mu y}{2}\right)$	$\cos\left(\frac{\pi \eta x}{2}\right) \cos\left(\frac{\pi \mu y}{2}\right)$
v	$\cos\left(\frac{\pi \eta x}{2}\right) \sin\left(\frac{\pi \mu y}{2}\right)$	$\cos\left(\frac{\pi \eta x}{2}\right) \cos\left(\frac{\pi \mu y}{2}\right)$	$\sin\left(\frac{\pi \eta x}{2}\right) \cos\left(\frac{\pi \mu y}{2}\right)$	$\sin\left(\frac{\pi \eta x}{2}\right) \sin\left(\frac{\pi \mu y}{2}\right)$
w	$\cos\left(\frac{\pi \eta x}{2}\right) \cos\left(\frac{\pi \mu y}{2}\right)$	$\cos\left(\frac{\pi \eta x}{2}\right) \sin\left(\frac{\pi \mu y}{2}\right)$	$\sin\left(\frac{\pi \eta x}{2}\right) \sin\left(\frac{\pi \mu y}{2}\right)$	$\sin\left(\frac{\pi \eta x}{2}\right) \cos\left(\frac{\pi \mu y}{2}\right)$

where  $\eta = n/a$ , and  $\mu = m/b$ , with  $m$  and  $n$  odd numbers, and  $a$  and  $b$  are the dimensions in the  $x$  and  $y$  directions, respectively. Substitution of the solution into Eqs. (1-3) results in three equations with three unknowns for each value of  $m$  and  $n$ , leading to

$$\begin{bmatrix} A_{11} & A_{12} & A_{13} \\ A_{21} & A_{22} & A_{23} \\ A_{31} & A_{32} & A_{33} \end{bmatrix} \begin{Bmatrix} u \\ v \\ w \end{Bmatrix} = \rho h (\omega^{mn})^2 \begin{Bmatrix} u \\ v \\ w \end{Bmatrix} \quad (8)$$

The explicit expression for the entries of matrix  $A$  can be found in Ref. [1], and they are the same for all four cases of boundary conditions. Thus, for the four cases investigated, one gets the surprising result that the frequencies are the same but the associated mode shapes are very different, as can be seen in Figure 3 where the first four modes are plotted.

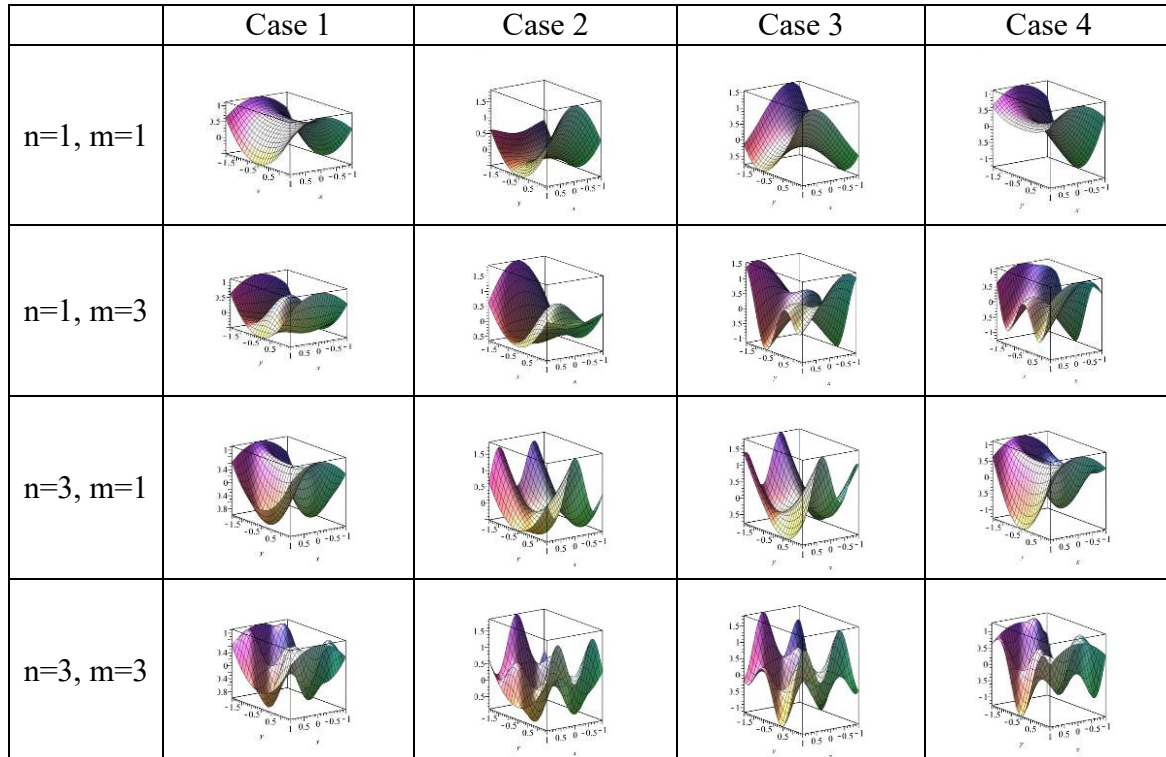


Figure 3: Four mode shapes for the four combinations of boundary condition investigated, for an hyperboloidal shallow shell ( $a = 1$ ,  $b = 1.5$ ,  $R_x = 100$ ,  $R_y = -150$ ,  $\nu = 0.3$ )

For the shallow shells, the present results indicate that the specific changes in boundary conditions investigated have a consequence on the modes of vibration but do not affect the natural frequencies of the shell.

#### References

- [1] Leissa, A.W. and Kadi, A.S.; Curvature effects on shallow shell Vibrations, JSV, Vol. 16, pp. 173-187, 1971.
- [2] Godoy, L.A. and de Souza, V.C.M.; Vibrations of shallow shells due to removal of formwork, JSV, Vol. 215, pp. 425-437, 1998.



# Total Lagrangian Large Amplitude Beam Vibrations and the Limits of Poisson and von Karman

Paul R. Heyliger\*

\* Department of Civil and Environmental Engineering  
Colorado State University  
Fort Collins, Colorado, USA  
prh@engr.colostate.edu

## Summary

In the linear theory of one-dimensional solids, the vibrational behavior of the cross-section is usually split into deformation patterns associated with axial, torsional, and flexural mode shapes. Each of these behaviors is represented by a single ordinary differential equation in the axial, rotational, and transverse displacement components that are completely uncoupled. The natural frequencies associated with these classes of displacement are well known and depend on the material density, cross-sectional area, moments of inertia, material properties, and length of the section. In all of these cases, the problem has been linearized and it is not possible to determine the unique value of the amplitude of the vibrational motion. Since many if not most structural applications rely on design constraints in which the displacements must remain infinitesimal, this is a reasonable assumption.

The difficulty comes when the amplitude of vibration is no longer small. The earliest and most dramatic example of this was presented by Woinowsky-Krieger in 1950 for the case of the planar hinged-hinged beam. In this case, the axial and transverse displacements are no longer independent and are represented by the two coupled ordinary differential equations

$$\frac{\partial}{\partial x} \left\{ AE \left[ \frac{\partial u}{\partial x} + \frac{1}{2} \left( \frac{\partial w}{\partial x} \right)^2 \right] \right\} + f = \rho \frac{\partial^2 u}{\partial t^2} \quad (1)$$

$$\frac{\partial^2}{\partial x^2} \left( EI \frac{\partial^2 w}{\partial x^2} \right) + \frac{\partial}{\partial x} \left\{ AE \frac{\partial w}{\partial x} \left[ \frac{\partial u}{\partial x} + \frac{1}{2} \left( \frac{\partial w}{\partial x} \right)^2 \right] \right\} + q = \rho \frac{\partial^2 w}{\partial t^2} \quad (2)$$

Here  $A$  is the section area,  $I$  is the second moment of area,  $f$  and  $q$  are distributed axial and transverse forces,  $u$  and  $w$  are the axial and transverse displacements,  $\rho$  is the material density,  $x$  is the independent axial coordinate, and  $t$  is time. Woinowsky-Krieger (1950) found the relationship between the frequencies under large deformations for an Euler-Bernoulli beam to be considerably larger than those of the linear theory. Many other studies have confirmed this behavior. Most of these studies focused on Euler-Bernoulli descriptions of the beam bending. The Timoshenko theory was used by Sarma and Varadan (1985) and a higher-order beam theory was used by Heyliger and Reddy (1988). Recent work by Pagani and Carrera (2018) and Filippi, Pagani, and Carrera (2018) used the Carrera Unified Formulation to condense many of these theories under a single generalized class of approximation.

There are several limitations with many existing one-dimensional beam theory formulations. The first is inclusion of only the dominant nonlinear term  $(\partial w/\partial x)^2$  in the governing equations of motion. This is the so-called von Karman nonlinearity, and for thin beams in particular, this term does in fact dominate the nonlinear behavior and is the primary source of axial-flexural coupling. But as the beam becomes shorter in length, the inclusion of other nonlinear terms have have some impact. Second, most theories used to describe the beam kinematics are necessarily restricted to displacement fields that are of relatively low order in the thickness coordinate of the beam. By far, most studies have used the Euler-Bernoulli model in which the transverse shear strains are equal to zero. But more flexible fields, including the Timoshenko and higher-order displacements, have also been explored and generally show an increase in nonlinear frequency ratio over Euler-Bernoulli models. Finally, there is the additional issue of Poisson effects near fixed supports. Most beam models assume that the Poisson ratio is zero and that only the axial and transverse displacements at the centerline need constraining. But such assumptions have consequences of unknown magnitude.

In the present formulation, the nonlinear aspects of the problem are directly considered by including the nonlinear terms in the Green-Lagrange strain tensor as they appear in the original statement of Hamilton's principle. The dominant nonlinear term for most bending theories is the square of the transverse displacement gradient  $(\partial w/\partial x)$ . In the full planar elasticity formulation, however, there are far more terms that can appear. Related observations have been made by Carrera and co-workers (2018). In this study, a combination of analytic functions along the beam axis is combined with power series in the thickness of the beam.

Several representative results will be given for the dominant modes of deformation for the nonlinear beam. One special case is the purely axial mode of vibration. This is the case where the mode of vibration is not associated with flexure or shear but rather the longitudinal deformation along the axis of the beam. Such modes are purely linear according to the one-dimensional theories since in this case the transverse displacement of the beam centroid is exactly zero. But for the elasticity model, there are nonlinear terms associated with the squares of the displacement gradients along with non-zero transverse normal strains that are usually neglected in one-dimensional theories. This problem, although simple in structure, has seen extremely limited study (Cveticanin 2016, Kovacic 2018).

There is another behavior that influences frequency response, and that is the Poisson effect in the region of bar supports. In one-dimensional models, these effects are neglected. Yet there is a stiffening effect that can occur in such regions, and this changes the nature of the displacement field in the region of, for example, fixed supports. The results are shown in Figure 1, and indicate the physical nature of the difference of including Poisson effects near the beam supports under large deformation.

In this study, direct comparisons are made between results from existing beam theories and those using more comprehensive elasticity-based results. For longer beams and fairly small amplitudes, the results among various formulations are in very good agreement. But it is shown that as the beam becomes thick relative to its length and the amplitude increases, the beam theories underpredict the ratio of linear to nonlinear frequency. Hence more inclusive kinematic models may be required under these conditions to accurately capture the influence of large deformations on the frequency and actual deformed mode shape of the beam.

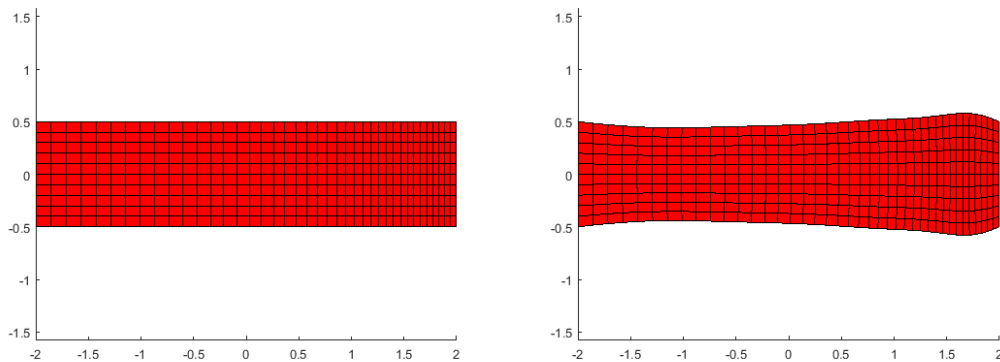


**Figure 1.** The lowest nonlinear axial mode for the fixed-fixed bar of length  $L=4$  with  $a/r=2$ , plotted to scale without (left) and with (right) Poisson effects at the supports. Surprisingly, although the frequencies for the bar on the right are notably higher than those neglecting Poisson ratio, the ratio between linear and nonlinear frequencies are nearly identical.

## References

- [1] L. Cveticanin, Period of vibration of axially vibrating truly nonlinear rod, *J. Sound Vib.*, Vol. 374, pp. 199-210, 2016.
- [2] Filippi, M., Pagani, A. and Carrera, E. Accurate Nonlinear Dynamics and Mode Aberration of Rotating Blades, *Journal of Applied Mechanics*, Vol. 85, 111004, 2018.
- [3] Heyliger, P. R. and Reddy, J. N., A higher order beam finite element for bending and vibration problems, *J. Sound Vib.* Vol. 126, pp. 309-326, 1988.
- [4] Kovacic, I. and Zukovic, M. On the response of some discrete and continuous oscillatory systems with pure cubic nonlinearity: Exact solutions, *Int. J. Non-Linear Mech.* Vol. 98, pp. 13-22, 2018.
- [5] Pagani, A. and E. Carrera, E., Unified formulation of nonlinear refined beam theories, *Mechanics of Advanced Materials and Structures*, Vol. 25, pp. 15-31, 2018.
- [6] Sarma, B. S. and Varadan, T. K. Ritz finite element approach to nonlinear vibration of a Timoshenko beam, *Comm. Appl. Num. Meth.* Vol. 1, pp. 23-32, 1985.
- [7] Woinowsky-Krieger, S. The effect of an axial force on the vibration of hinged bars, *J. Appl. Mech.*, Vol. 17, pp. 35-56, 1950.
- [8] Leissa, A.W.; MacBain, J.C.; Kielb, R.E.: Vibrations of Twisted Cantilevered Plates—Summary of Previous and Current Studies. *Journal of Sound and Vibration*, Vol. 96, No. 2, pp. 159–173, 1984.



## Vibration optimization of variable-stiffness composites fabricated by tailored fiber placement machine and electrodeposition molding

Shinya Honda<sup>\*</sup>, Kazuaki Katagiri<sup>#</sup>, Katsuhiko Sasaki<sup>\*</sup>

<sup>\*</sup> Faculty of Engineering  
Hokkaido University  
Kita-13 Nishi-8 Kita-ku, 060-8628,  
Sapporo, Hokkaido, Japan  
[honda, katsu]@eng.hokudai.ac.jp

<sup>#</sup> Department of Applied Material  
Chemistry, Osaka Research Institute  
of Industrial Science & Technology  
Ayumino 2-7-1, 594-1157, Izumi,  
Osaka, Japan  
katagirika@tri-osaka.jp

### Summary

Due to development of manufacturing techniques of carbon fiber reinforced plastics (CFRP), it becomes possible to fabricate variable stiffness composites with curvilinearly shaped reinforcing fibers. It was revealed that the variable stiffness composites indicate superior mechanical properties to the constant stiffness composites [1]. There are some manufacturing approaches for variable stiffness composites, and the authors employ a tailored fiber placement (TFP) machine that is an application of embroidering technique to fabricate preforms with curved carbon fibers. To impregnate resins into carbon fiber preforms efficiently, we have recently developed a new manufacturing method, an electrodeposition molding (EDM) [2, 3]. An electrodeposition solution based on epoxy is filled in a steel tank that becomes an anode in the process, and the carbon preform for a cathode is sunk in the solution. The schematic illustration of the EDM mechanism is shown in Figure 1. By energization to the system, the resin precipitates around the carbon fiber surface and fills in the space between fibers. This electrochemical process reduces voids and defects for the molded composites. Convergence of the current reduction in the system indicates enough impregnating of the resin. After this, composites are heat-cured at 170 °C. Figure 2 is a microstructure of test specimen. Few voids are observed, and it is known that resin is impregnated well between fibers. **Compared to other molding methods including a resin transfer molding (RTM), the present method is more effective and suitable for mass production since the technique of electrodeposition is established well and employed to paintings of automobiles. From the following, we propose an approach to predict and optimize vibration behaviors of composites by the TFP and EDM.**

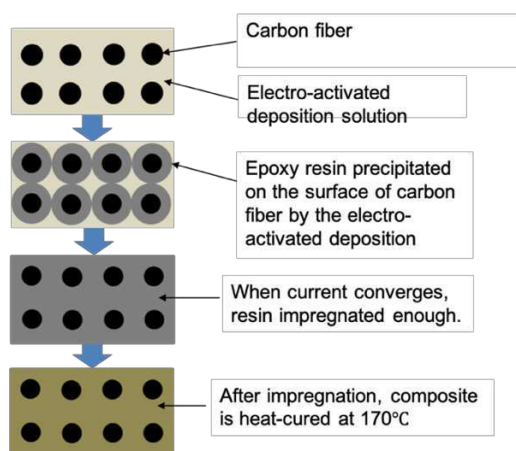


**Figure 1.** Schematic illustration of EDM system.

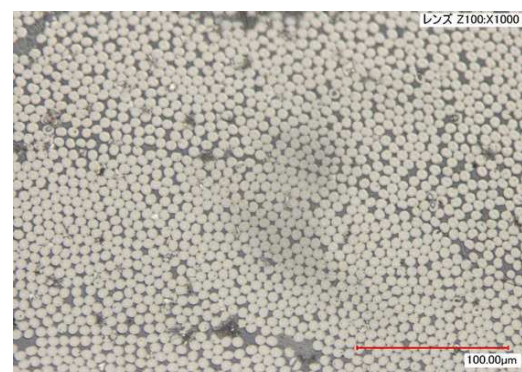


**Figure 2.** Microstructure of test specimen

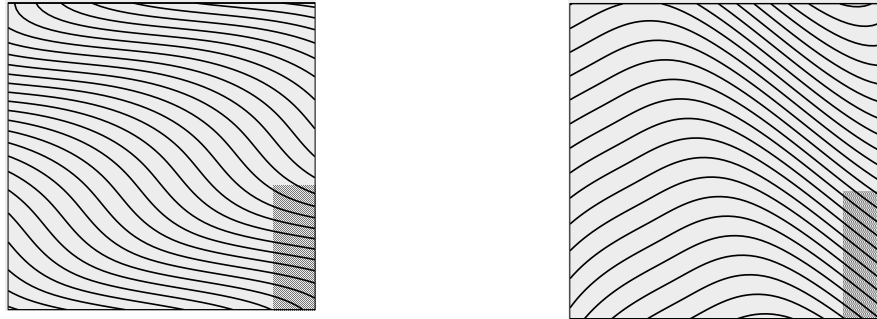
Since the variable stiffness composite has curvilinear reinforcing fibers, adjacent tows overlap each other because of their curvatures. This causes partial thickness increases and affects vibration characteristics of laminated plate significantly. Thus, these thickness distributions or variable thicknesses should be estimated correctly and be included to the prediction of vibration behavior of variable stiffness composites. When a fiber shape is given by  $f(x, y)$ , the overlap rate  $\lambda$  of fiber tows can be estimated by

$$\lambda = 1 - \frac{1}{|\nabla f(x, y)|} \quad (1)$$

where a cubic spline function is used as the fiber shape function. With the overlap rate  $\lambda$ , we can estimate the thickness of laminated plates with the experimental data as

$$t = \frac{0.68}{(1 - \lambda)(0.12\lambda^2 + 0.051\lambda + 0.44)} \text{ [mm]} \quad (2)$$

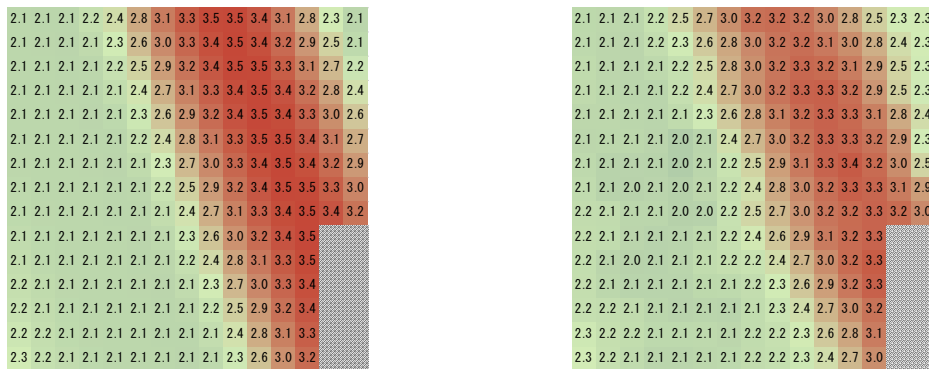
Using Equations (1) and (2), we can predict frequencies and mode shapes of variable stiffness composites correctly, and details are omitted in this report. Hereafter, the optimization of fiber shapes to maximize fundamental frequency of variable stiffness composites is mentioned for the cases with and without thickness distributions. Design variables are shape determining factors of cubic spline  $y_i (i = 1, 2, 3, \dots, 7)$  and same fiber shapes are defined in the  $y$  direction. Rotating angle  $\phi$  of spline function in terms of center of plate is also assigned as the design variable. The particle swarm optimization (PSO) is used as an optimizer and obtained fiber shapes with and without thickness distributions are indicated in Figure 3. Each plate is square and has 150 mm length. Right bottom corner (grayed area) is clamped.



(a) Without thickness distribution

(b) With thickness distribution

**Figure 3.** Obtained optimum fiber shapes with and without thickness distribution.



Estimated thickness distribution

Measured thickness distribution

**Figure 4.** Estimated and measured thickness distribution for the optimum fiber shape.

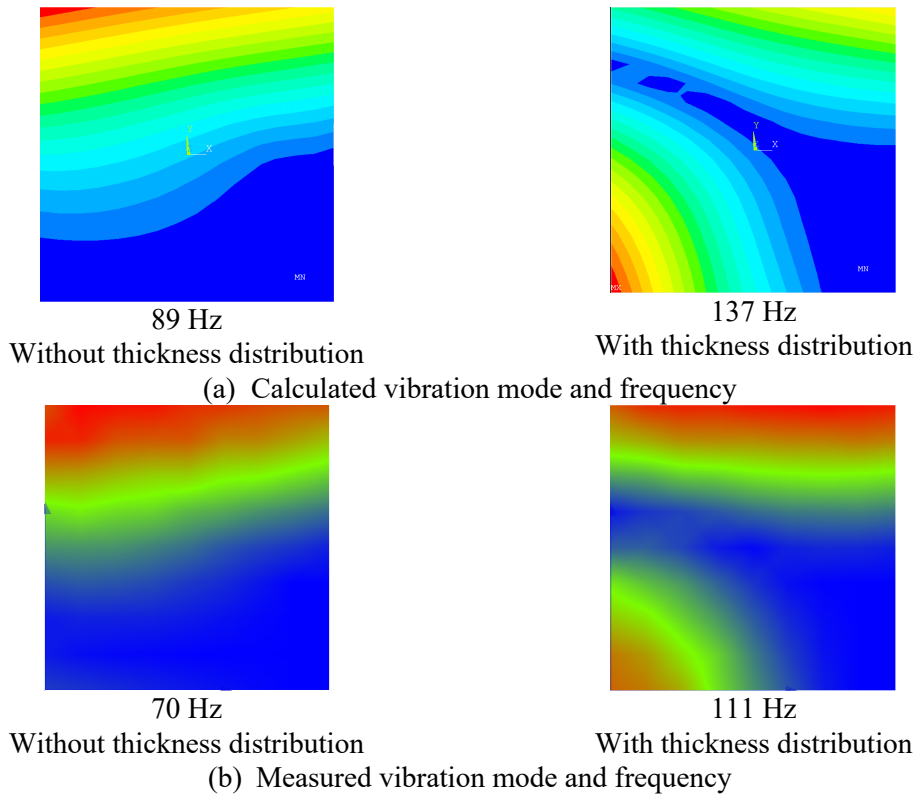


**Figure 5.** Comparison of vibration mode shapes and fundamental frequencies between calculation and experiments.

Figure 4 shows estimated and measured thickness distribution for the plate in Figure 3 (b), and Figure 5 indicates the vibration mode shapes and fundamental frequencies from the finite element analysis and experiment. It is known from Figures 4 and 5 that the present thickness estimation method agrees well with the experimental results and the optimization approach with thickness estimation results in higher frequencies, both numerical and experiential results indicate more than 50 % higher frequencies, than result without thickness distribution.

From above discussions, we conclude that it becomes possible to manufacture fibrous composites with curvilinear reinforcing fibers effectively with the present molding method or EDM, and it is also found that including variable thicknesses due to fiber curvature is important to predict and optimize vibration behavior of laminated composites with curvilinear fibers even it has been already revealed in Ref. [1] that the curvilinear fibers without thickness distributions enhance frequencies of composites over straight fibers.

## References

- [1] S. Honda, T. Igarashi, Y. Narita, Multi-Objective Optimization of Curvilinear Fiber Shapes for Laminated Composite Plates by Using NSGA-II, *Composites Part B: Engineering*, Vol. 45, 2013, pp. 1071-1078.
- [2] K. Katagiri, K. Sasaki, S. Honda, et. al., Resin molding by using electro-activated deposition for efficient manufacturing of carbon fiber reinforced plastic, *Composite Structures*, Vol.182, 15, 2017, pp 666-673.
- [3] K. Katagiri, S. Honda, et. al., An efficient manufacturing method for I-shaped cross section CFRP beam with arbitrary arrangement of carbon fiber using electro-activated resin molding, *Mechanics of Advanced Materials and Structures*, DOI: 10.1080/15376494.2018.1516324.



## Separating the effect of crack severity and location in a skeletal structure with a single crack

S. Ilanko<sup>\*</sup>, Y. Mochida<sup>\*</sup>, J. De Los Rios<sup>#</sup>, D. Kennedy<sup>†</sup>

<sup>\*</sup> The School of Engineering  
The University of Waikato  
Gate 1 Knighton Road Private Bag  
3105 Hamilton 3240 New Zealand

ilanko@waikato.ac.nz; yusuke.mochida@waikato.ac.nz

<sup>#</sup>Guachene, Columbia  
[juliandelosrios@hotmail.com](mailto:juliandelosrios@hotmail.com)

<sup>†</sup> School of Engineering  
Cardiff University  
Queen's Buildings, The Parade  
Cardiff CF24 3AA, United Kingdom  
KennedyD@cardiff.ac.uk

### Summary

One of the challenges in using frequency measurements to detect the presence of a crack, and to solve the inverse problem of finding its severity and location, is that even with a single crack, is that different combinations of severity and location can result in the same natural frequencies. A method of using a roving rotary inertia to detect and identify the location of cracks in skeletal structures was presented at ISVCS11 [1] and subsequently published in a journal [2]. In this presentation we discuss the use of a relationship between the determinants of the exact dynamic stiffness of the following three structures: the structure with a crack; the corresponding structure with a hinge at the crack location; the original (undamaged) structure. The corresponding determinants are denoted by  $D_c$ ,  $D_h$  and  $D_o$  where the subscripts c, h and o refer to cracked, hinged and original states of the structure. In terms of the equivalent rotational stiffness of the beam at the crack  $k$ , the following linear relationship has been established [3].

$$D_c(x, \omega, k) = D_h(x, \omega) + kD_o(\omega) \quad (1)$$

Here  $\omega$  is any frequency and  $x$  is the location of the crack from a given convenient origin.

By rearranging this equation, we obtain the following expression for the rotational stiffness of the beam at the crack.

$$k = (D_c(x, \omega, k) - D_h(x, \omega)) / D_o(\omega) \quad (2)$$

Since at the natural frequency  $\omega_i$  of the cracked structure  $D_c(x, \omega_i, k) = 0$ , equation (2) may be reduced further giving

$$k = -D_h(x, \omega_i) / D_o(\omega_i) \quad (3)$$

If several natural frequencies of a cracked structure are found through measurements, then equation (3) can be used to obtain an expression for the stiffness at any "potential" crack location  $x$ . As the crack location is not known, the locations are only trial values or potential locations. However, if the trial value is the correct location of the crack then irrespective of which natural frequency is being considered, the calculated stiffness would be the same. So the method of identifying the location relies on the fact that where the calculated stiffness vs potential crack location curves for various modes meet is the correct crack location.

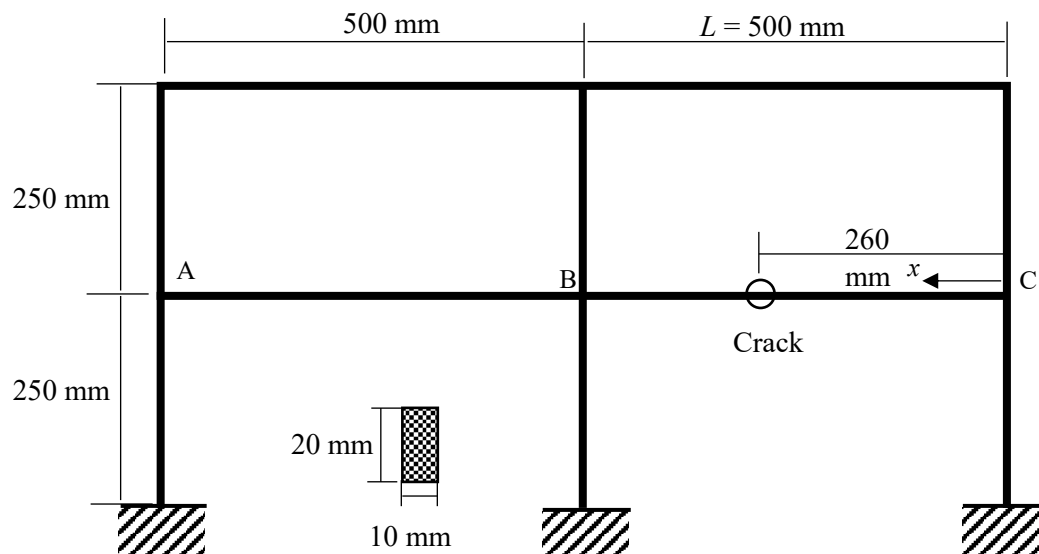


Figure 1. Two bay, two storey frame used by Labib.

The application of the methodology and its effectiveness in a simple search is demonstrated using the natural frequencies of the two bay two storey frame in Figure 1. Table 1 lists calculated values of the natural frequencies based on defined cracks (pseudo-experimental natural frequencies) obtained in a previous study [4] by numerical simulation. The respective values for  $D_0(\omega_i)$  and  $D_h(x, \omega_i)$  for a set of 99 locations within beam BC were calculated and the results are presented here.

Using equation (3) the stiffness values that nullify Eq. (1) are obtained for each measured frequency and plotted in Figure 2. All the obtained curves are located on the positive side of the stiffness, and intercept in a unique crossover point at  $x = 0.52L$  and in the stiffness value of  $k = 0.146EI/L$ . The positive value of stiffness is consistent with the reduction in the natural frequencies for the intact beam and the crossing point indicates that, for this particular member, from all the possible stiffness values there is just one possible crack location.

While this example demonstrates the potential use of the determinantal relationship (1) in separating the severity and location effects, it has to be borne in mind that the changes in the frequencies due to cracks are usually small and the effect of noise in measurements may make this method difficult to implement, even for a structure with a single crack. Following [4], the effect of noise is considered by evaluating equation (3) at the two frequencies  $\omega_i \pm \varepsilon$  where  $\varepsilon$  is a tolerance on the measured natural frequency  $\omega_i$ . The two resulting values of  $k$  give a range of possible stiffness values  $k_L \leq k \leq k_U$  for each potential crack location  $x$ . Each curve in Figure 2 is replaced by two curves and the crossover point is predicted as a range of values of  $x$  and  $k$ .

Table 1. Pseudo-experimental natural frequencies for intact and cracked frame

	$\omega_3$ (Hz)	$\omega_4$ (Hz)	$\omega_5$ (Hz)	$\omega_6$ (Hz)
Intact	142.635	169.112	177.238	194.562
Crack at $x=0.52L, k= 0.146EI/L$	142.625	169.082	177.212	194.495

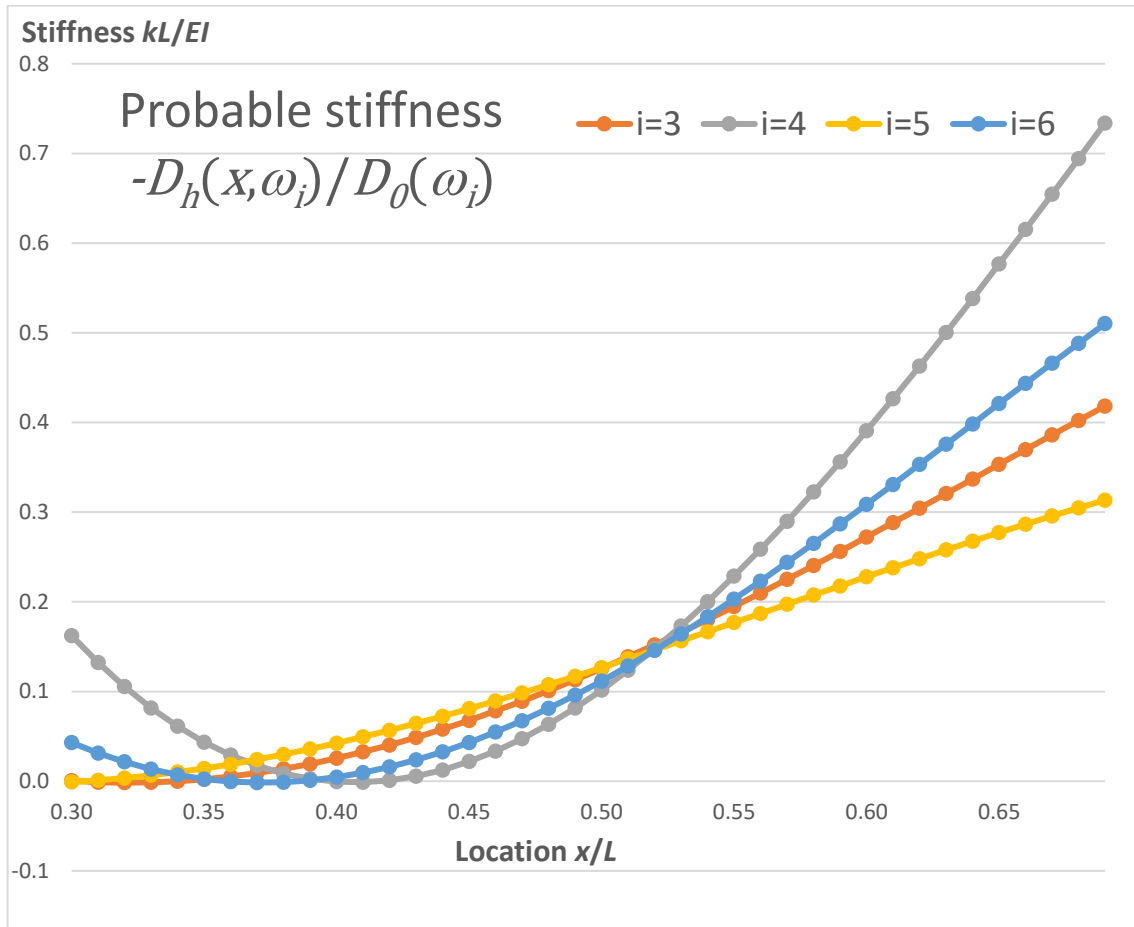


Figure 2. Numerical search from pseudo-experimental natural frequencies of Labib's frame

It should be noted that for a symmetric structure the crack location cannot be predicted uniquely. For the frame of Figure 1 the analysis would predict an alternative crack location symmetrically placed in beam AB.

## References

- [1] Ilanko, S.; De Los Rios, J.; Caddemi, S.; Kennedy, D.: The effect of roving rotary inertia as it passes a crack. ISVCS 2017 – Proceedings of 11th International Symposium on Vibrations of Continuous Systems, pp. 34-37, 2017.
- [2] Cannizzaro, F.; De Los Rios, J.; Caddemi, S.; Calio, I.; Ilanko, S.: On the use of a roving body with rotary inertia to locate cracks in beams. Journal of Sound and Vibration, 425, 275-300, 2018: doi:10.1016/j.jsv.2018.03.020
- [3] De Los Rios Giraldo, J.O. Damage identification in skeletal structures: A dynamic stiffness approach (Thesis, Doctor of Philosophy (PhD)). The University of Waikato, Hamilton, New Zealand. 2017
- [4] Labib, D.; Kennedy, D.; Featherston, C.A.: Crack localisation in frames using natural frequency degradations. Computers and Structures, 157, pp. 51-59, 2015: doi: 10.1016/j.compstruc.2015.05.001



## **From semi-analytical to Finite Element integrated low-dimensional models for nonlinear dynamic analysis of composite cylindrical shells**

**Eelco Jansen<sup>\*</sup>, Tanvir Rahman<sup>#</sup>**

<sup>\*</sup> Institute of Structural Analysis  
Leibniz Universität Hannover  
Appelstrasse 9A, 30167 Hannover,  
Germany  
e.jansen@isd.uni-hannover.de

<sup>#</sup> DIANA FEA BV  
Delftechpark 19a, 2628 XJ Delft,  
The Netherlands  
t.rahman@dianafea.com

### **Summary**

Composite cylindrical shells are basic components in mechanical and aerospace engineering. Stability and nonlinear dynamic analysis are of main importance for these structures, since they are prone to buckling instabilities under static and dynamic compressive loading. Moreover, under dynamic loads they may be directly or parametrically excited into resonance at their natural frequencies. The notorious discrepancy between the experimental results and the theoretical predictions for the buckling load of a cylindrical shell under axial compression led to an enormous research effort since the 1960s. The important problem of the nonlinear vibration behavior of cylindrical shells has also been studied since that time and has received a considerable amount of attention [1].

The nonlinear structural behavior of shell structures can be studied by means of Finite Element analysis, but this requires considerable effort and expertise from the user and corresponds to high computational costs. In particular in the area of nonlinear dynamics it has been recognized, that low-dimensional models (i.e. models with a relatively small number of degrees of freedom) are indispensable in order to gain insight into the nonlinear behavior of the structure. Another obvious advantage of using low-dimensional models lies in the quick evaluation of the dynamic response characteristics that can be attained, so that the methods can be used within a design context. Instead of carrying out a transient analysis with a (large) Finite Element model, one solves a relatively small set of nonlinear ordinary differential equations through numerical time integration. The current contribution presents characteristics of two different types of low-dimensional models.

Work in the field of nonlinear dynamics is often rooted in a semi-analytical framework based on the governing differential equations. In earlier work, semi-analytical models for buckling and vibration of anisotropic, composite cylindrical shells have been developed and were presented in a unified, simplified analysis framework based on Donnell-type governing equations using a Galerkin-type approach (Figure 1) [2]. These low-dimensional semi-analytical models are believed to capture important characteristics of the nonlinear static and dynamic behavior of composite cylindrical shells. Basic analysis cases which have been analyzed using these analytical methods include

- dynamic buckling (buckling under step loading)
- parametric excitation (vibration buckling under pulsating loads)
- nonlinear vibrations

Several reduced-order models for the nonlinear, large amplitude vibration analysis of composite shells are available [2, 3, 4]. These models can be used in a systematic, three-level hierarchical approach, based on the level of complexity of the description of the spatial behavior of the structure:

- Level-1 Analysis (Simplified Analysis) [3]: Semi-analytical approach based on a limited number of assumed spatial modes, approximately satisfying simply supported boundary conditions at the shell edges. The Method of Averaging is used to approximate the temporal behavior;
- Level-2 Analysis (Extended Analysis) [4]: Semi-analytical approach in which the boundary conditions at the shell edges are satisfied accurately. A perturbation method is used to approximate the temporal behavior;
- Level-3 Analysis: Numerical analysis corresponding to a detailed Finite Element discretization.

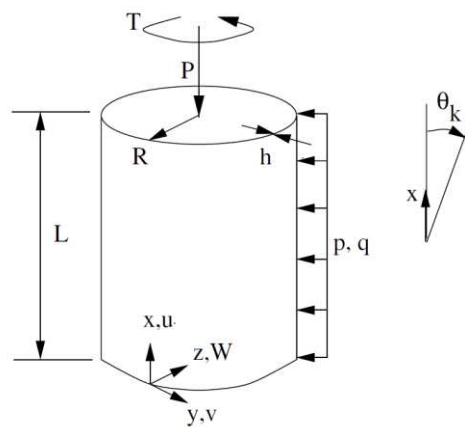


**Figure 1.** Shell geometry, applied loading and laminate layer orientation within semi-analytical nonlinear dynamic analysis of composite cylindrical shells [2].

Semi-empirical methods and the „classical” semi-analytical methods [3,4] are very helpful, but are available for specific structures with relatively simple geometries only. A second type of low-dimensional models is constituted by Finite Element integrated reduced complexity approaches, which provide a way to systematically carry out nonlinear analyses for arbitrary structures (Figure 2) [5]. The usefulness of this type of reduced complexity models, based on perturbation approaches, to gain insight into the characteristics of the nonlinear static and dynamic behavior of cylindrical shell structures and to reduce the computational effort involved in the nonlinear Finite Element calculations has been demonstrated in earlier work, see e.g. [6, 7, 8].

The Finite Element integrated low dimensional models make use of an analytical approach to approximate the nonlinear behavior, Koiter’s perturbation approach for buckling and dynamic buckling analysis and a Lindstedt–Poincaré type perturbation approach for nonlinear vibrations, respectively. Similar to the „classical” semi-analytical methods, they are also using „buckling modes” and „vibration modes” to establish a set of appropriate generalized coordinates for the nonlinear structural analysis. A modal-based reduced-order model for dynamic buckling of imperfection-sensitive structures was presented [7], while an extension of this reduced-order modelling approach to dynamic response analysis is currently under development. In parallel, Finite Element based reduced order-models for nonlinear, large amplitude vibrations of thin-walled structures have been developed and applied to composite cylindrical shells [8].

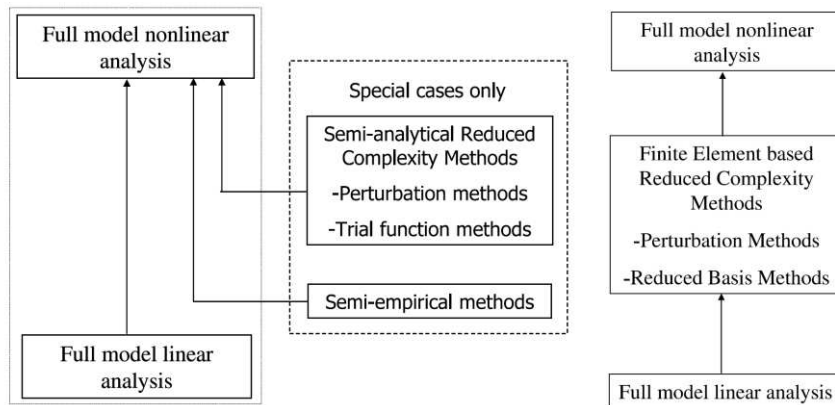


**Figure 2.** Standard Finite Element approach versus approach using Finite Element integrated low-dimensional reduced complexity methods for nonlinear structural analysis [5].

In the present contribution, results of the two types of low-dimensional models developed are illustrated. Firstly, two „classical” semi-analytical approaches (Simplified Analysis and Extended Analysis) demonstrate nonlinear vibration characteristics of specific composite cylindrical shells. Moreover, results of the second type of low-dimensional model, the Finite Element integrated reduced-order modelling approach, illustrate important features of the dynamic buckling and nonlinear vibration behavior of various composite cylindrical shells.

## References

- [1] Amabili, M.; Paidoussis, M.: Review of studies on geometrically nonlinear vibrations and dynamics of circular cylindrical shells and panels, with and without fluid-structure interaction. *Applied Mechanics Reviews*, Vol. 56, No. 4, pp. 349–381, 2003.
- [2] Jansen, E.L.: Buckling, vibration and flutter of shells via a simplified analysis. In: *Shell Structures, Theory and Applications*, W. Pietraszkiewicz and C. Szymczak, Eds., Taylor and Francis Group, London, 2006.
- [3] Jansen, E.L.: The effect of static loading and imperfections on the nonlinear vibrations of laminated cylindrical shells. *Journal of Sound and Vibration*, Vol. 315, pp.1035–1046, 2008.
- [4] Jansen, E.L.; Rolfes, R.: Non-linear free vibration analysis of laminated cylindrical shells under static axial loading including accurate satisfaction of boundary conditions. *International Journal of Non-Linear Mechanics*, Vol. 66, pp. 66-74, 2014.
- [5] Jansen, E.L.; Rahman, T.; Rolfes, R.: Reduced-order models for static and dynamic analysis of composite panels based on a perturbation approach. *Applied Mechanics and Materials*, Vol. 828, pp. 199–212, 2016.
- [6] Rahman, T.; Jansen, E.L.: Finite element based coupled mode initial post-buckling analysis of a composite cylindrical shell. *Thin-Walled Structures*, Vol. 48, pp. 25–32, 2010.
- [7] Rahman, T.; Jansen, E.L.; Gürdal, Z.: Dynamic buckling analysis of composite cylindrical shells using a finite element based perturbation method. *Nonlinear Dynamics*, Vol. 66, pp. 389–401, 2011.
- [8] Rahman, T.; Jansen, E.L.; Tiso, P.: A finite element-based perturbation method for nonlinear free vibration analysis of composite cylindrical shells. *International Journal of Structural Stability and Dynamics*, Vol. 11, No. 4, pp. 717–734, 2011.



## Natural Frequency Degradations in Cracked Plates

Yulin Luo\*, David Kennedy\*, Carol A. Featherston\*

\* School of Engineering  
 Cardiff University  
 Queen's Buildings, The Parade, Cardiff CF24 3AA, Wales, United Kingdom  
 [LuoY9, KennedyD, FeatherstonCA]@cardiff.ac.uk

### Summary

Plates and stiffened panels are widely used in aerospace and other applications. Their structural performance is degraded by the presence of damage such as delaminations and cracks, which are difficult to detect visually, particularly in built-up structures such as wing and fuselage panels. Changes in the natural frequencies enable damage to be identified using non-destructive testing.

Dynamic stiffness analysis provides an efficient, accurate alternative to finite element (FE) analysis by using a transcendental stiffness matrix based on exact solutions to the governing differential equations. Plates and their loading are required to be invariant in the longitudinal ( $x$ ) direction, so that the vibration modes vary sinusoidally in this direction [1]. Arbitrarily damaged structures violate this restriction, but can be modelled using a hybrid method [8] which combines an exact strip model of the undamaged regions with a rectangular FE model of the longitudinal strips containing the damage, see Figure 1(a). Displacements and rotations at the boundaries are coupled using Lagrangian multipliers, and natural frequencies are found using the Wittrick-Williams algorithm [9]. Previous analyses have been restricted to cracks located at the centre or at a plate edge, running parallel to the edges, over the full length or width, or through the full thickness [3, 5, 7]. The present analysis permits cracks of arbitrary length, depth, location and orientation. Figure 1(b) shows part of the FE model. A crack runs along the line  $PQRS$  through elements  $a$ ,  $b$  and  $d$ . It is modelled as a rotational spring with depth-dependent compliance  $C$  per unit length [4] which is resolved into rotational components ( $C_x, C_y$ ) about the  $x$  and  $y$  axes. The components in element  $a$  are integrated along  $PQ$  to allocate compliances to nodes (1, 2, 4, 5). Similarly the compliances in elements  $b$  and  $d$  are allocated to nodes (2, 3, 5, 6) and (5, 6, 8, 9).

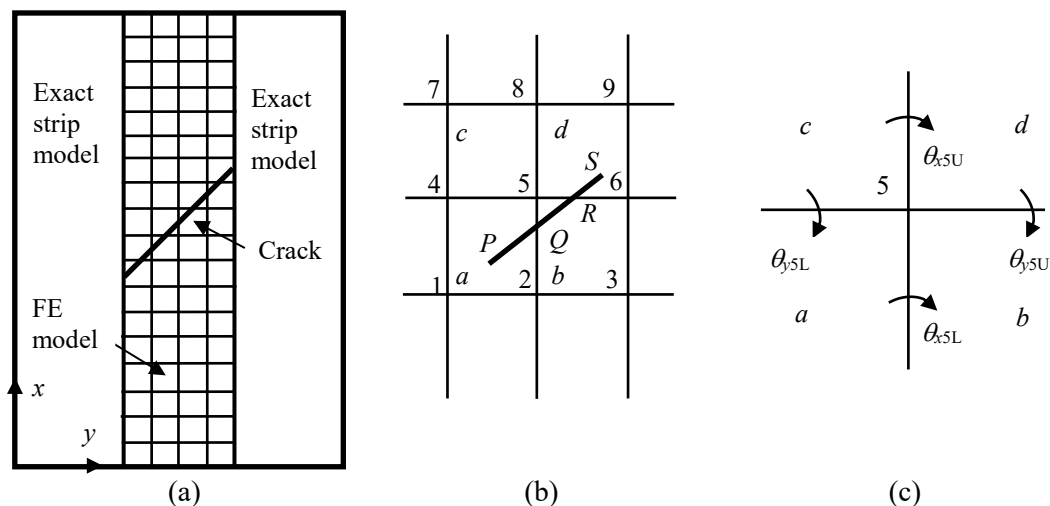


**Figure 1.** (a) Cracked plate, showing coupled exact strip and FE models. (b) Detail of a portion of the FE model. (c) Rotational degrees of freedom at node 5.

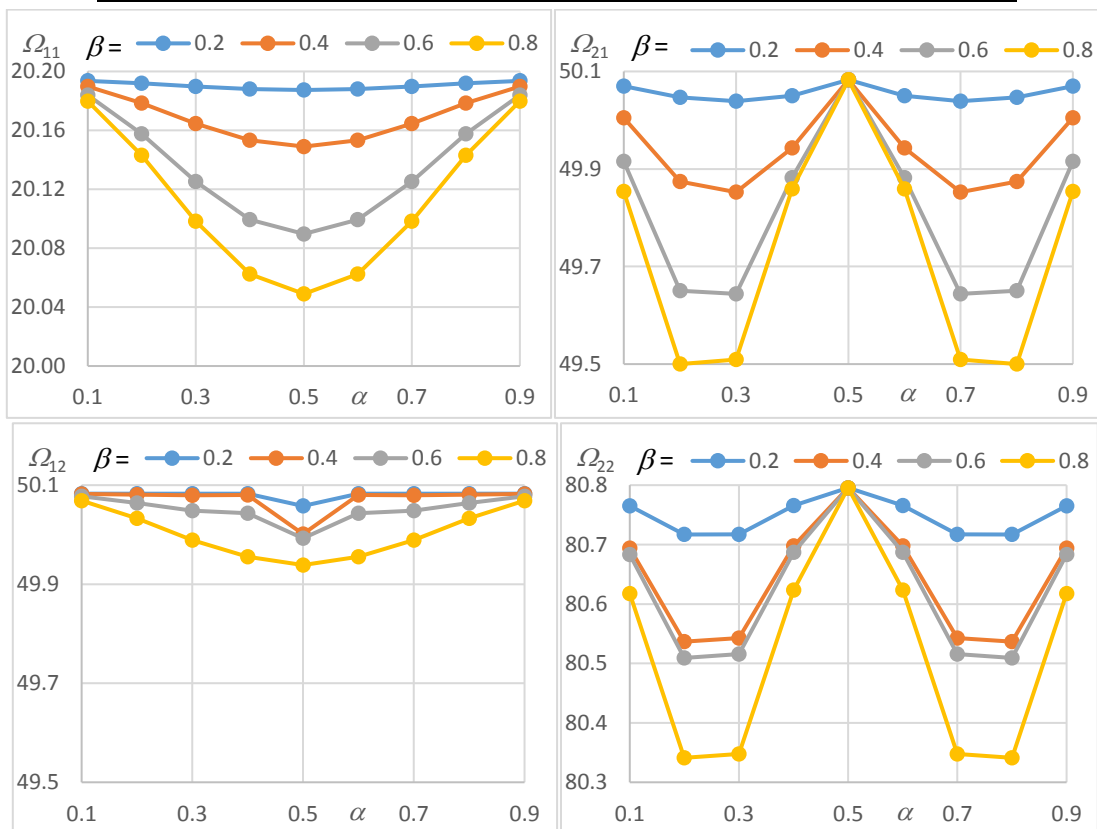
The finite elements have three degrees of freedom at each node: vertical displacement  $w$  and rotations  $\theta_x$  and  $\theta_y$  about the  $x$  and  $y$  axes. Nodes to which rotational compliances  $(C_x, C_y)$  have been allocated are given additional rotational degrees of freedom, e.g. as shown in Figure 1(c) for node 5. Element  $a$  connects to  $(w_5, \theta_{x5L}, \theta_{y5L})$  while element  $b$  connects to  $(w_5, \theta_{x5L}, \theta_{y5U})$ . Rotational springs of stiffness  $(1/C_x, 1/C_y)$  connect freedoms  $(\theta_{x5L}, \theta_{x5U})$  and  $(\theta_{y5L}, \theta_{y5U})$ .

Table 1 lists normalised natural frequencies with  $(m, n)$  half-waves in the  $(x, y)$  directions for an undamaged simply supported square plate of length  $l$ , thickness  $h$ , Young's modulus  $E$ , Poisson's ratio  $\nu$  and density  $\rho$ . Results obtained from the present method using a  $40 \times 40$  FE mesh are seen to be close to classical results [2]. A crack of depth  $0.4h$  is now introduced to the plate, running from  $(x, y) = (\alpha l, 0)$  to  $(\alpha l, \beta l)$  where  $\alpha$  is a location parameter in the range  $0.1 \leq \alpha \leq 0.9$  and  $\beta$  is a length parameter in the range  $0.2 \leq \beta \leq 0.8$ . The four lowest non-dimensional natural frequencies are shown in Figure 2.

Figure 3 shows contour plots of two of the vibration modes for four different locations of a crack of length  $0.4l$ . The mode shapes show increasing skewing as the crack is moved towards the centre line of the plate. But as a result of symmetry the pure  $(2,1)$  and  $(1,2)$  modes return when the crack runs along the centre line, with no degradation in the natural frequency  $\Omega_{21}$  (see Figure 2). Care is needed to identify such crossovers when tracking the natural frequencies.

**Table 1.** Non-dimensional natural frequencies  $\Omega_{mn} = 2\pi l^2 \omega_{mn} \sqrt{12\rho(1-\nu^2)/Eh^2}$  for undamaged simply supported square plate.

$(m, n)$	(1, 1)	(1, 2)	(2, 1)	(2, 2)	(1,3)	(3,1)
Present analysis	20.194	50.083	50.083	80.796	99.532	99.532
Classical results [2]	19.739	49.348	49.348	78.957	98.696	98.696



**Figure 2.** Degradation of natural frequencies with crack location and length.

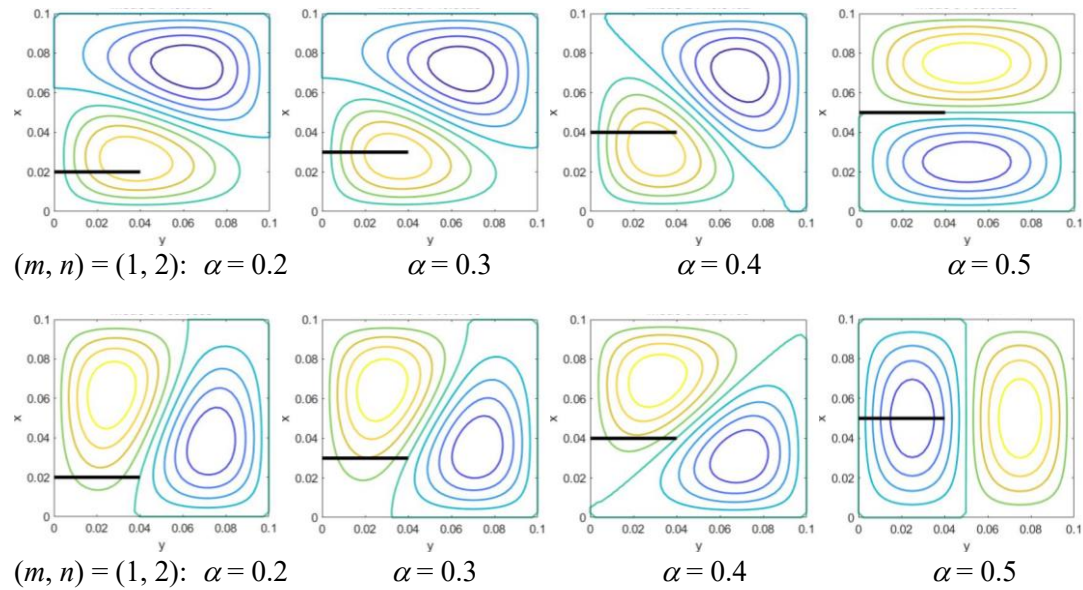


**Figure 3.** Variation of mode shapes with crack location  $\alpha$ , for  $\beta = 0.4$ .

Morassi [6] demonstrated that the natural frequency degradation for a cracked beam is proportional to the square of the curvature in the vibration mode of the corresponding uncracked beam, measured at the crack location. This result will be generalised to cracked plates.

## References

- [1] Anderson, M.S.; Williams, F.W.; Wright, C.J.: Buckling and vibration of any prismatic assembly of shear and compression loaded anisotropic plates with an arbitrary supporting structure. *International Journal of Mechanical Sciences*, Vol. 25, No. 8, pp. 585–596, 1983.
- [2] Beards, C.F.: *Structural Vibration: Analysis and Damping*. Elsevier, 1996.
- [3] Bose, T.; Mohanty, A.R.: Vibration analysis of a rectangular thin isotropic plate with a part-through surface crack of arbitrary orientation and position. *Journal of Sound and Vibration*, Vol. 332, No. 26, pp. 7123–7141, 2013.
- [4] Dimarogonas, A.D.: Vibration of cracked structures: a state of the art review. *Engineering Fracture Mechanics*, Vol. 55, No. 5, pp.831–857, 1996.
- [5] Liew, K.M.; Hung, K.C.; Lim, M.K.: A solution method for analysis of cracked plates under vibration. *Engineering Fracture Mechanics*, Vol. 48, No. 3, pp. 393–404, 1994.
- [6] Morassi, A.: Crack-induced changes in eigenparameters of beam structures. *Journal of Engineering Mechanics*, Vol. 119, No. 9, pp. 1798–1803, 1993.
- [7] Stahl, B; Keer, L.M.: Vibration and stability of cracked rectangular plates. *International Journal of Solids and Structures*, Vol. 8, No. 1, pp. 69–91, 1972.
- [8] Suliman, B.; Featherston, C.A.; Kennedy, D.: A hybrid method for modelling damage in composites and its effect on natural frequency. *Computers and Structures*, Vol. 213, pp. 40–50, 2019.
- [9] Wittrick, W.H.; Williams, F.W.: A general algorithm for computing natural frequencies of elastic structures. *Quarterly Journal of Mechanics and Applied Mathematics*, Vol. 24, No. 3, pp. 263–284, 1971.



## Wave propagation analysis within multilayer media by using the dynamic stiffness method

Xiang Liu<sup>#†</sup>

<sup>#</sup> Joint International Research Laboratory of Key Technology for Rail Traffic Safety,  
410075 Changsha, China

<sup>†</sup> School of Traffic & Transportation Engineering, Central South University  
410075 Changsha, China  
xiangliu06@gmail.com

### Summary

Wave propagation or dynamic response of multilayer media is commonly encountered in many areas[1]. For example, environmental vibration caused by traffic loads may become irritating[2], seismic wave may lead to disasters, rock blasting may give rise to slope instabilities, and ultrasonic waves in media facilitate structural health monitoring purposes[3]. The first two examples are in the low frequency ranges whereas the latter two fall into the mid- to high-frequency ranges. Hence, an efficient and accurate model, hopefully within the whole frequency range, has been always an essential objective for engineers.

This research presents a dynamic stiffness formulation for multilayer media. Firstly, given an elastic layer in the  $xz$  plane ( $z \in [0, h]$ ,  $h$  is the thickness), the differential equation governing the vibration of elastic media in the plane strain deformation is essentially the Navier equation in the  $xz$  plane

$$\sigma_{zz,z} + \tau_{zx,x} - \rho W_{,tt} = 0, \quad (1a)$$

$$\tau_{xz,z} + \sigma_{xx,x} + \rho U_{,tt} = 0, \quad (1b)$$

in which,  $W$  and  $U$  denote the displacements in  $z$  and  $x$  respectively,  $\rho$  is the media's density, and the stresses are given as

$$\sigma_{zz} = (\lambda + 2G)W_{,z} + \lambda U_{,x}, \quad (2a)$$

$$\tau_{xz} = G(W_{,x} + U_{,z}), \quad (2b)$$

$$\sigma_{xx} = (\lambda + 2G)U_{,x} + \lambda W_{,z} \quad (2c)$$

where  $\lambda, G$  are Lamé constant in plane strain. The boundary conditions on the top and bottom surfaces are described as Eqs. (2a) and (2b).

Now we introduce a frequency parameter  $\omega_m$  and a wavenumber parameter  $k_n$  in the  $x$  direction, namely,

$$W(x, z, t) = \sum_{m=0}^{\infty} \sum_{n=0}^{\infty} W_{mn}(z) \exp(i\omega_m t) \exp(ik_n x),$$

$$U(x, z, t) = \sum_{m=0}^{\infty} \sum_{n=0}^{\infty} U_{mn}(z) \exp(i\omega_m t) \exp(ik_n x).$$

Therefore, we have  $(\cdot)_{tt} = -\omega_m^2(\cdot)$ , and  $\partial^j(\cdot)/\partial x^j = (ik_n)^j(\cdot)$ . Then Eq. (1) becomes

$$\sigma_{zz,z} + ik_n \tau_{zx} + \rho \omega^2 W = 0, \quad (3a)$$

$$\tau_{xz,z} + ik_n \sigma_{xx} + \rho \omega^2 U = 0 \quad (3b)$$

and Eq.(2) results in

$$\sigma_{zz} = (\lambda + 2G)W_{,z} + ik_n\lambda U, \quad (4a)$$

$$\tau_{xz} = G(ik_nW + U_{,z}), \quad (4b)$$

$$\sigma_{xx} = ik_n(\lambda + 2G)U + \lambda W_{,z} \quad (4c)$$

Based on Eqs. (3) and (4), we may rewrite the governing different equation in the form of a first-order differential equation of state space in the frequency-wavenumber domain to be

$$\frac{\partial \mathbf{U}(z)}{\partial z} = \mathbf{A}\mathbf{U}(z), \quad (5)$$

where the state space vector  $\mathbf{U}(z)$  and the coefficient matrix  $\mathbf{A}$  are

$$\mathbf{U}(z) = \begin{Bmatrix} \mathbf{f} \\ \mathbf{d} \end{Bmatrix} = \begin{Bmatrix} \sigma_{zz}(z) \\ i\tau_{xz}(z) \\ W(z) \\ iU(z) \end{Bmatrix}, \quad \mathbf{A} = \begin{bmatrix} 0 & -k_n & -\rho\omega^2 & 0 \\ \frac{\lambda k_n}{\lambda+2G} & 0 & 0 & \frac{4G(\lambda+G)k^2}{\lambda+2G} - \rho\omega^2 \\ \frac{1}{\lambda+2G} & 0 & 0 & -\frac{\lambda k_n}{\lambda+2G} \\ 0 & 1/G & k_n & 0 \end{bmatrix}.$$

Therefore, the general solution of the elastic layer is  $\mathbf{U}(z) = \exp(\mathbf{A}z)$ . Letting  $\mathbf{T} = \exp(\mathbf{A}h)$ , the boundary conditions on the two surfaces can be related in the transfer matrix (or propagator matrix) form

$$\mathbf{U}(h) = \mathbf{T}\mathbf{U}(0), \quad (6)$$

where

$$\mathbf{U}(h) = \begin{Bmatrix} \mathbf{f}_2 \\ \mathbf{d}_2 \end{Bmatrix} = \begin{Bmatrix} \sigma_{zz}(h) \\ i\tau_{xz}(h) \\ W(h) \\ iU(h) \end{Bmatrix}, \quad \mathbf{T} = \begin{bmatrix} \mathbf{T}_{11} & \mathbf{T}_{12} \\ \mathbf{T}_{21} & \mathbf{T}_{22} \end{bmatrix}, \quad \mathbf{U}(0) = \begin{Bmatrix} \mathbf{f}_1 \\ \mathbf{d}_1 \end{Bmatrix} = \begin{Bmatrix} \sigma_{zz}(0) \\ i\tau_{xz}(0) \\ W(0) \\ iU(0) \end{Bmatrix}.$$

It is straightforward to rewrite the transfer matrix form into the following dynamic stiffness formulation

$$\mathbf{f}^e = \mathbf{K}^e \mathbf{d}^e, \quad (7)$$

where

$$\mathbf{f}^e = \begin{Bmatrix} \mathbf{f}_1 \\ \mathbf{f}_2 \end{Bmatrix}, \quad \mathbf{K}^e = \begin{bmatrix} -\mathbf{T}_{21}^{-1}\mathbf{T}_{22} & \mathbf{T}_{21}^{-1} \\ \mathbf{T}_{12} - \mathbf{T}_{11}\mathbf{T}_{21}^{-1}\mathbf{T}_{22} & \mathbf{T}_{11}\mathbf{T}_{21}^{-1} \end{bmatrix}, \quad \mathbf{d}^e = \begin{Bmatrix} \mathbf{d}_1 \\ \mathbf{d}_2 \end{Bmatrix}.$$

Now we have formulated the dynamic stiffness matrix of a single elastic layer within the frequency-wavenumber domain, the global dynamic stiffness matrix of multilayer elastic media can be easily formulated by assembling the dynamic stiffness elements just like assembling bar or beam elements in the classical dynamic stiffness method or the finite element method.

If we need to perform wave propagation (dynamic response) analysis, the formulation of Eq. (7) in the frequency-wavenumber domain can be utilized combined with some proper form of linear transform. In this research, we adopt Double Fast Fourier transform because there are many well-developed efficient algorithms in a wide range of computational platforms. The procedure is described as follows.

1. Determine the sampling time window  $T_s$  based on the duration of input force and the response of the considered multilayer media; identify the sampling space window  $X_s$  in the  $x$  direction based on the width of the applied force as well as that of the multilayer elastic media in consideration;

2. Determine the highest frequency  $f_{max}$  and largest wavenumber  $k_{max}$  based on the input force, therefore, according to Nyquist condition, we have the sampling time interval  $\Delta t \leq 1/(2f_{max})$  and the sampling space interval in  $x$  direction  $\Delta x \leq 1/(2k_{max})$ ;
3. According to the sampling number requirement of Double Fast Fourier transform, determine the number of time samples  $N_t = 2^{p_t}$  and the number of space samples in the  $x$  direction  $N_x = 2^{p_x}$ , in which  $p_t = \lceil \log_2(T_s/\Delta t) \rceil$  and  $p_x = \lceil \log_2(X_s/\Delta x) \rceil$  are integers,  $\lceil \cdot \rceil$  stands for ceiling function of ' $\cdot$ '. Finally, the final sampling time interval  $dt = T_s/N_t$  and  $dx = X_s/N_x$ ;
4. If external excitation applied on the  $i$ th surface  $f_i(x, t)$  is given in an analytical manner, we can evaluate the numerical values at  $t = (0 : N_t - 1) \times dt$  and  $x = (0 : N_x - 1) \times dx$  as a matrix  $[f_i^{num}(t, x)]$  of size  $N_t \times N_x$ ;
5. Apply the Double Fast Fourier transform,  $\text{fft2}[f_i^{num}(t, x)]$  leading to the external force on the  $i$ th surface in the frequency-wavenumber domain  $[F_i(\omega_m, k_n)]$  in a matrix form where  $m \in \{0, 1, \dots, N_t - 1\}$ ,  $n \in \{0, 1, \dots, N_x - 1\}$ . For each combination of  $\omega_m$  and  $k_n$ , put all the component  $F_i(\omega_m, k_n)$  together, we have the overall force vector  $\mathbf{F}(\omega_m, k_n)$ ;
6. Calculate the displacement response in the frequency-wavenumber domain, we will have  $\mathbf{D}(\omega_m, k_n) = \mathbf{K}(\omega_m, k_n)^{-1} \mathbf{F}(\omega_m, k_n)$ ;
7. Apply the inverse Double Fast Fourier transform to the displacement response of the  $i$ th surface  $\text{ifft2}[D_i(\omega_m, k_n)]$  leading to the displacement response of the  $i$ th surface in the time and space domain (in  $x$  direction)  $d_i^{num}(t, x)$ .

The method described in this paper has been used for the pavement vibration analysis induced by travelling traffic. Further special attempts have been made to speed up the calculation process for one order of magnitude, this is for the purpose that it could be used for parameters studies and inverse problems. It has been demonstrated that this method is of two order of magnitude faster than the FEM. The superiority is much more significant in the mid- to high-frequency ranges.

## References

- [1] E. Kausel, Fundamental Solutions in Elastodynamics, Cambridge University Press, 2006.
- [2] Y. Yang, H. Hung, Wave Propagation for Train-induced Vibrations A Finite Infinite Element Approach, World Scientific, 2009.
- [3] S. Gopalakrishnan, A. Chakraborty, D. R. Mahapatra, Spectral finite element method, Springer-Verlag, London, 2008.



## Sensitivity Analysis of Eigenproblems and Application to Wave Propagation in Timber

**Brian R Mace**<sup>\*</sup>, **Alice Cicirello**<sup>#</sup>, **Michael J Kingan**<sup>\*</sup>, **Yi Yang**<sup>\*</sup>

<p><sup>*</sup> Acoustics Research Centre Dep of Mechanical Engineering University of Auckland Private Bag, Auckland, New Zealand [b.mace, m.kingan, yi.yang]@auckland.ac.nz</p>	<p><sup>#</sup> Department of Engineering Science Oxford University Parks Road, Oxford, OX1 3PJ, UK alice.cicirello@eng.ox.ac.uk</p>
--	--

### Summary

Eigenproblems arise in many areas of structural dynamics, including modal analysis and analysis of wave propagation. The right and left eigenproblems (EPs) are

$$\mathbf{B}(p)\mathbf{u} = \lambda\mathbf{C}(p)\mathbf{u}; \quad \mathbf{z}^T\mathbf{B}(p) = \lambda\mathbf{z}^T\mathbf{C}(p) \quad (1)$$

where  $\mathbf{B}(p)$  and  $\mathbf{C}(p)$  are  $m \times m$  matrices, while  $\lambda$ ,  $\mathbf{u}$  and  $\mathbf{z}$  are the eigenvalues and right and left eigenvectors and  $p$  is some parameter (e.g. a material or geometric property). The sensitivities of the eigenvalues and eigenvectors with respect to  $p$  are of interest for reasons including uncertainty modelling, stability analysis, model updating and design. Linear perturbations can be developed to estimate changes in the eigensolutions without the need to re-solve the eigenproblem multiple times, reducing computational cost drastically.

Much attention has been applied to the sensitivity analysis of eigenproblems. Of relevance here is the generalised, asymmetric eigenproblem (1), involving asymmetric and complex matrices, applied to a wave and finite element (WFE) model to analyse wave propagation in a waveguide with uncertain parameters. For some value  $p_0$  of the parameter  $p$ , the EP becomes

$$\mathbf{B}_0\mathbf{u}_0 = \lambda_0\mathbf{C}_0\mathbf{u}_0; \quad \mathbf{z}_0^T\mathbf{B}_0 = \lambda_0\mathbf{z}_0^T\mathbf{C}_0; \quad \mathbf{z}_0^T\mathbf{C}_0\mathbf{u}_0 = 1 \quad (2)$$

where the last equation is a normalisation condition. Assuming that  $\lambda_0$  is distinct, its derivative with respect to  $p$  is (see for example Seyranian and Mailybaev, section 2.12 [1])

$$\frac{d\lambda}{dp} = \mathbf{z}_0^T \left[ \frac{d\mathbf{B}}{dp} - \lambda_0 \frac{d\mathbf{C}}{dp} \right] \mathbf{u}_0 \quad (3)$$

Expressions for eigenvector derivatives and for multiple eigenvalues can be found in [1]. This result reduces to that for symmetric eigenproblems for which  $\mathbf{B}$ ,  $\mathbf{C}$  are real and symmetric and the left and right eigenvectors are equal.

### WFE eigenproblems and sensitivity analysis

The WFE method for free wave propagation in a waveguide [2] involves determining the mass and stiffness matrices  $\mathbf{M}$  and  $\mathbf{K}$  of a short segment of length  $\Delta$ , forming the dynamic stiffness

matrix (DSM)  $\mathbf{D} = \mathbf{K} - \omega^2 \mathbf{M}$  relating the left-hand and right-hand degrees of freedom  $\mathbf{q}_L$  and  $\mathbf{q}_R$  of the segment, and applying periodicity equations. Damping can be included by a viscous damping matrix  $\mathbf{C}$  or by  $\mathbf{K}$  being complex. An eigenproblem follows, the solutions yielding the eigenvalues  $\lambda = \exp(-ik\Delta)$ , with  $k$  being the (generally complex) wavenumber. The WFE eigenproblem can be phrased in a number of ways. Numerical issues are common [3], with two forms of the eigenproblem being especially attractive for sensitivity analysis. In the first, the equations of motion are projected onto the left-hand DOFs  $\mathbf{q}_L$  leading to an eigenproblem with

$$\mathbf{B} = \begin{bmatrix} \mathbf{0} & \mathbf{I} \\ -\mathbf{D}_{RL} & -(\mathbf{D}_{LL} + \mathbf{D}_{RR}) \end{bmatrix}, \quad \mathbf{C} = \begin{bmatrix} \mathbf{I} & \mathbf{0} \\ \mathbf{0} & \mathbf{D}_{LR} \end{bmatrix} \quad (4)$$

where the subscripts denote the partitions of the DSM. Alternatively, using Zhong's method [4], the most numerically robust approach, the matrices in the eigenproblem are such that

$$[\mathbf{B} - \mu \mathbf{C}] \begin{Bmatrix} \mathbf{q} \\ \lambda \mathbf{q} \end{Bmatrix}, \quad \mathbf{B} = \begin{bmatrix} \mathbf{D}_{RL} & \mathbf{0} \\ \mathbf{0} & \mathbf{D}_{LR} \end{bmatrix}, \quad \mathbf{C} = \begin{bmatrix} -(\mathbf{D}_{LL} + \mathbf{D}_{RR}) & -(\mathbf{D}_{LR} - \mathbf{D}_{RL}) \\ (\mathbf{D}_{LR} - \mathbf{D}_{RL}) & -(\mathbf{D}_{LL} + \mathbf{D}_{RR}) \end{bmatrix}, \quad (5)$$

$$\mu = \frac{1}{(\lambda + 1/\lambda)}, \quad \frac{\partial \lambda}{\partial p} = \frac{(1 + \lambda^2)^2}{(1 - \lambda^2)} \frac{\partial \mu}{\partial p}, \quad \frac{\partial k}{\partial p} = \frac{i \exp(ik\Delta)}{\Delta} \frac{\partial \lambda}{\partial p} \quad (6)$$

### Applications to timber and CLT panels

Radiata pine is widely used as a building material in New Zealand and elsewhere and consequently its acoustic and vibration behaviour is of interest for noise control. Recently, use of CLT panels, which involve layers of bonded timber (Figure 1), has grown rapidly, but their vibroacoustic behavior is poorly understood and is a subject of current research activity. Timber is



Figure 1. CLT panel.

highly anisotropic and properties are variable, depending on the growth site, the part of the tree from which the timber is cut, age, knots, moisture content etc. The density of radiata pine varies from 340-540 kg/m<sup>3</sup> while the along-grain elastic modulus ranges from 6-14 GPa, correlates to some degree with density and is substantially higher than the cross-grain value [5].

Figure 2 shows the sensitivity  $\partial k / \partial E$  of the axial and bending wavenumbers of a timber beam with elastic modulus  $E = 7.2$  GPa,  $\rho = 500$  kgm<sup>-3</sup> and width and thickness 100mm  $\times$  50mm.

Axial waves contribute primarily to structure-borne sound and flanking transmission in buildings, while bending waves dominate airborne sound transmission. Analytical and WFE results agree well except for finite element discretisation effects at high frequency (in particular for the axial

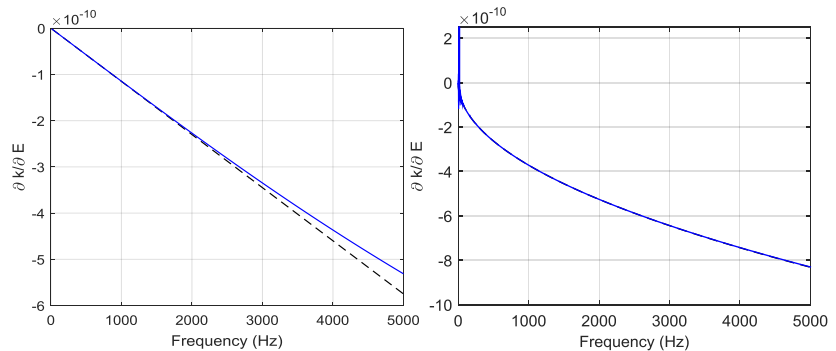
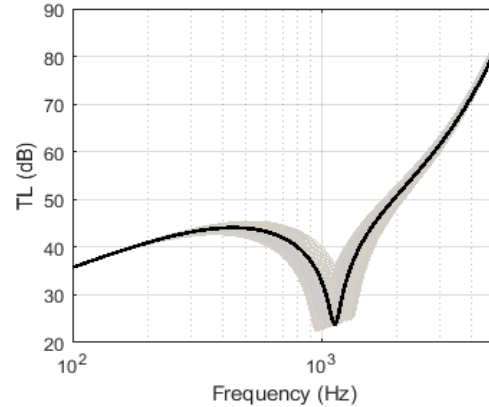


Figure 2. Sensitivity of wavenumber with respect to  $E$  for timber beam: axial (left) and bending (right) waves: - - - analytical, —WFE.

waves) and numerical noise at low frequency due to rounding errors [3] (in particular for bending waves, for which the segment is shorter). Finally Figure 3 shows the oblique transmission loss of a  $6 \times 33$ mm layer CLT panel, stacking sequence [0/90/0/0/90/0], modelled using WFE. Full details in [6]. The nominal value of the along-grain elastic modulus  $E_{xx} = 1.1 \times 10^{10}$  but a range is plotted to reflect the inherent uncertainty. Each line shows a coincidence notch when the trace wavenumber equals the bending wavenumber.



**Figure 3.** Transmission loss of CLT panel, incidence angles  $(\theta, \phi) = (30^\circ, 0^\circ)$ ,  $E_{xx} = 0.8 \times 10^{10}$  Pa to  $1.4 \times 10^{10}$ , thick line  $E_{xx} = 1.1 \times 10^{10}$  Pa.

### Concluding remarks

The sensitivity of the eigenvalues of complex, non-symmetric matrices was applied to WFE models to estimate the sensitivity of the wavenumber with respect to a parameter. From this, together with either a probabilistic or possibilistic description of the parameter, the variability of response quantities can be estimated at low cost: these quantities include natural frequencies, frequency response and sound transmission loss. In principle, spatially varying uncertainty can be included, e.g. through WKB methods. There is a real practical issue of an accurate description of the parameter variability. The sensitivity (3) breaks down for the case of equal (or very close) eigenvalues: there are two situations, corresponding to mode crossing or veering/instability in modal analysis, or wavenumber crossing or veering/locking for wave propagation. For spatially varying properties, additional problems arise at and around any critical sections where wave modes cut off. These situations are the subject of future work.

### Acknowledgements

The authors gratefully acknowledge the support of the MBIE Smart Ideas grant entitled “A Wave and Finite Element Method for Calculating Sound Transmission in Lightweight Buildings” and the Royal Society for the International Exchanges programme IES\R3\170279.

### References

- [1] Seyranian A.P.; Mailybaev A.A.: Multiparameter Stability Theory with Mechanical Applications, World Scientific Publishing, Singapore, 2003.
- [2] Mace B.R.; Duhamel D.; Brennan M.J.; Hinkel.: Finite element prediction of wave motion in structural waveguides. J Acoust Soc Amer, 117, 2835-2843, 2005.
- [3] Waki Y.; Mace B.R.; Brennan M.J.: Numerical issues concerning the wave and finite element method for free and forced vibrations of waveguides. J Sound Vib, 327, 92-108, 2009.
- [4] Zhong W.X.; Williams F.E.: Wave Problems for Repetitive Structures and Symplectic Mathematics, Proc Institution of Mechanical Engineers, Part C 206, 371-379, 1992.
- [5] Xu P.: The mechanical properties and stability of radiata pine structural timber, *PhD thesis, University of Canterbury*, 2000.
- [6] Yang Y.; Kingan M.; Mace B.R.: Analysis of the acoustic characteristics of CLT panels using a wave and finite element method. 26<sup>th</sup> ICSV, Montreal, 2019.



## Analysis on Nonlinear Forced Vibrations of a Thin Shell-panel Including Clamped Edges

**Shinichi Maruyama<sup>\*</sup>, Ken-ichi Nagai<sup>#</sup>, Daisuke Kumagai<sup>†</sup>, Takumi Okawara<sup>†</sup>**

<sup>\*</sup> Division of Mechanical Science and  
 Technology, Graduate School of  
 Science and Technology, Gunma  
 University, 1-5-1 Tenjin-cho, Kiryu,  
 Gunma 376-8515, JAPAN  
 maruyama@gunma-u.ac.jp

<sup>#</sup> Professor emeritus  
 Gunma University,  
 1-5-1 Tenjin-cho, Kiryu, Gunma  
 376-8515, JAPAN  
 kennagai@gunma-u.ac.jp

<sup>†</sup> Graduate School of Science and Technology,  
 Gunma University,  
 1-5-1 Tenjin-cho, Kiryu, Gunma 376-8515, JAPAN

### Summary

A new analytical procedure is presented on nonlinear vibrations of a thin rectangular shell-panel including clamped edges as shown in Figure 1. We introduce the  $x$ ,  $y$  axes along the in-plane directions of the shell-panel and the  $z$  axis in the lateral direction. The origin is taken at the center of the panel. The symbols  $\alpha_x$ ,  $\alpha_y$  are non-dimensional curvatures in  $x$  and  $y$  directions, respectively. The symbol  $W$  denotes the deflection, and  $U$ ,  $V$  are in-plane displacements in the  $x$  and  $y$  directions, respectively. At the boundaries of two opposite edges along  $x$  direction, the shell-panel is classically simply-supported (shear diaphragm), while at the other two edges along  $y$  direction the panel is classically simply-supported or clamped in the lateral direction. The in-plane boundary conditions are expressed by elastic constraint with springs  $K_x^*$ ,  $K_y^*$  in normal direction and shear springs along the edges  $K_{xy}^*$ ,  $K_{yx}^*$ . When an edge is fixed in one or both of the in-plane directions, the corresponding in-plane spring constants are taken as sufficiently large value. The spring constants are taken as zero when the edge is free in the in-plane direction. At the outer ends of the elastic constraints, initial uniform in-plane displacements  $U_{0x}^*$ ,  $V_{0y}^*$  are applied in the normal in-plane directions, but these displacements are taken as zero in this research. The Poisson's ratio of the panel is denoted by  $\nu$ . In the lateral direction, the shell-panel is subjected to periodic acceleration  $a_d \cos \Omega t$ , where  $a_d$ ,  $\Omega$  and  $t$  are amplitude of periodic acceleration, the excitation frequency and the time, respectively.

To reduce computational costs in the analysis, we express the in-plane motion with the stress function assuming that the panel is sufficiently thin and that the in-plane inertia can be neglected, instead of expanding in-plane displacements with multiple terms. The non-dimensional equation of motion of the shell-panel is expressed as follows:

$$L(w, f) = w_{,\tau\tau} + \bar{\nabla}^4 w - \alpha_x \beta^2 f_{,\eta\eta} - \alpha_y f_{,\xi\xi} - \beta^2 (f_{,\xi\xi} w_{,\eta\eta} - 2f_{,\xi\eta} w_{,\xi\eta} + f_{,\eta\eta} w_{,\xi\xi}) - p_d \cos \omega \tau - q_s \delta(\xi - \xi_1) \delta(\eta - \eta_1) = 0 \quad (1)$$

$$\bar{\nabla}^4 f = c \{ -\alpha_x \beta^2 w_{,\eta\eta} - \alpha_y w_{,\xi\xi} + \beta^2 (w_{,\xi\eta}^2 - w_{,\xi\xi} w_{,\eta\eta}) \} \quad (2)$$

Equation (1) denotes the equation of motion of the panel in the lateral direction, and Eq. (2) is the compatibility equation of the in-plane strain in terms of the stress function  $f$ , which is related to the in-plane resultant force  $n_x$ ,  $n_y$  and  $n_{xy}$  as follows.

$$n_x = \beta^2 f_{,\eta\eta}, \quad n_y = f_{,\xi\xi}, \quad n_{xy} = -\beta f_{,\xi\eta} \quad (3)$$

We employ single-term expansion to derive an ordinary differential equation.

$$w(\xi, \eta, \tau) = \hat{b}_{11}(\tau)(d_4 \bar{\xi}^4 + d_3 \bar{\xi}^3 + d_2 \bar{\xi}^2 + d_1 \bar{\xi} + d_0) \sin \pi \bar{\eta}, \quad \bar{\xi} = (\xi + 1/2), \quad \bar{\eta} = (\eta + 1/2) \quad (4)$$

The notation  $\hat{b}_{11}(\tau)$  is an unknown time function. Coordinate function of deflection is assumed with the product of power series with respect to  $\xi$  and trigonometric function with respect to  $\eta$ , in which the constants  $d_i$  are chosen to satisfy the lateral boundary conditions of edges perpendicular to the  $\xi$  direction. The solution of the compatibility equation (2) can be expressed as  $f = f_0 + f_1$ , where  $f_0$  and  $f_1$  are homogeneous and particular solutions, respectively. Assuming that the particular solution  $f_1$  has same form as the deflection as shown in Eq. (4),  $f_1$  can be determined by equating coefficients in the compatibility equation. The homogeneous solution is assumed as follow:

$$\begin{aligned} f_0 = & \frac{1}{2} p_y \xi^2 + \frac{1}{2} p_x \eta^2 + p_{xy} \xi \eta + \frac{1}{6} p_{ya} \xi^3 + \frac{1}{6} p_{xa} \eta^3 \\ & + \sum_{ns} \left\{ C_{8ns+1} \cosh(\beta ns' \xi) + C_{8ns+2} \sinh(\beta ns' \xi) + C_{8ns+3} \xi \cosh(\beta ns' \xi) + C_{8ns+4} \xi \sinh(\beta ns' \xi) \right\} \sin ns' \bar{\eta} \\ & + \sum_{nc} \left\{ C_{8nc+5} \cosh(\beta nc' \xi) + C_{8nc+6} \sinh(\beta nc' \xi) + C_{8nc+7} \xi \cosh(\beta nc' \xi) + C_{8nc+8} \xi \sinh(\beta nc' \xi) \right\} \cos nc' \bar{\eta} \\ & + \sum_{sn} \sin sn' \bar{\xi} \left\{ C_{8sn+1} \cosh\left(\frac{sn'}{\beta} \eta\right) + C_{8sn+2} \sinh\left(\frac{sn'}{\beta} \eta\right) + C_{8sn+3} \xi \cosh\left(\frac{sn'}{\beta} \eta\right) + C_{8sn+4} \xi \sinh\left(\frac{sn'}{\beta} \eta\right) \right\} \\ & + \sum_{cn} \cos cn' \bar{\xi} \left\{ C_{8cn+1} \cosh\left(\frac{cn'}{\beta} \eta\right) + C_{8cn+2} \sinh\left(\frac{cn'}{\beta} \eta\right) + C_{8cn+3} \xi \cosh\left(\frac{cn'}{\beta} \eta\right) + C_{8cn+4} \xi \sinh\left(\frac{cn'}{\beta} \eta\right) \right\} \end{aligned} \quad (5)$$

In the above expression, the terms with  $p_x, p_y$  correspond to uniform normal stresses,  $p_{xy}$  denotes uniform shear stress and  $p_{xa}, p_{ya}$  denote normal stresses proportionally distribute along the edges. The other terms denote stress distribution with trigonometric functions along  $\xi$  or  $\eta$  directions. The unknown coefficients in the above homogeneous solution can be determined by equating the virtual work by the in-plane forces, which corresponds to the in-plane boundary condition, to be zero as follows.

$$\begin{aligned} & \left[ \int_{-\frac{1}{2}}^{\frac{1}{2}} \left\{ n_x + k_{xp} (u - u_{0ps}) \right\} \delta u d\eta \right]_{\xi=\frac{1}{2}} - \left[ \int_{-\frac{1}{2}}^{\frac{1}{2}} \left\{ n_x - k_{xm} (u - u_{0ms}) \right\} \delta u d\eta \right]_{\xi=-\frac{1}{2}} + \left[ \int_{-\frac{1}{2}}^{\frac{1}{2}} \left\{ n_{xy} + k_{yyp} v \right\} \delta v d\eta \right]_{\xi=\frac{1}{2}} - \left[ \int_{-\frac{1}{2}}^{\frac{1}{2}} \left\{ n_{xy} - k_{ym} v \right\} \delta v d\eta \right]_{\xi=-\frac{1}{2}} \\ & + \left[ \beta \int_{-\frac{1}{2}}^{\frac{1}{2}} \left\{ n_y + k_{yp} (v - v_{0ps}) \right\} \delta v d\xi \right]_{\eta=\frac{1}{2}} - \left[ \beta \int_{-\frac{1}{2}}^{\frac{1}{2}} \left\{ n_y + k_{ym} (v - v_{0ms}) \right\} \delta v d\xi \right]_{\eta=-\frac{1}{2}} + \left[ \beta \int_{-\frac{1}{2}}^{\frac{1}{2}} \left\{ n_{xy} + k_{yxp} u \right\} \delta u d\xi \right]_{\eta=\frac{1}{2}} - \left[ \beta \int_{-\frac{1}{2}}^{\frac{1}{2}} \left\{ n_{xy} - k_{xym} u \right\} \delta u d\xi \right]_{\eta=-\frac{1}{2}} = 0 \end{aligned} \quad (6)$$

Then, substituting Eqs. (4) and (5) to Eq. (1) and applying the Galerkin procedure, the equation of motion is reduced to ordinary differential equations in terms of  $\hat{b}_{11}$  in single-degree-of-freedom system as follows.

$$\hat{b}_{11, \tau\tau} + 2\alpha \omega_1 \hat{b}_{11, \tau} + \alpha^2 \hat{b}_{11} + \beta \hat{b}_{11}^2 + \gamma \hat{b}_{11}^3 - p_d \cos \omega \tau G_1 = 0 \quad (7)$$

Dynamic periodic responses are calculated with the harmonic balance method.

First, a backbone curve is calculated with the present method for a cylindrical shell-panel  $\alpha_x = 10$  whose all edges are classically simply-supported (SSSS). Terms taken for the in-plane stress functions are as follows:  $ns=sn=0, 2, 4, \quad nc=cn=1, 3, 5$ . The rigid line in Figure 2 shows the backbone curve obtained with the present method. The ordinate denoted the frequency normalized by the lowest natural frequency, while the abscissa denotes the maximum amplitude at the center of the panel in free vibration normalized by the thickness of the panel. The backbone curve corresponds to the spring characteristics of softening-and-hardening type. The dotted-and-dashed line is the backbone curve obtained by Kobayashi and Leissa[2], which agree

well with the result obtained with the present method. Figure 2 shows a numerical example of characteristics of restoring force and nonlinear frequency response curve of a cylindrical shell-panel  $\alpha_x = 10, 20, 30$ , one of the edges perpendicular to  $\xi$  direction is clamped while the others are classically simply-supported (SSSC). Terms taken for the in-plane stress functions are as follows:  $ns=sn=0, 1, 2, nc=cn=1, 2, 3$ . As the curvature of the shell-panel increased, the natural frequency becomes higher and softening feature becomes predominant.

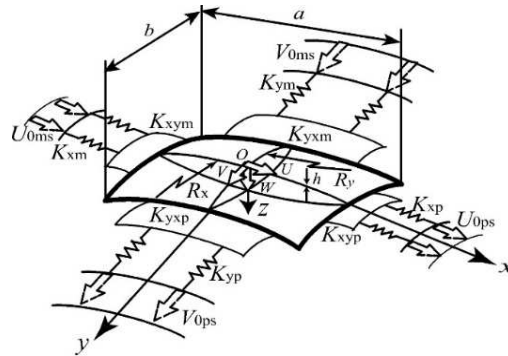


Figure 1. Analytical model of a thin shell-panel.

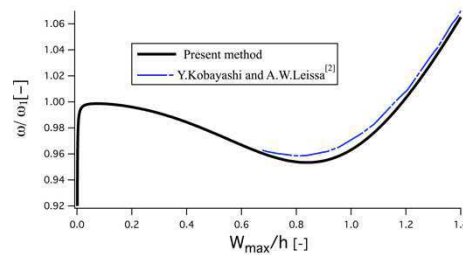


Figure 2. Backbone curves of the thin shell-panel (SSSC).

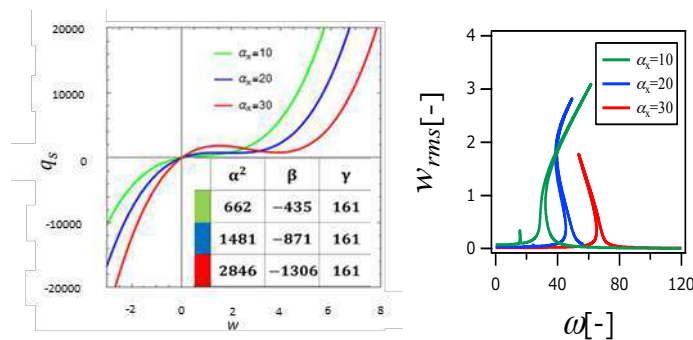


Figure 3. Characteristics of restoring force and nonlinear frequency response curves of the thin shell-panel (SSSC).

## References

- [1] Maruyama, S.; Nagai, K.; Tsuruta, Y.: Modal Interaction in Chaotic Vibrations of a Shallow Double-Curved Shell-Panel. Journal of Sound and Vibration, Vol. 315, pp. 607-625, 2008.
- [2] Kobayashi, Y.; Leissa, A.W.: Large Amplitude Free Vibration of Thick Shallow Shells Supported by Shear Diaphragms. Int. J. Non-Linear Mechanics, Vol. 30, No.1, pp.57-66, 1995.



## Vibration analysis of multi-cracked plates with a roving body using the Rayleigh-Ritz Method

**Yusuke. Mochida<sup>\*</sup>, Sinnah Ilanko**

<sup>\*</sup> The School of Engineering  
The University of Waikato  
Gate 1 Knighton Road Private Bag  
3105 Hamilton 3240 New Zealand  
yusuke@waikato.ac.nz, ilanko@waikato.ac.nz

### Summary

The natural frequencies of a plate having multi-cracks with a roving mass were computed using the Rayleigh-Ritz Method. It is observed that there sudden shifts in the natural frequencies as a roving body crosses cracks. Identifying cracks through frequency measurements attract many researchers for decades for decades but it still remains a challenge due to two main reasons. The frequency changes due to cracks are usually very small and the inverse problem of identifying cracks is further complicated by the fact that the frequencies depend on the number, severity and locations of cracks. However, recently it is shown that for a beam, a roving body that has a rotary inertia causes a sudden shift in frequencies as it passes a crack. In this presentation, we discuss this phenomena for a plate with a roving body and show that the frequencies of a plate with a crack will change abruptly as a mass attached to the plate is moved from one side of the crack to the other. This is potentially useful in detecting cracks in structures, as it is possible to track the changes in the natural frequencies of a structure as a test body (e.g. a vehicle on a bridge) moves and identify points where sudden frequency changes occur. These would then correspond to potential crack locations irrespective of the number and severity of the cracks. To identify a crack and its location all that is needed is an observation of a sudden change in the natural frequencies. The location of the roving body then corresponds to a crack location. This sudden shift in frequency occurs in all modes with the exception of certain cases where the crack is at the nodal line and the use of a cumulative frequency shift parameter also helps to address the difficulty due to frequency changes being too small.

In order to find the natural frequencies of rectangular plates with cracks and a roving body (Figure 1), the Rayleigh-Ritz Method is used. The type of crack considered is that there is a discontinuity in flexural rotation but the translation is continuous such as those considered in beams [1]. The differential rotation is related to the bending moment at the crack and a rotational spring stiffness representing the effective stiffness of the joint. In plates, the crack can also go through the full thickness and in this case, both translation and rotation are discontinuous. The plate is also subject to a roving body, that is, a body whose location is changed to track any change in the frequencies but the body has no velocity relative to the plate. The results are plotted against the location of the roving body.

The crack is modelled in the following way. The plate is formed by assembling several rectangular plates and the coupling between the plates is enforced through distributed penalty stiffness that control the relative translations and rotations between the plate components. A length along which a crack is present is subject to zero or low penalty stiffness but elsewhere along the joint sufficiently high penalty stiffness is applied. To represent a complete (through

thickness) crack both translational and rotational penalty stiffness are set to zero while for flexural cracks, the translational stiffness is set to a high value but rotational stiffness is set to a smaller value. Suitable magnitude of penalty stiffness can be determined by using positive and negative stiffness values [2] which help to ensure that any error due to violation of the continuity is kept within the required accuracy.

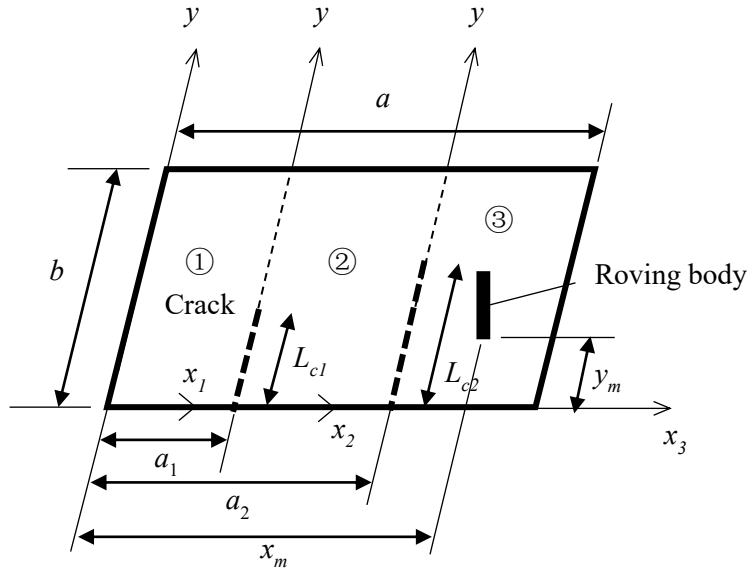


**Figure 1.** A multi-cracked plate with a roving mass.

The plate was subdivided into two rectangular segments (Segment 1, 2, 3) that have the separate coordinates  $(x_1, y)$  and  $(x_2, y)$ , and so on, and for each segment the admissible functions in  $x, y$  directions consisted of a constant, a linear function, a quadratic function and a cosine series [3]. The out-plane displacement plate of a segment of a completely free plate,  $W_k$  ( $k = 1, 2, 3$ ) can be defined by the following equations.

$$w_k(x_k, y, t) = W_k(x_k, y) \sin \omega t \quad (1)$$

with

$$W_k(x_k, y) = \sum_{i=1}^N \sum_{j=1}^N G_{ij} \phi_i(x_k) \phi_j(y) \quad (2)$$

and

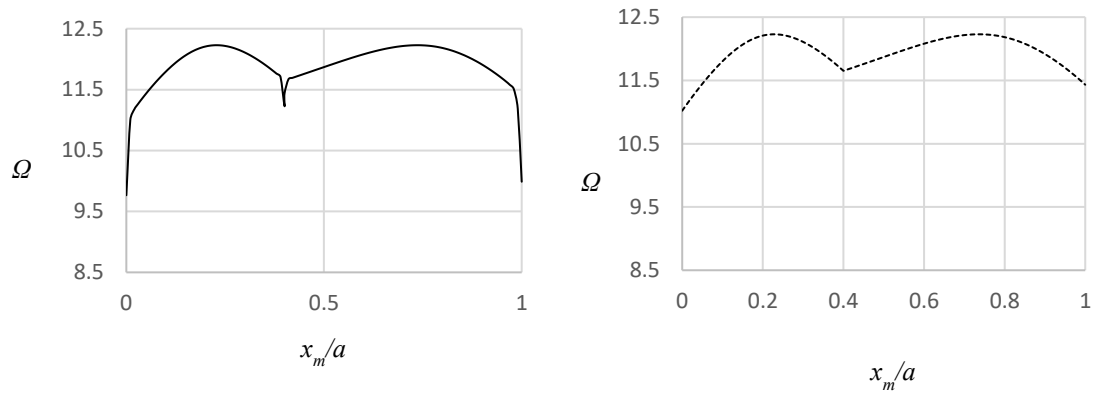
$$\phi_i(x_k) = \left(\frac{x_k}{a_k}\right)^{i-1} \quad \text{for } i = 1, 2 \text{ and } 3$$

$$\phi_i(x_k) = \cos\left(\frac{(i-3)\pi x_k}{a_k}\right) \quad \text{for } i \geq 4$$

where  $\omega$  is the circular frequency and  $t$  is time.  $G_{i,j}$  are undetermined weighting coefficients. The above equations are used to find the strain energy expression and kinetic energy expression, from which the stiffness matrix and mass matrix used in the Rayleigh – Ritz analysis are derived

Figure 2 shows the variation of a non-dimensional first frequency parameter  $\Omega = \omega a^2 (\rho h / D)^{0.5}$  for a completely free square plate with single crack against the location  $(x_m/a)$  of a roving body with (continuous line) and without (dotted line) rotary inertia, for  $y_m = 0.3b$ . With the roving mass

having rotary inertia, it can be seen that there is a sudden change in the frequency parameter when the roving mass passes the crack [4]. The results for other boundary conditions and with multiple cracks will also be presented at the symposium.



The natural frequencies of a plate with cracks parallel to an edge were computed using the Rayleigh-Ritz Method. The obtained frequencies exhibit a sudden shift as a roving body crosses a crack. If the crack is only partial and continuity of translation is maintained, then the frequency shift occurs only when the body possesses a rotary inertia, as has been observed in beams. If the crack is complete (through thickness), which permits differential translation to occur on either side of the crack, a particle having mass only (translatory inertia) is sufficient to cause a sudden shift. Future work would be to study the effect of cracks that are not parallel to an edge, and non-straight cracks. The body used in this study was assumed to possess mass and rotary inertia at a point. The effect of a body of small but finite dimensions also would be investigated.

## References

- [1] Cannizzaro, F.; De Los Rios, J.; Caddemi, S. Calìò, I, Ilanko, S.: On the use of a roving body with rotary inertia to locate cracks in beams, *Journal of Sound and vibration*, Vol 425. pp. 275-300, 2018.
- [2] Monterrubio, L.: The use of eigenpenalty parameters in structural stability analysis, *Proceedings of the Institution of Mechanical Engineers, Part C: Journal of Mechanical Engineering Science*, Vol. 226, pp. 861–870, 2012.
- [3] Monterrubio, L. E.; Ilanko, S.: Proof of convergence for a set of admissible functions for the Rayleigh–Ritz analysis of beams and plates and shells of rectangular planform, *Computers & Structures*, Vol. 147, pp. 236-243, 2014.
- [4] Ilanko, S.; Mochida, Y.; De Los Rios, J.: Vibration analysis of cracked structures as a roving body passes a crack using the Rayleigh-Ritz Method. *EPI International Journal of Engineering*, Vol. 1, No. 2, pp. 30-34, 2018.



## Some Topics on In-plane Vibration of Laminated Rectangular Plates: Analysis, Optimization and Combination

Yoshihiro Narita<sup>\*</sup>, Nobuo Innami<sup>#</sup>

<sup>\*</sup> Hokkaido University (Prof. Emeritus)  
JICA C-Best Project, Faculty of Eng.,  
Hasanuddin University, Gowa,  
Sulawesi Selatan, 92171 Indonesia,  
ynarita@eng.hokudai.ac.jp

<sup>#</sup> Hokkaido Polytechnic College,  
Otaru, Hokkaido, Japan  
innami@hokkaido-pc.ac.jp

### 1. Introduction

The target of research on plate vibration is mainly directed toward bending (out-of-plane) vibration due to practical concern in low frequency range. A vast literature has resulted since 1960's and the famous monograph was compiled by Leissa [1]. It is known, however, that addition of slight curvature to plates causes the coupling between bending and in-plane vibrations, and acoustic noises are often transmitted through inplane vibration of plates embedded in the structure. Considering these, it is meaningful to develop analytical methods for the in-plane vibration of plates. In the past literature, the problem of in-plane vibration has been studied for isotropic plates [2-6] and anisotropic plates [7-11], but comprehensive analytical methods have not been fully developed to cover the laminated rectangular plates under arbitrary boundary conditions. This paper deals with such problem under any sets of free, supported (two types) and clamped edges. The optimization and counting problems are also mentioned.

### 2. Outlines of Analysis, Optimization and Combination

#### 2.1 Ritz method

Consider a symmetrically laminated rectangular plate with dimension of  $a \times b$  and thickness  $h$ . The strain energy and kinetic energy are formulated by

$$V = \frac{1}{2} \iint \{\varepsilon\}^T [A] \{\varepsilon\} dArea, \quad T = \frac{1}{2} \rho \iint \left[ \left( \frac{\partial u}{\partial t} \right)^2 + \left( \frac{\partial v}{\partial t} \right)^2 \right] dArea \quad (1)$$

where  $\{\varepsilon\}$  is a strain vector,  $[A]$  is a  $3 \times 3$  matrix composed of stretching stiffness  $A_{ij}$  and  $\rho$  is mass per unit area. Two in-plane displacements  $u$  and  $v$  in  $x$  and  $y$  directions, respectively, are introduced and written by using non-dimensional coordinates of  $\xi=2x/a$ ,  $\eta=2y/b$  as

$$u(\xi, \eta, t) = \sum_{i=0}^{M-1} \sum_{j=0}^{N-1} P_{ij} X_i(\xi) Y_j(\eta) \sin \omega t, \quad v(\xi, \eta, t) = \sum_{k=0}^{M-1} \sum_{l=0}^{N-1} Q_{kl} X_k(\xi) Y_l(\eta) \sin \omega t \quad (2)$$

where  $P_{ij}$  and  $Q_{kl}$  are unknown coefficients, and  $X_i(\xi)$ ,  $Y_l(\eta)$ ,  $X_k(\xi)$  and  $Y_l(\eta)$  are the functions where geometrical boundary conditions are adjustable [12]. The kinematical boundary conditions for in-plane problem are

$$u \neq 0, v \neq 0 (B_{ul} = B_{vl} = 0): \text{ a free edge (denoted by F)} \quad (3a)$$

$$u \neq 0, v = 0 (B_{ul} = 0, B_{vl} = 1): \text{ a supported edge, (by S1)} \quad (3b)$$

$$u = 0, v \neq 0 (B_{ul} = 1, B_{vl} = 0): \text{ a supported edge (by S2)} \quad (3c)$$

$$u = v = 0 (B_{ul} = B_{vl} = 1): \text{ a clamped edge (by C)} \quad (3d)$$

which are presented along the left-hand edge of  $x = -a/2$  and  $B_{u1}, B_{v1}, \dots$  are boundary index [12].

A frequency parameter  $\Omega = \omega a [\rho(1 - \nu_{LT} \nu_{TL}) / E_T]^{1/2}$  is obtained by minimizing the functional as

$$\partial(T_{max} - V_{max}) / \partial P_{ij} = 0, \quad \partial(T_{max} - V_{max}) / \partial Q_{kl} = 0 \quad (i, k = 0, 1, 2, \dots, (M-1); j, l = 0, 1, 2, \dots, (N-1)) \quad (4)$$

## 2.2 The finite element method

This problem may also be solved by using the finite element method, and the energy expressions used are the same as Eq.(1). Two displacements  $u$  and  $v$  are formulated in the  $x$  and  $y$  directions, respectively, for a rectangular element with four nodes labeled as  $i, j, k, l$ .

$$\begin{Bmatrix} u(x, y) \\ v(x, y) \end{Bmatrix} = \begin{bmatrix} 1 & 0 & x & 0 & y & 0 & xy & 0 \\ 0 & 1 & 0 & x & 0 & y & 0 & xy \end{bmatrix} \{\beta\} \quad \text{with } \{\beta\} = \{\beta_0, \gamma_0, \beta_1, \gamma_1, \beta_2, \gamma_2, \beta_3, \gamma_3\}^T \quad (5)$$

with the four coordinates  $(x_i, y_i), \dots, (x_l, y_l)$  and coefficients  $\beta$  and  $\gamma$  for interpolation, the nodal displacement vector  $\{d_e\}$  and the strain vector  $\{\varepsilon\}$  become

$$\{d_e\} = \{u_i, v_i, u_j, v_j, u_k, v_k, u_l, v_l\}^T = [C]\{\beta\}, \quad \text{i.e., } \{\beta\} = [C]^{-1}\{d_e\} \quad (6)$$

$$\{\varepsilon\} = [Q]\{\beta\} = [Q][C]^{-1}\{d_e\} \quad (7)$$

respectively, where  $[Q]$  is derived from Eq.(5). Substitution of Eq.(7) into (1) yields the strain energy in terms of nodal displacements, and the element strain energy and the element stiffness matrix are given, respectively, by

$$V_e = \frac{1}{2} \{d_e\}^T [K_e] \{d_e\}, \quad [K_e] = \left([C]^{-1}\right)^T \cdot \iint_{Area} [Q]^T [A] [Q] dA \cdot [C]^{-1} \quad (8)$$

Similarly, the element kinematic energy and element mass matrix are derived as

$$T_e = \frac{1}{2} \omega^2 \{d_e\}^T [M_e] \{d_e\}, \quad [M_e] = \left([C]^{-1}\right)^T \cdot \iint_{Area} \rho (u^2 + v^2) dA \cdot [C]^{-1} \quad (9)$$

By using Eqs.(8)(9), the frequency equation for total system is constructed for eigenvalues.

## 2.3 Optimization

The frequency parameters calculated from the Ritz and FEM solutions can be utilized in the optimization, for such purposes as maximizing fundamental frequencies. Since these solution processes are independent from optimization process, any general purpose optimization schemes are applicable, typically the genetic algorithm (GA). Unlike the bending problem where distance of each layer from the middle plane counts, the number of different stacking cases is reduced, for example, the laminates of  $[10^\circ/30^\circ]_s$  and  $[30^\circ/10^\circ]_s$  ( $s$ : symmetric)(first fiber angle being for the outer-most layer) give the identical in-plane stiffness. Because the Ritz method is computationally efficient, search of all combinations for relatively small number of layer is feasible by directly comparing the frequencies of all the combinations.

## 2.4 Combination of boundary conditions

One of the authors has been interested in clarifying the total number of combinations with the same vibration frequencies for all possible sets of boundary conditions along four edges. In bending vibration [12], such counting problem was solved by using Polya counting theory. The same combinatorics approach is used for in-plane vibration of plates.

## 3. Results and Discussion

In numerical examples, the material constants are used that are averaged among three typical sets of constants [13]:  $E_L=150.0$  GPa,  $E_T=10.0$  GPa,  $G_{LT}=5.0$  GPa,  $\nu=0.3$ . Table 1(a) presents convergence characteristics of Ritz method by changing number of term in displacement functions (2) from six terms to twelve in one direction (the resulting matrix sizes are  $72 \times 72, \dots, 288 \times 288$ ). The boundary conditions are denoted, for example, by C-S1-S2-F (in counter-clockwise starting from the left edge with  $x=-a/2$ ). In the table, a solution of  $10 \times 10$  terms generates frequency in well converged values, although the convergence speeds are different depending upon order of modes.

In Table 1(b), the number of elements in the finite element calculation (FEM) is varied from 12×12 to 20×20 in the  $x, y$  directions. Except for the third modes, Ritz solution agree well with values of FEM. The differences are within one percent. It is also noted in Table 1(b) that the all FEM solutions give values monotonically decreasing, thereby showing the solution being upper-bounds. This means that the present two-dimensional element resulted in conforming element in the in-plane vibration problem, while the resulting element derived from similar simple polynomials for the bending is non-conforming element [14] with the slope not being continuous along boundaries of adjoining elements.

Table 2 presents the maximum and minimum frequency parameters  $\Omega_1$  by Ritz 10×10 solution for symmetrically laminated, balanced eight-layer square plates  $[(\theta_1/-\theta_1)/(\theta_2/-\theta_2)]_s$ . The search was made for all combinations of 36×36=1296 times ( $\Delta\theta=5^\circ$ ), and therefore they are exact optimum solutions. One see an index value  $\langle \Omega_{1,max} / \Omega_{1,min} \rangle$  to evaluate the effect of optimization. For five different sets of boundary conditions, the ratios were almost same, being about 2.5.

**Table 1.** Convergence of solutions for symmetric 8-layer square plates with  $[(30^\circ/-30^\circ)_2]_s$ , (BC: C-S1-S2-F,  $b/a=1$ ).

**Table 2.** Optimum design for maximum and minimum frequencies of 8-layer square plate with balanced sequence of  $[(\theta_1/-\theta_1)/(\theta_2/-\theta_2)]_s$ .

Number of term		(a) Ritz solution					B.C.					
$m \times n$	$\Omega_1$	$\Omega_2$	$\Omega_3$	$\Omega_4$	$\Omega_5$		$\Omega_{1,max}$	$\theta_1$	$\theta_2$	$\Omega_{1,min}$	$\Omega_{1,max}/\Omega_{1,min}$	
6x6	2.439	4.183	6.271	6.509	7.560	S1S1S1S1	5.199	65	30	2.215	2.35	
8x8	2.436	4.183	6.248	6.501	7.553	S2S2S2S2	8.718	0	90	3.132	2.78	
10x10	2.434	4.183	6.242	6.501	7.553	CFFF	1.753	35	15	0.690	2.54	
12x12	2.434	4.183	6.240	6.501	7.553	CS1S2F	2.554	40	40	0.991	2.58	
Number of elements		(b) FEM solution					CCCC	9.149	0	90	3.835	2.39
(div.x) × (div.y)	$\Omega_1$	$\Omega_2$	$\Omega_3$	$\Omega_4$	$\Omega_5$							
12x12	2.450	4.219	6.502	6.642	7.642							
16x16	2.444	4.203	6.396	6.579	7.603							
20x20	2.441	4.196	6.343	6.550	7.585							
dif.(%)*	0.3	0.3	1.7	0.8	0.4							
*Difference with Ritz(12x12) solution.												

## References

- [1] Leissa, A.W., NASA SP-160, (1969).
- [2] Bardel, N.S., et al., *J. Sound Vib.*, vol.191 (1996), 459.
- [3] Gorman, D.J., *J. Sound Vib.*, vol.272 (2004), 831.
- [4] Gorman, D.J., *J. Sound Vib.*, vol.276 (2004), 311.
- [5] Gorman, D.J., *J. Sound Vib.*, vol.294 (2006), 131.
- [6] Xing, Y.F., et al., *Int. J. Mech. Sci.*, vol.51 (2009), 246.
- [7] Gorman, D., *J. Sound Vib.*, vol.323 (2009), 426.
- [8] Liu, B., et al., *Euro. J. Mech. A/Solids*, vol.30 (2011), 383.
- [9] Zhang, Y., et al., *Int. J. Mech. Sci.* vol.79 (2014), 15.
- [10] Woodcock, R.L., et al., *J. Sound Vib.*, vol.312 (2008), 94.
- [11] Dozio, L., *Compo. Struct.* vol.93 (2011), 1787.
- [12] Narita, Y., *J. Appl. Mech., Trans.ASME*, vol.67 (2000), 568.
- [13] Narita, Y., et al., *EPI Intl. J. Eng.*, vol.2 (2019) (accepted).
- [14] Narita, Y., *Intl. J. Solids Struct.*, vol.43 (2006), 4342.



## Vibration around non-trivial equilibrium of highly flexible composite thin-walled structures and plates

Alfonso Pagani, Erasmo Carrera, Matteo Filippi, Bin Wu

Mul<sup>2</sup>, Department of Mechanical and Aerospace Engineering  
Politecnico di Torino  
Corso Duca degli Abruzzi 24, 10129 Torino, Italy  
alfonso.pagani@polito.it, erasmo.carrera@polito.it,  
matteo.filippi@polito.it, bin\_wu@polito.it

### Summary

Highly flexible composite thin-walled booms and plates are constantly employed in spacecraft science; applications include, but are not limited to, deployable satellites' instrumentation, antennas, and solar arrays. Generally subjected to large displacements and rotations, these composite structures are prone to suffering vibration and instability phenomena as a consequence of external excitations and operational loadings [1, 2]. Thus, predicting accurately the in-service nonlinear response and the modal characteristics around non-trivial equilibrium states of these thin-walled composite flexible structures is of great importance for design and verification.

In this work, the governing nonlinear equations of lower- to higher-order 1D (beam) and 2D (plate) structural theories for composite laminates are derived as degenerated cases of the three-dimensional elasticity equilibrium via an appropriate index notation and by employing the Carrera unified formulation (CUF), see Ref. [3]. According to CUF, 1D beam theories, for example, can be formulated from the three-dimensional displacement field ( $\mathbf{u}$ ) as an arbitrary expansion of the generalized unknowns ( $\mathbf{u}_\tau$ ); i.e.,

$$\mathbf{u}(x, y, z) = F_\tau^{\text{1D}}(x, z) \mathbf{u}_\tau(y), \quad \tau = 1, 2, \dots, M \quad (1)$$

where  $F_\tau$  are generic functions on the beam cross-section domain,  $M$  is the number of expansion terms, and  $\tau$  denotes summation. In contrast, the generalized displacements are functions of the  $(x, y)$  in-plane coordinates in the case of plate models and  $F_\tau$  represent thickness functions to give:

$$\mathbf{u}(x, y, z) = F_\tau^{\text{2D}}(z) \mathbf{u}_\tau(x, y), \quad \tau = 1, 2, \dots, M \quad (2)$$

Depending on the choice of  $F_\tau$  and the number of expansion terms  $M$ , different classes of beam and plate structural theories can be formulated and, thus, implemented in a straightforward manner [4].

Regardless of the use of 1D or 2D formulations, quasi-static and eventually nonlinear equilibrium states of elastic structures can be found by using the principle of virtual work, which states that the sum of the virtual variation of the internal strain energy and the virtual variation of the work of external loadings is null. As a consequence, small-amplitude vibration of beams and plates subjected to initial pre-stress states and undergoing large displacements and rotations can be analysed by linearizing the virtual variation of the internal work, which – by using CUF, standard finite elements (FEs), the constitutive relations, and the Green-Lagrange strains – reads [5]

$$\begin{aligned} \delta(\delta L_{\text{int}}) &= \langle \delta(\delta \boldsymbol{\varepsilon}^T \boldsymbol{\sigma}) \rangle \\ &= \langle \delta \boldsymbol{\varepsilon}^T \delta \boldsymbol{\sigma} \rangle + \langle \delta(\delta \boldsymbol{\varepsilon}^T) \boldsymbol{\sigma} \rangle \\ &= \delta \mathbf{u}_{\tau i}^T (\mathbf{K}_0^{ij\tau s} + \mathbf{K}_{T_1}^{ij\tau s} + \mathbf{K}_\sigma^{ij\tau s}) \delta \mathbf{u}_{s j} \\ &= \delta \mathbf{u}_{\tau i}^T \mathbf{K}_T^{ij\tau s} \delta \mathbf{u}_{s j} \end{aligned} \quad (3)$$

In Eq. (3),  $\langle \cdot \rangle = \int_V (\cdot) dV$ ,  $\boldsymbol{\varepsilon}$  and  $\boldsymbol{\sigma}$  are respectively the strain and stress vectors,  $\mathbf{u}_{\tau i}$  is the vector of the FE nodal unknowns, and  $\mathbf{K}_T^{ij\tau s}$  is the tangent stiffness matrix in the form of  $3 \times 3$  fundamental nucleus. Note that  $\mathbf{K}_T^{ij\tau s}$  is the sum of  $\mathbf{K}_0^{ij\tau s}$ , which represent the linear stiffness matrix,  $\mathbf{K}_{T_1}^{ij\tau s}$ , which is the nonlinear contribution due to the linearization of the Hooke's law, and  $\mathbf{K}_\sigma$ , which comes from the linearization of the nonlinear form of the strain-displacement equations and is often called the *geometric stiffness*. Given the theory approximation order, these fundamental nuclei can be opportunely expanded in order to obtain the element tangent stiffness matrices of any arbitrarily refined beam and plate models. In other words, by opportunely choosing the theory kinematics (Eqs. (1) and (2)), classical to higher-order FE stiffness arrays can be implemented in an automatic manner by exploiting the index notation of CUF. The explicit derivation of the tangent stiffness matrix is not provided here for the sake of brevity, but it can be found in [6]. Once the global tangent stiffness matrix  $\mathbf{K}_T$  is known, the natural frequencies and mode shapes of the structure can be evaluated by solving the usual eigenvalue problem, which holds:

$$(\mathbf{K}_T - \omega^2 \mathbf{M}) \bar{\mathbf{u}} = 0 \quad (4)$$

where  $\mathbf{M}$  is the FE mass matrix, assumed linear in the present study.

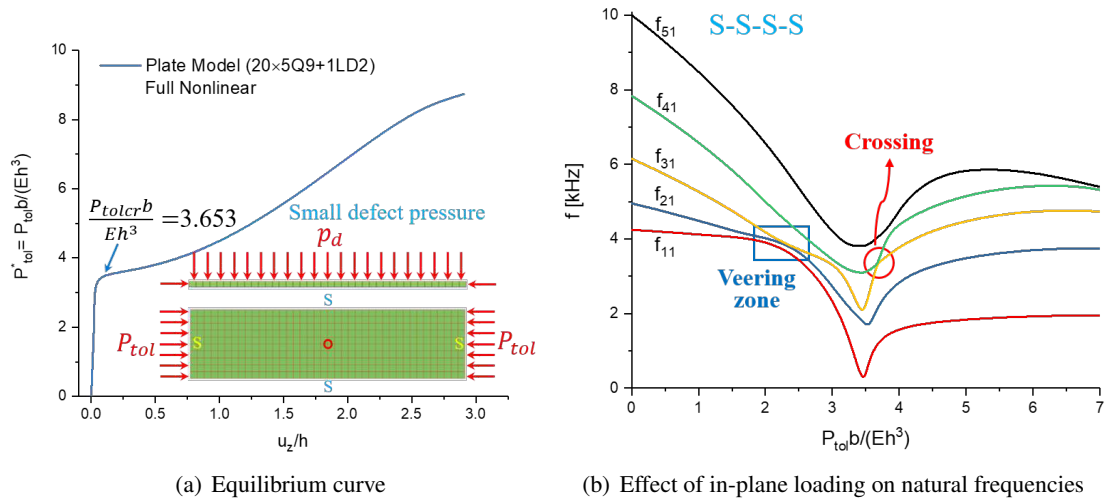


Figure 1: Vibration of simply-supported plate under uni-axial compression.

For representative purposes, Fig. 1 shows the mode aberration of a metallic simply-supported rectangular plate subjected to uni-axial in-plane compression. In particular, Fig. 1(a) shows the static equilibrium curve of the elastic structure under consideration. Note that a small defect pressure is applied to avoid singularities close to the buckling load. Important natural frequencies are thus analysed all along the equilibrium path and shown in Fig. 1(b). It is clear that instabilities, veering phenomena as well as crossing frequencies may arise as a consequence of the operational loadings. Some further considerations can be done:

- The accuracy of the proposed methodology, of course, depends on the capability of the structural theory to describe nonlinear analysis in an accurate manner, which is the case of the present CUF methodology.
- In fact, internal stress distributions are accurate and large-displacement states are described by 3D Green-Lagrange relations.
- The nonlinear vibrations have low amplitudes, so the linearization around discrete states of the equilibrium path and the assumption of harmonic oscillations are legit.

- Inertial work is neglected in the evaluation of the equilibrium path. In other words, vibrations are evaluated around quasi-static equilibrium states.
- The proposed method is able to identify bifurcations, elastic instabilities or buckling phenomena as those conditions which render the tangent stiffness matrix singular.

## References

- [1] Virgin, L. N.: *Vibration of Axially Loaded Structures*. Cambridge University Press, 2007.
- [2] Leissa, A.W.: Looking Back at Curve Veering. *ISVCS9 - Proceedings of 9th International Symposium on Vibrations of Continuous Systems*, pp. 46–48, 2013.
- [3] Carrera, E.; Cinefra, M.; Petrolo, M.; Zappino, E.: *Finite Element Analysis of Structures through Unified Formulation*. John Wiley & Sons, 2014.
- [4] Carrera, E.; Petrolo, M.: Preliminary assessments on the development of refined shell models for free vibrations via machine learning. *ISVCS 2019 - Proceedings of 12th International Symposium on Vibrations of Continuous Systems*, 2019.
- [5] Pagani, A.; Augello, R.; Carrera, E.: Frequency and mode change in the large deflection and post-buckling of compact and thin-walled beams. *Journal of Sound and Vibration*, Vol. 432, pp. 88–104, 2018.
- [6] Pagani, A.; Carrera, E.: Unified formulation of geometrically nonlinear refined beam theories. *Mechanics of Advanced Materials and Structures*, Vol. 25, no. 1, pp. 15–31, 2018.



## Complex Dynamics of Shells under Different Thermal Conditions

**Francesco Pellicano<sup>\*</sup>, Antonio Zippo<sup>#</sup>, Giovanni Iariccio<sup>†</sup>, Marco Barbieri<sup>‡</sup>**

Dept. of Engineering Enzo Ferrari  
University of Modena and Reggio Emilia  
V. Pietro Vivarelli, 10, 41125 Modena, Italy

<sup>\*</sup> [francesco.pellicano@unimore.it](mailto:francesco.pellicano@unimore.it)

<sup>#</sup> [antonio.zippo@unimore.it](mailto:antonio.zippo@unimore.it)

<sup>†</sup> [giovanni.iariccio@unimore.it](mailto:giovanni.iariccio@unimore.it)

<sup>‡</sup> [mark@unimore.it](mailto:mark@unimore.it)

### Summary

Thin walled structures play a key role in different fields of structural engineering thanks to the high strength-to-weight ratio. For example: in aerospace industry, shells and plates are commonly used in the structural part of fuselages and wings of aircrafts; in energy production industry, pipes and heat exchangers are made of thin structures subjected to strong temperature gradients. Despite the simplicity of plates and shells, the dynamics of these components exhibit a great complexity.

In 1992, Noor and Burton [1] published an extensive review on computational models applied to thermomechanical problems of plates and shells made of composite material.

Alijani and Amabili [2] on the subject of the nonlinear vibrations of shells.

Zippo et al [32] investigated the dynamics of pre-compressed circular cylindrical shells by experiments, both in linear and nonlinear fields.

The aim of the present work is to investigate the dynamic scenario of shells under mechanical and thermal loads. The nonlinear dynamics of polymeric circular cylindrical shells with top mass subjected to axial harmonic excitation has been investigated. The present work is fully experimental.

### Test description

A thin circular cylindrical shell made of polyethylene terephthalate (PET) is tested. The position of the shell is vertical and the base is vibrating. A cylindrical mass made of aluminum alloy is glued to the top edge of the shell. The bottom side of the structure is clamped to a vibration table adapter (VTA) by means of a steel bolted ring.

a)

b)

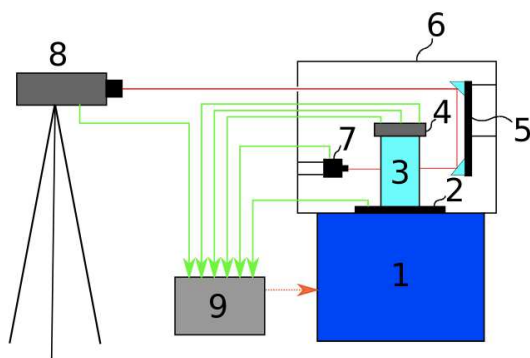


**Figure. 1** - Experimental setup: (1) shaker, (2) VTA, (3) shell, (4) top mass, (5) periscope, (6) climatic chamber, (7) laser telemeter, (8) laser vibrometer, (9) control and data acquisition.

A stepped sine vibration is imposed to the seismic base with the aim of exciting the first axisymmetric mode of vibration of the shell.

Several homogeneous temperature conditions are considered ( $-5^{\circ}\text{C}$ ,  $10^{\circ}\text{C}$ ,  $25^{\circ}\text{C}$ ,  $45^{\circ}\text{C}$ ) as well as different drive excitation levels (0.1 V, 0.2 V, 0.3 V, 0.4 V).

Fig. 2 shows amplitude-frequency curves at 0.4 V of drive excitation amplitude with upward frequency variations. The voltage input amplitude is related to the vibration level of the shaker base. For example, the base acceleration amplitude varies from 210  $\text{m/s}^2$  to 110  $\text{m/s}^2$  at  $25^{\circ}\text{C}$ .

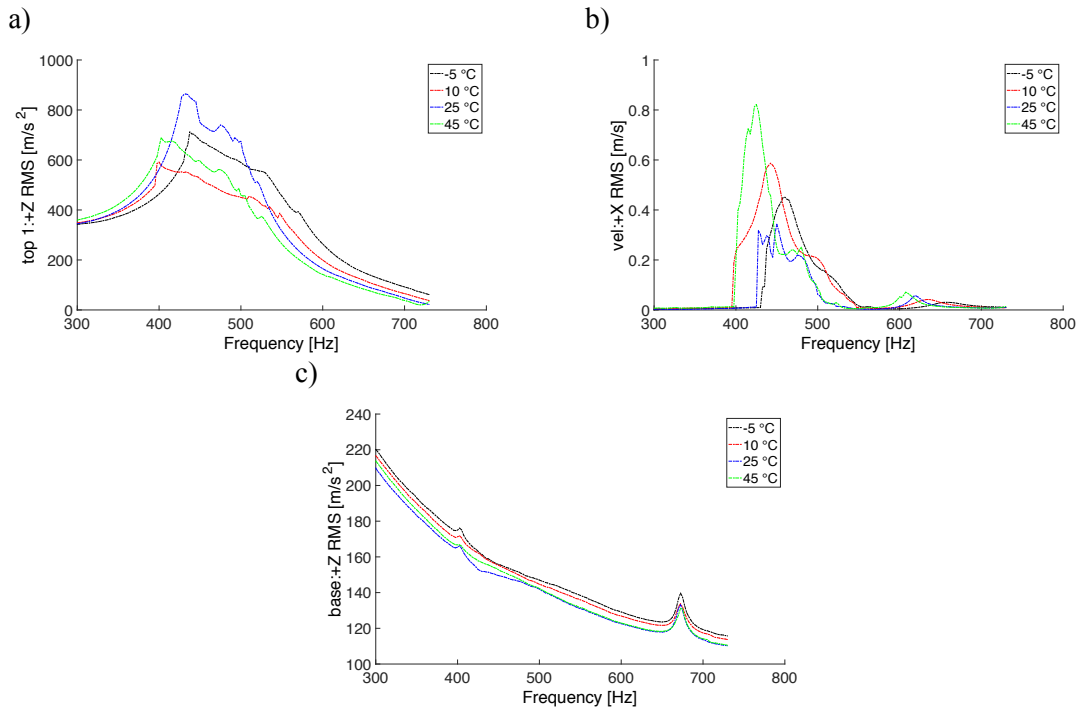


Figure. 2 – Amplitude-frequency: a) Top, b) Shell, c) Base

The top mass acceleration amplitude shows the resonance of the first axisymmetric mode (at about 473 Hz at  $25^{\circ}\text{C}$ ); far from the exact resonance, the amplitude frequency curves of the three top accelerometers (vertical direction) follow the expected behavior of a linear resonance; conversely, there is a region close to the resonance where the response does not present the standard aspect and a saturation phenomenon takes place.

In order to complete the analysis of the dynamic scenario, in this section the bifurcation diagrams of the Poincaré maps are presented.

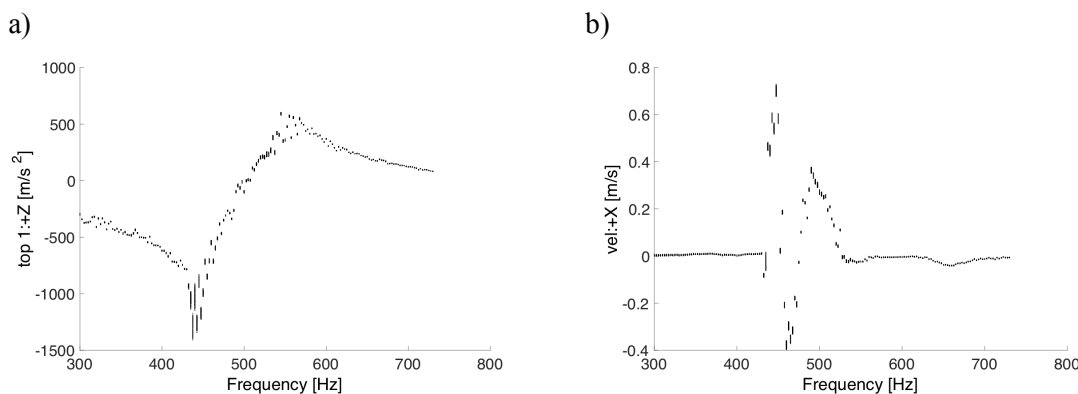
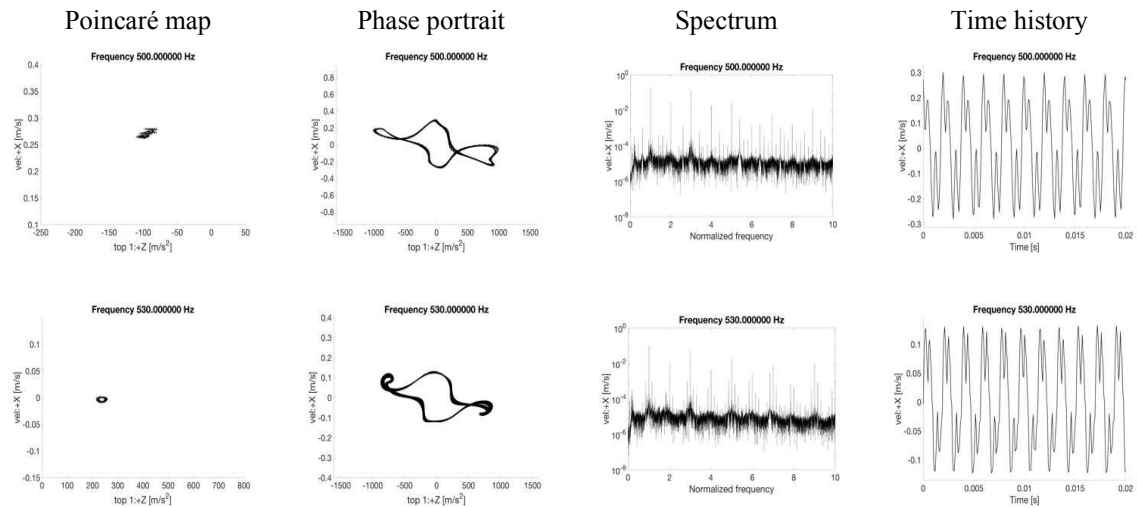


Figure. 3 – Bifurcation diagrams: a) Top, 2) Shell,

Fig. 3 shows the bifurcation diagrams and the spectrograms carried out with 0.4 V of drive amplitude at  $T=-5^{\circ}\text{C}$ . Upward frequency variation is considered. The top mass motion is periodic up to 430Hz; when the saturation/instability occurs, a non-stationary motion takes place from 430 to 570Hz, at higher frequencies the top mass vibration becomes regular, i.e. periodic. This is in perfect agreement with the analysis of the amplitude-frequency diagrams and the instability region identified in the previous section.

Table 1 shows details of the dynamic scenario for the most interesting regimes, in particular: i) 1/3 sub-harmonic response, three point on the Poincaré map and a spike in the spectrum at 1/3 the excitation frequency; ii) a quasi-periodic response characterized by a continuous closed trajectory on the Poicaré map and sidebands on the spectrum.

**Tab. 1-** Poincaré maps , Phase portraits, Fourier spectra, Time histories, - 0.4 V -  $T = -5^{\circ}\text{C}$  –



## Conclusions

The effects of extreme homogeneous temperature conditions on nonlinear dynamics of polymeric shell, interacting with a top mass, have been experimentally analyzed. Tests are carried out in controlled environmental conditions.

A parametric excitation is induced by the base motion and a saturation of the top mass vibration takes place the first axisymmetric vibration mode is resonant.

Through the bifurcation analysis, it was possible to obtain deeper information. Within the saturation region, shell nonlinear dynamics is emphasized by high temperature. For low temperatures, the response is periodic or quasi-periodic with the spectra dominated by the fundamental harmonics. On the other hand, high temperatures lead to a less stable behavior of the structure, i.e. a tendentially more chaotic response, with broad spectra.

## References

- [1] A. K. Noor and W. S. Burton, "Computational Models for High-Temperature Multilayered Composite Plates and Shells," *Appl. Mech. Rev.*, vol. 45, no. 10, p. 419, 1992.
- [2] F. Alijani and M. Amabili, "Non-linear vibrations of shells: A literature review from 2003 to 2013," *Int. J. Non. Linear. Mech.*, vol. 58, pp. 233–257, 2014.
- [3] A. Zippo, M. Barbieri, and F. Pellicano, "Experimental analysis of pre-compressed circular cylindrical shell under axial harmonic load," *Int. J. Non. Linear. Mech.*, vol. 94, no. June 2016, pp. 417–440, 2017.



## On the analysis of 1D impacting rods of arbitrary cross section and with arbitrary material parameters.

Burgert Jens, Seemann Wolfgang

Institute of Dynamics/Mechatronics  
 Karlsruhe Institute of Technology  
 Kaiserstraße 10, 76131 Karlsruhe, Germany  
 jens.burgert@kit.edu, wolfgang.seemann@kit.edu

Impacting rods are used in several applications of every day life tools. In this contribution a theoretical model to calculate the stress wave propagation of two impacting rods of arbitrary cross section and arbitrary material properties is presented. Finally, the semi-analytical results are compared with experimental results which yields good agreement.

### Theoretical model

The theoretical model presented is based on traveling waves in rods. The geometries of the rods are approximated by a large number of elements with different lengths  $\ell_j$ . The material properties density  $\rho$ , Young's modulus  $E$  and the geometry  $A$  can vary from element to element but are constant within each element. On an element with constant material parameters the solution of the governing partial differential equation for the displacements of the rods simplifies to the well-known wave equation which can be solved analytically [1]. The element lengths are determined so that all wave fronts of the elements arrive after the time step  $\Delta t$  at the end of the element

$$\ell_j = \sqrt{\frac{E_j}{\rho_j}} \Delta t = c_j \Delta t, \quad (1)$$

where  $c_j$  is the constant wave propagation speed in element  $j$ .

At the beginning of each timestep at  $t = t^-$  the rods are in equilibrium, which means that both the stress  $\sigma$  and the velocity  $v$  is constant within the elements (Figure 1 a)). The superscripts  $+/-$  relate to the right/left element border. In case of the time  $t$  the superscripts refer to the time immediately after (superscript  $+$ ) or just before (superscript  $-$ )  $t$ . If  $\sigma_{j-1,t^-} \neq \sigma_{j,t^-}$  stress waves start to

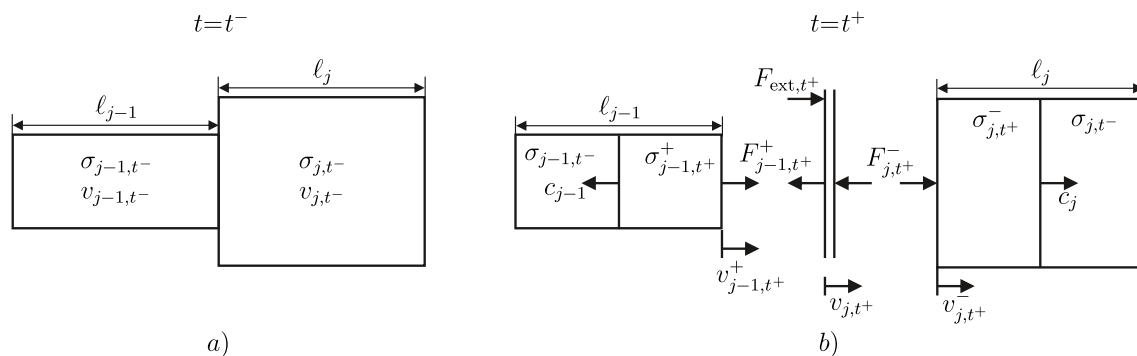


Figure 1: Elements in equilibrium at time  $t = t^-$  a) and straight after at  $t = t^+$  b).

propagate into the elements at time  $t^+$ . By claiming force and displacement/velocity equilibrium

at the transition zones

$$F_{j-1,t^+}^+ + F_{j,t^+}^- = F_{\text{ext},t^+} \quad (2)$$

$$v_{j-1,t^+}^+ = v_{j,t^+} = v_{j,t^+}^- \quad (3)$$

and applying the momentum conservation formula [2]

$$F_{j,t^+}^- = -F_{j,t^-} + \rho_j A_j c_j (v_{j,t^+}^- - v_{j,t^-}) \quad (4)$$

$$F_{j-1,t^+}^+ = F_{j-1,t^-} + \rho_{j-1} A_{j-1} c_{j-1} (v_{j-1,t^+}^+ - v_{j-1,t^-}) \quad (5)$$

the velocities  $v_{j,t^+}^-$ ,  $v_{j-1,t^+}^+$  and the forces  $F_{j,t^+}^-$ ,  $F_{j-1,t^+}^+$  at  $t^+$  can be calculated. Applying the momentum conservation formula within each element leads to

$$F_{j,t+\Delta t^-} = F_{j,t^+}^+ - F_{j,t^+}^- - F_{j,t^-} \quad (6)$$

$$v_{j,t+\Delta t^-} = v_{j,t^+}^+ + v_{j,t^+}^- - v_{j,t^-} \quad (7)$$

the new forces  $F_{j,t+\Delta t^-}$  and velocities  $v_{j,t+\Delta t^-}$  in equilibrium at time  $t + \Delta t^-$ . Finally, the external forces  $F_{\text{ext}}$  are updated and a new timestep begins.

### Setup of the test rig

In Figure 2 the schematic sketch of the setup of the single hit test rig is depicted. The gun pneumatically accelerates a piston that hits a rod which is at rest. At the exit of the gun channel the impact velocity is measured by a photoelectronic fork sensor.

On the rod, several strain gauges are attached. Its signals are amplified and filtered by a low pass filter with cutoff frequency 40kHz. In order to get a better insight during the impact, i.e. to detect the impact time, a high speed camera which is illuminated by an LED light records the impact.

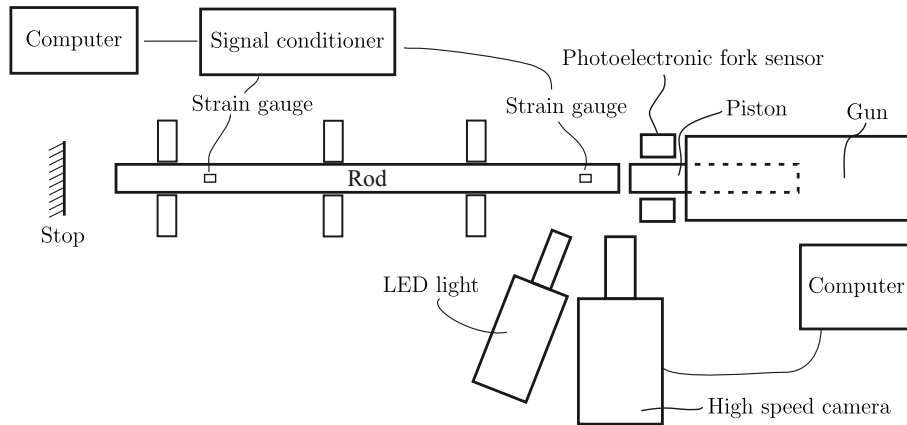


Figure 2: Schematic sketch of the test rig.

### Results and discussion

The PE rod is mounted freely at its other end. The dimensions of both steel piston and PE rod and the position of the strain gauges (SG) are depicted in Figure 3. In Figure 4 the results yielded by the strain gauge measurements are compared with the semi-analytical results. After a short dead time the wave front arrives at the first strain gauge (Figure 4 a)) with a compression stress

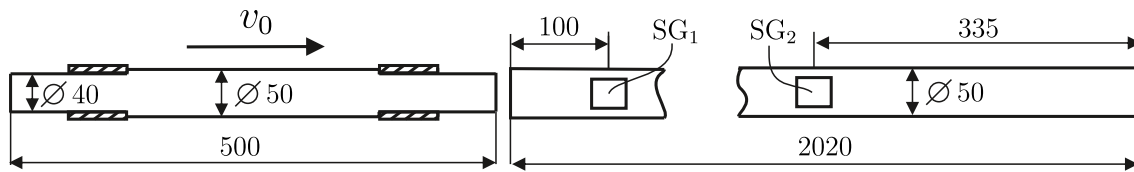


Figure 3: Dimensions in mm of piston (left) and rod (right) and position of the strain gauges (SG).

jump. The wave propagation speed of the piston is faster and the length is smaller compared to the rod. Therefore, the incident waves of the piston are reflected several times at its free end and transmitted into the rod at the impact zone before the wave front of the rod first reaches its free end. Thus, the absolute value of the compression stress decreases continuously. At  $t \approx 3.6$  ms the reflected tensile stress arrives at the first strain gauge which leads to a positive stress jump. Shortly after, when the tensile stress wave reaches the transition zone, rod and piston separate.

After  $t \approx 1.3$  ms the wave front reaches the second strain gauge and leads to a smaller compression

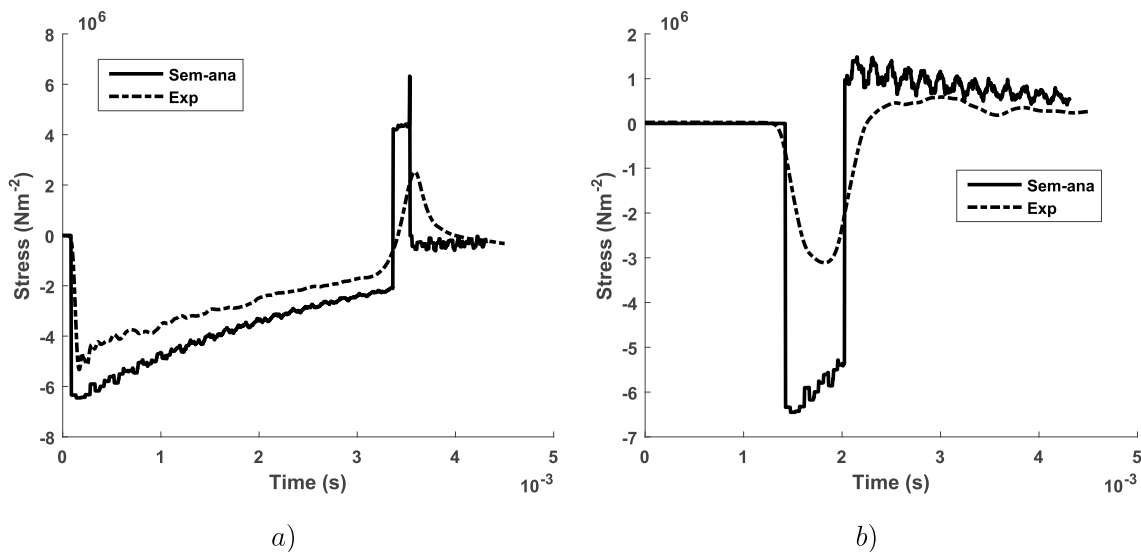


Figure 4: Comparison of semi-analytical and experimental results at first *a)* and second *b)* strain gauge.

stress jump. Since the position of the second strain gauge is close to the free end, the width of the stress pulse is much smaller compared to the first strain gauge as the reflected tensile stress arrives shortly after the compression stress wave arrived.

Comparing the semi-analytical with the experimental results yields good qualitative accordance. However, the quantitative behavior does not match perfectly, especially for the second strain gauge. A possible reason is that the internal damping is not yet considered in the semi-analytical model.

## References

- [1] Hagedorn, P.; DasGupta, A.: Vibrations and Waves in Continuous Mechanical Systems. Wiley, 2007.
- [2] Shorr, B. F.: The Wave Finite Element Method. Springer, 2004.



## On the Stability of Parametrically Excited Continuous Gyroscopic Systems

Alessandro De Felice, Silvio Sorrentino

Department of Engineering *Enzo Ferrari*  
University of Modena and Reggio Emilia  
Via Vivarelli 10, 41125 Modena, Italy  
[alessandro.defelice, silvio.sorrentino]@unimore.it

### Summary

Gyroscopic effects on the stability of parametrically excited continuous rotor systems are clarified with respect to incomplete and/or incorrect conclusions found in the literature, presenting novel theoretical developments and computational results.

Stability analysis of continuous parametrically excited rotor systems is a topic of both relevant theoretical interest and practical importance. Several studies can be found in the literature, dealing on stability analysis of continuous rotating shafts [1, 2] or continuous cylindrical shells [3, 4] under periodic axial forces, or more in general on conditions for rotordynamic stability under combined axial forces and torques. In all the mentioned works (and in many others, as reported in [5]), however, an improper application of Bolotin's method [6] led to wrong conclusions (single and double period critical solutions with apparent destabilizing effects due to gyroscopic terms).

As case-study including all features of interest, a continuous perfectly balanced shaft is herein considered, modelled as a spinning Timoshenko beam loaded by axial end thrust and twisting moment oscillating at the same period. The equations of motion of this parametrically excited continuous system, in the form of a set of coupled partial differential Mathieu–Hill equations with gyroscopic terms, read:

$$\begin{cases} \rho A \ddot{v} - \kappa GA (v'' - \vartheta_z') - N \vartheta_z' = 0 \\ \rho A \ddot{w} - \kappa GA (w'' + \vartheta_y') + N \vartheta_y' = 0 \\ \rho J \ddot{\vartheta}_y + \rho J_0 \omega \dot{\vartheta}_z + (\kappa GA - N)(w' + \vartheta_y) - EJ \vartheta_y'' - T \vartheta_z' = 0 \\ \rho J \ddot{\vartheta}_z - \rho J_0 \omega \dot{\vartheta}_y - (\kappa GA - N)(v' - \vartheta_z) - EJ \vartheta_z'' + T \vartheta_y' = 0 \end{cases} \quad (1)$$

where (according to Fig. 1 left and adopting dots and roman numbers for differentiation with respect to time  $t$  and to the spatial variable  $x$ ),  $v$  and  $w$  are the displacements in the  $y, z$  directions,  $\vartheta_y$  and  $\vartheta_z$  are the angular displacements about the  $y, z$  axes,  $\rho$  is the density of the shaft,  $A$  is its cross-section area,  $J$  its moment of inertia,  $E$  is the Young's modulus,  $G$  is the shear elasticity modulus,  $\kappa$  is the transverse shear factor,  $\omega$  is the angular speed,  $N$  is the time-dependent (harmonic) external end thrust (positive if tensile),  $T$  is the time-dependent (harmonic) external twisting moment (positive if counterclockwise) [7]. Damping terms can be added to Eqs. (1), for modelling either external (non rotating) and/or internal (rotating) damping distributions.

Since in this kind of problem the classical Bolotin method cannot be applied (due to the presence of gyroscopic terms), and the computation of the transition matrix within Floquet analysis would carry overwhelming difficulties, a different approach is herein adopted: after Galerkin discretization of the equations of motion, stability of Floquet solutions is studied via eigenproblem formulation, obtained by applying the harmonic balance method. A numerical algorithm is then developed to compute global stability thresholds for the whole continuous system in presence of both gyroscopic and damping terms. Stability charts are represented as Ince–Strutt diagrams, with a frequency parameter  $\delta$  and an amplitude parameter  $\varepsilon$  defined as for the single degree of freedom Mathieu–Hill equation:

$$\delta = \Omega^2 / \omega_L^2, \quad \varepsilon = \Delta L \quad \delta = \Delta L (\Omega^2 / \omega_L^2) \quad (2)$$

In Eq. (2)  $\omega_L$  is the angular frequency of the external load harmonic component,  $\Delta L$  its amplitude, and  $\Omega$  a characteristic angular frequency defined by the mechanical properties of the shaft, replacing the natural angular frequency of the single degree of freedom system.

Gyroscopic effects on stability are first investigated in the undamped case, considering the angular speed (in dimensionless form  $\hat{\omega} = \omega / \Omega$ ) as independent from the frequency parameter  $\delta$ , and noticing that the associated time-invariant system (at  $\varepsilon = 0$ ) is merely stable [8].

As a first result, in this study it has been demonstrated that due to gyroscopic terms in the continuous system, the single-period and double-period solutions are not critical solutions anymore, meaning that the collision points of the Floquet multipliers [9] (laying on the unit-circle, in absence of damping) are no longer the two points on the real axis (+1, 0) and (-1, 0), as shown in Fig. 1 right. In fact, when  $\hat{\omega} \neq 0$  each pair of coincident values of natural frequency  $\omega_n$  separate into two distinct values  $\omega_{nf} > \omega_{nb}$  (forward and backward values), and consequently also the Floquet multipliers for each eigenvalue separate into two pairs of counter-rotating points on the unit circle. In addition, simple analytical expressions have been found for the critical values of  $\delta$  at  $\varepsilon = 0$  (points on the  $\delta$  axis of the stability chart from which the instability regions originate, as shown Fig. 2 left) and for the related critical eigenvalues  $\lambda$  (which on the unit circle form quadruplets of points out of the real axis, as shown in Fig. 1 right), in both cases as functions of the  $n$ -th forward and backward eigenfrequencies:

$$\delta_{nk,\varepsilon=0}^{crit} = \frac{k^2}{(\omega_{nf} + \omega_{nb})^2}, \quad \lambda_{nk,\varepsilon=0}^{crit} = \frac{ik}{2} \left[ 1 \pm \left( \frac{\omega_{nf} - \omega_{nb}}{\omega_{nf} + \omega_{nb}} \right) \right] \quad (3)$$

in which  $k$  is an integer index defining the sequence.

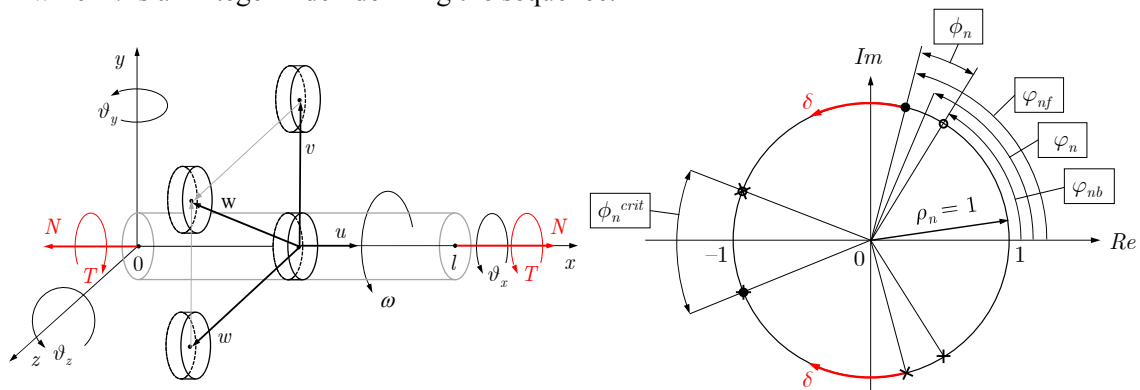


**Figure 1.** Left: Schematic of the continuous rotating shaft. Right: Floquet multipliers on the unit circle in presence of gyroscopic effects.

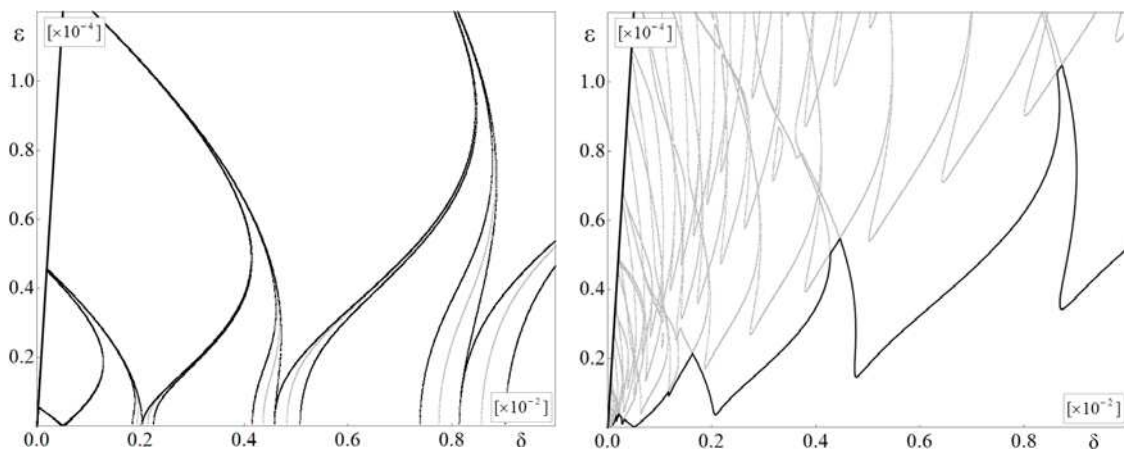


**Figure 2.** Left: Ince-Strutt stability map with undamped gyroscopic effects for eigenvalue 1. Right: gyroscopic effects with external damping for the continuous shaft ( $\zeta_0 = 0.01$ ).

Figure 2 left displays the sequence of stability thresholds obtained for the first eigenvalue of the continuous shaft: the black curve with downward spikes represents the actual threshold, while the lateral grey and black curves lay in the stable domain (the whole areas between each pair of grey curves, due to single and double period solutions, were erroneously identified as instability regions in several studies).

Another result comes from considering the effect of continuous damping distributions. They play an essential role in making stability charts readable for practical purposes, producing substantial clearing of high-order mode contributions to global stability regions, with great advantage in terms of reduction of computational load, which would otherwise become prohibitive.

On stability charts, external damping affects mainly the downward spikes of modal instability regions (producing smoothing and contractions, with stabilizing effects, as in Fig. 2 right), while it has been found that internal damping (even in very small amount) acts significantly on their lateral borders (producing merging, with potential destabilizing effects induced by angular speed).

In Fig. 2 right a superposition of modal sequences of instability regions is displayed (grey curves), and the black curve identifies the stability threshold (global stability region in the lower part of the map, given by the complement area with respect to the union of all sequences of modal instability regions). Modal interactions grow with  $\Delta L$ , due to coupling of the equations of motion, showing that the stability charts for the continuous system cannot be represented by mere superpositions of scaled single degree of freedom Ince–Strutt diagrams.

Regarding the external load components, the effects of harmonic axial end thrusts are dominant, while those of harmonic twisting moments are practically negligible. It is also worth pointing out that in all cases considered the operation lines ( $\varepsilon = \Delta L \delta$ ) related to equivalent first Euler's critical loads are well into the unstable regions, which clearly means that critical load analysis is generally not sufficient for assessing the stability of parametrically excited continuous rotors.

## References

- [1] Chen L.W.; Ku D.M.: Dynamic stability analysis of a rotating shaft by the finite element method. *Journal of Sound and Vibration*, Vol. 143, No. 1, pp. 143–151, 1990.
- [2] Lee H.P.: Effects of axial base excitations on the dynamic stability of spinning pre-twisted beams. *Journal of Sound and Vibration*, Vol. 185, No. 2, pp. 265–278, 1995.
- [3] Ng Y.T.; Lam K.Y.; Reddy J.N.: Parametric resonance of a rotating cylindrical shell subjected to periodic axial loads. *Journal of Sound and Vibration*, Vol. 214, No. 3, pp. 513–529, 1998.
- [4] Liew K.M.; Hu Y.G.; Ng T.Y.; Zhao X.: Dynamic stability of rotating cylindrical shells subjected to periodic axial loads. *International Journal of Solids and Structures*, Vol. 43, pp. 7553–7570, 2006.
- [5] Yong-Chen P.: Stability boundaries of a spinning rotor with parametrically excited gyroscopic system. *European Journal of Mechanics A / Solids*, Vol. 28, pp. 891–896, 2008.
- [6] Bolotin V.V.: *The dynamic stability of elastic systems*. Holden–Day, 1964.
- [7] De Felice A.; Sorrentino S.: Insights into the gyroscopic behaviour of axially and torsionally loaded rotating shafts. *ICSV24 – Proceedings of 24<sup>th</sup> International Conference on Sound and Vibration*, London, United Kingdom, paper 879, 2017.
- [8] Lancaster P.: Stability of linear gyroscopic systems: a review. *Linear Algebra and its Applications*, Vol. 439, pp. 686–706, 2013.
- [9] Yakubovich V.A.; Starzhinskii V.M.: *Linear differential equations with periodic coefficients*. Wiley, 1975.



## Free Vibrations of Curved Periodic Beams and Combinations

Shudong Ding, Jinghui Wu, Chunlei Bian, Yangyang Zhang, Longtao Xie, Ji Wang

MOE Key Laboratory of Impact and Safety Engineering,  
School of Mechanical Engineering and Mechanics, Ningbo University  
818 Fenghua Road, Ningbo, Zhejiang 315211, CHINA  
{wangji, zhangyangyang, xielongtao}@nbu.edu.cn

### Summary

Curved beams are frequently used in modern structures of civil and mechanical engineering as typical loading resistance elements and the latest use of curved beams is directly related to the 3D-printing technology for the rapid generation of periodic patterns and their combinations to form structures of novel configurations. To satisfy the needs of conceptual initiation and evaluation of structural properties, the vibration characteristics of curved periodic beams are studied. With existing knowledge of curved beams, the analysis can only be done with numerical methods for the considerations of arbitrary configurations. In our study, we choose the Rayleigh-Ritz method as the analytical procedure with accuracy and efficiency. By using the simple functions for displacement approximation, accurate results of vibration frequencies and mode shapes are obtained. The approximate results have also been validated with finite element analysis.

With the successful analysis of vibrations of curved plane beams, the curved periodic beams and the combinations of beam elements can also be analyzed. We shall present the analytical results with the comparison from finite element analysis to establish a complete procedure. In the future study, the higher-order theory of curved beams can be established and more vibration modes including torsion will be included. It is expected that our analytical method and procedure will be able to calculate all vibration modes of curved beams and combinations for accurate design of curved beam elements in association with the 3D-printing technology. Eventually, we should be able to analyze vibrations of curved beams with an efficient analytical method. This study will concentrate on beam theories and the analytical procedure which is further complicated due to the introduction of additional deformation in curved beams.

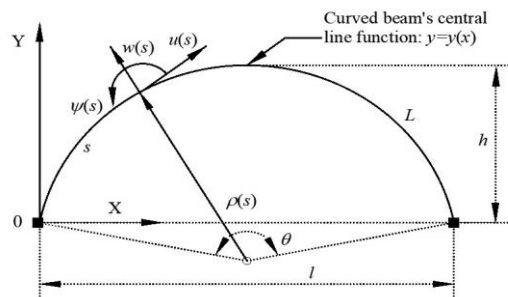


Fig 1. The geometry of a curved beam

For a generalized plane curved beam shown in Fig 1, the popular Euler-Bernoulli beam theory can be used for the analysis of vibrations for the frequency and mode shapes with known functions of the axial curve and boundary conditions. However, generally speaking, the analytical solutions are only available with special cases of the axial curve and boundary conditions. In most cases, numerical methods including the Rayleigh-Ritz and finite element methods have to be employed for accurate solutions.

If a curved beam has a smaller length and large area of cross-section, or the shear deformation cannot be neglected, the Timoshenko variational equation of vibrations of a curved beam will have the form of

$$\delta \int_{t_1}^{t_2} \left[ \frac{1}{2} \int_L (\gamma A w_{,t}^2 + \gamma I \psi_{,t}^2 + \gamma A u_{,t}^2) ds - \frac{1}{2} \int_L (EI \psi_{,s}^2 + k_q G A \beta^2 + E A u_{T,s}^2) ds \right] dt = 0 \quad (1)$$

where  $L$ ,  $\gamma$ ,  $A$ ,  $E$ ,  $I$ ,  $k_q$ ,  $G$ ,  $\beta$ ,  $w$ ,  $u$ ,  $\psi$  and  $u_T$  ( $du_T(s)/ds = du(s)/ds + w(s)/\rho(s)$ ) are the full length of curved beam, material density, cross-sectional area, the Young's modulus, the area moment of inertia, the shear correction factor, shear modulus, the rotation due to shear, the radial displacement, the tangential displacement, the rotation due to bending along the tangential direction, and the total tangential displacement, respectively. Equation (1) now includes the flexural, shear, and extensional displacements. With the increase of numbers of displacements and couplings of vibration modes, the analytical solutions will be more difficult and only the numerical solutions can be expected in general cases.

With the objective of accurate analysis of in-plane vibrations of curved beams, the actual models are typically curved elements we frequently encounter from the 3D-printing technology. In addition to the rare configuration we are not familiar with from traditional manufacturing process, there are also periodic beam elements with large number of unit cells from today's manufacturing technology. As mentioned earlier, we choose the Rayleigh-Ritz method to calculate natural frequencies and modes. The formulation of the solution procedure with the Rayleigh-Ritz method is straightforward with displacement solutions satisfying boundary conditions. The differences in the beam theories require the different displacements in the calculation of strain and kinetic energies. Our analysis has been shown that with the increase of independent displacements, the resulted eigenvalue problem will also be larger, and the numerical procedure will then be challenging because of a much larger matrix problem which is also sensitive in numerical calculations. To provide accurate solutions to the benchmark problems, the simplest approach is the finite element solutions with COMSOL. The results from this study and earlier publications have been validated with examples [2]. Table 1 shows nondimensional frequency parameters for circular curved beams by the Euler-Bernoulli beam theory. It is shown that the larger length to radius ratio will require more computing time and the

**Table 1.** Nondimensional Frequency  $\Omega = \omega L^2 \sqrt{\gamma A / EI}$  for Circularly Curved Beams with Simply Supported Ends

$L/R$	$m=1$			$m=2$			$m=3$		
	FEM	Ref. [2]	Present	FEM	Ref. [2]	Present	FEM	Ref. [2]	Present
--	9.8685	9.8696	9.8696	39.478	39.478	39.478	88.825	88.827	88.826
0.01	10.352	10.351	10.351	39.478	39.478	39.478	88.834	88.832	88.832
0.1	32.466	32.467	32.467	39.452	39.453	39.453	89.500	89.501	89.501
1	37.093	37.092	37.092	82.191	82.184	82.184	155.47	155.48	155.47
$\pi$	22.371	22.367	22.367	68.296	68.288	68.287	137.89	137.92	137.87

convergence is also not uniformly stable. Table 2 shows nondimensional frequency parameters for sinusoidally shaped curved beams formulated and calculated by the Timoshenko beam theory with the inclusion of extensional deformation. And the value of ratio of arc height to span of sinusoidal-shaped curved beams is 0.0318, which is a relatively small number. It is found that the convergence is quite sensitive to this ratio. We presented the validated results for small arc height

to span ratios, and further investigation is being performed to find limitations and remedies for beams with larger ratios. Since the vibration frequencies of curved beams are normalized with the nondimensional frequency  $\Omega = \omega L^2 \sqrt{\gamma A / EI}$ , the actual frequencies in Table 2 are to be calculated for different length.

**Table 2.** Nondimensional Frequency  $\Omega = \omega L^2 \sqrt{\gamma A / EI}$  for Sinusoidally Curved Beams with Simply Supported Ends

Order	One half wavelength		Two half wavelengths		Three half wavelengths		Four half wavelengths	
	FEM	Present	FEM	Present	FEM	Present	FEM	Present
1	57.910	57.906	14.537	14.537	14.552	14.552	14.555	14.555
2	130.56	130.54	129.51	129.51	57.930	57.929	58.150	58.150
3	232.22	232.16	231.64	231.62	228.35	228.34	129.53	129.53
4	356.08	356.11	362.45	362.41	360.96	360.94	353.21	353.17
5	362.92	362.76	522.24	522.16	521.19	521.15	518.07	518.03
6	522.66	522.33	711.05	710.90	710.18	710.11	708.18	708.12
7	711.44	710.84	928.89	928.63	928.12	928.00	926.57	926.49
8	929.26	928.24	1175.8	1175.4	1175.0	1174.9	1173.7	1173.6

Expectedly, the validation of the procedure and results has been successful and the method and procedure have been proven to be accurate. After the validation of beam equations with their implementation by the Rayleigh-Ritz method, we turn to the typical structures with periodic patterns for the first two vibration modes of a beam with up to four half sinusoidal waves as shown in Fig 2. The results, again, are exactly the same with COMSOL. Our current results prove that the Rayleigh-Ritz method for the free vibrations of general curved beams has been successful and it can be further extended to combinations of periodic elements for the needed analysis.

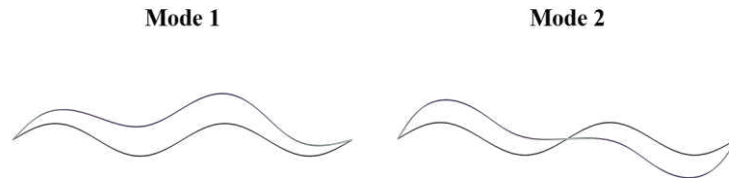


**Fig 2.** The first two vibration modes of a sinusoidally curved beam of two full sinusoidal waves.

From vibrations of beams of sinusoidal cells, it is found the convergence of the Rayleigh-Ritz method needs to be improved with larger number functions of deformation. Although we have obtained validated results in this study, careful study of the slow convergence and improving strategies is needed.

### References

- [1] Yang F; Sedaghati R; Esmailzadeh E.: Free in-plane vibration of general curved beams using finite element method. Journal of Sound and Vibration, Vol. 318, No. 4-5, pp. 850-867, 2008.
- [2] Qatu M.S.; Elsharkawy A.A.: Vibration of laminated composite arches with deep curvature and arbitrary boundaries. Computers & Structures, Vol. 47, No. 2, pp. 305-311, 1993.



## A pinned-pinned beam with and without a distributed foundation: A simple exact relationship between their eigenvalues

W. Paul Howson\* and Andrew Watson#

\* Independent Consultant  
Gwanwyn, Craig Penlline, CF71 7RT, UK  
w.p.howson@gmail.com

# Dept. of Aero and Auto Engineering  
Loughborough University  
Loughborough, LE11 3TU, UK  
a.watson@lboro.ac.uk

### Introduction

The body of this paper considers a pinned-pinned Bernoulli-Euler beam, from which the core natural frequencies and critical buckling loads corresponding to in-plane flexure, can be determined easily. The theory is then developed to yield an exact relationship between the static axial load in the beam and the frequency of vibration. This enables the core eigenvalues to be related exactly to their counterparts when the beam is additionally supported on a two parameter elastic foundation. The relationship is simple, exact and obviates the complex problems involved in solving the foundation problem using more traditional techniques. A number of illustrative problems are solved to confirm the accuracy and efficacy of the approach.

### Theory

Consider first the exact, fourth order differential equation governing the harmonic motion of an axially loaded Bernoulli-Euler beam of length,  $L$ , that is supported on a two parameter, distributed foundation, whose transverse and rotational restraining stiffnesses per unit length are  $k_y$  and  $k_\theta$ , respectively. The resulting equation is well known, can be deduced easily from Howson and Watson [1] and can be written in the following non-dimensional form

$$[D^4 + p^{*2}D^2 - b^{*2}]V = 0 \quad (1)$$

where  $D = d/d\xi$ ,  $\xi = x/L$  is the non-dimensional length parameter and  $V$  is the amplitude of the transverse displacement

$$p^{*2} = p^2 - k_\theta^* \quad b^{*2} = b^2 - k_y^* \quad (2)$$

$$p^2 = PL^2/EI \quad k_\theta^* = k_\theta L^2/EI \quad b^2 = \rho AL^4 \omega^2/EI \quad k_y^* = k_y L^4/EI \quad (3)$$

$\rho$  and  $E$  are the density and Young's modulus of the member material respectively,  $A$  and  $I$  are the area and second moment of area of the cross-section,  $\omega$  is the radian frequency of vibration and  $P$  is the static axial load in the member, which is positive for compression, zero, or negative for tension.

Equations (2) and (3) establish the non-dimensional member parameters  $p^2$  and  $b^2$ , which uniquely define the member effects of static axial load and frequency, respectively [2, 3], together with  $p^{*2}$  and  $b^{*2}$  which define their interaction with the non-dimensional foundation parameters.

Imposing pinned-pinned boundary conditions enables Equation (1) to be solved by assuming a general solution of the form

$$V = C \sin(i\pi\xi) \quad i = 1, 2, \dots, \infty \quad (4)$$

where  $C$  is an arbitrary constant,  $V$  defines the modal (displaced) shape, which also satisfies the boundary conditions. Substituting for  $V$  in Equation (1) then yields

$$(i\pi)^4 - p^{*2}(i\pi)^2 - b^{*2} = 0 \quad (5)$$

or

$$b^{*2}/(i\pi)^4 + p^{*2}/(i\pi)^2 = 1 \quad (6)$$

It is now helpful to introduce the notion of ‘member environment’ which, for the remainder of this paper, will be defined as follows. An environment will relate to either vibration or buckling and can be established by allocating constant values to the appropriate independent parameters in Equation (6). The core vibration environment will be defined by  $p^2 = k_y^* = k_\theta^* = 0$  and will yield the classical natural frequency parameters

$$b_{c,i} = (i\pi)^2 \quad i = 1, 2, \dots, \infty \quad (7)$$

In similar fashion, the core buckling environment will be defined by  $b^2 = k_y^* = k_\theta^* = 0$  and will yield the classical buckling parameters

$$p_{c,i} = (i\pi) \quad i = 1, 2, \dots, \infty \quad (8)$$

and hence that

$$b_{c,i} = p_{c,i}^2 \quad i = 1, 2, \dots, \infty \quad (9)$$

A further result of this is to enable Equation (6) to be written as

$$b^{*2}/b_{c,i}^2 + p^{*2}/p_{c,i}^2 = 1 \quad (10)$$

It is interesting to note in passing that solutions to Equation (10) will lie on the arc of an ellipse when  $b^{*2}$  and  $p^{*2}$  are both positive and on the arc of the adjoining hyperbola when they are of opposite sign. Equation (10) can now be used to model a range of vibration or buckling problems in which any appropriate combination of the non-dimensional effects can be neglected by setting the relevant parameter to zero.

## Discussion and numerical examples

The remainder of this paper now seeks to highlight aspects of Equation (10) while demonstrating its simplicity and effectiveness when applied to practical structures. This is best achieved by expanding it out in symbolic form to its most general vibration and buckling environments, as given in Equations (11a) and (11b), respectively, i.e.

$$b_i^2 = b_{c,i}^2[1 - (p^2/p_{c,i}^2)] + [(b_{c,i}^2/p_{c,i}^2)k_\theta^* + k_y^*] \quad i = 1, 2, \dots, \infty \quad (11a)$$

and

$$p_i^2 = p_{c,i}^2[1 - (b^2/b_{c,i}^2)] + [(p_{c,i}^2/b_{c,i}^2)k_y^* + k_\theta^*] \quad i = 1, 2, \dots, \infty \quad (11b)$$

where the subscript  $i$  has now been introduced on the dependent variable to denote modal rank, since there will be an infinite number of solutions for each new environment created.

Consider first the asymmetric relationship between Equations (11a) and (11b), which can be put into context as follows. Assume a vibration environment in which  $k_y = k_\theta = 0$  and  $p^2 = 0.4p_{c,1}^2$ . Then from Equation (11a) the frequency of vibration that would reduce the member stiffness to zero would correspond to  $b_1^2 = 0.6b_{c,1}^2$ . A similar buckling environment could be written as  $k_y = k_\theta = 0$  and  $b^2 = 0.6b_{c,1}^2$  then from Equation (11b) the compressive axial load that would

reduce the member stiffness to zero would correspond to  $p_1^2 = 0.4p_{c,1}^2$ . The same problem is thus solved both through a vibration and a buckling context. Closer inspection of Equations (11a) and (11b) enable a number of helpful points to be made. Firstly, it is clear that  $b_i^2$  and  $p_i^2$  must always be zero or positive and that the values of  $b^2$  and  $p^2$  shape their respective (constant) environments. Hence, when  $k_y^* = k_\theta^* = 0$ ;  $0 \leq b^2 \leq b_{c,i}^2$  and  $p^2 \leq p_{c,1}^2$ . When  $k_y^* > 0$  and/or  $k_\theta^* > 0$ , the values of  $b^2 (\geq 0)$  and  $p^2$  are only constrained by the requirement that  $b_i^2$  and  $p_i^2$  remain positive in their respective environments. More generally it is clear that in both vibration and buckling problems, the rotational stiffness becomes more influential as the modal rank increases.

The data for the remaining examples are given below so that the hand solutions developed from Equations (11a) and (11b) and given in Table 1 can be checked by alternative means.

$$E = 2.0 \times 10^{11} \text{ N/m}^2, \quad I = 1.6 \times 10^{-5} \text{ m}^4, \quad \rho = 8 \times 10^3 \text{ kg/m}^3, \quad A = 10^{-2} \text{ m}^2, \quad L = 4 \text{ m},$$

$$k_y = 10^6 \text{ N/m}^2, \quad k_\theta = 10^7 \text{ N} \quad \text{and} \quad P = 2 \times 10^5 \text{ N} \text{ for compression and negative for tension.}$$

The problem parameters and solutions are given in Table 1 below.

Table 1: Relationship given by Equations (11a) and (11b) between the core eigenvalues and their counterparts in the required environment.

	Environment		Modal Rank <i>i</i>	Core Eigenvalues		Solution	
	$k_y^*$	$k_\theta^*$		$p_{c,i}^2$	$b_{c,i}^2$		
Vibration	$p^2$					$b_i^2$	
	80	0	0	1	9.86960	97.4091	177.409
	80	0	0	3	88.8264	7890.14	7970.14
	0	50	-1	2	39.4784	1558.55	3571.94
	80	50	-1	1	9.86960	97.4091	680.759
Buckling	$b^2$						$p_i^2$
	80	0	0	1	9.86960	97.4091	17.9753
	0	50	0	2	39.4784	1558.55	89.4784
	80	50	0	4	157.914	24936.7	208.420

## Conclusions

A simple formula that can be manipulated easily by hand and which can predict exactly the change in core eigenvalues of a simple pinned-pinned beam to their counterparts in any other allowable environment has been presented and its efficacy demonstrated.

## References

- [1] Howson, W.P.; Watson, A.: On the provenance of hinged-hinged frequencies in Timoshenko beam theory. *Computers and Structures*, Vol. 197, pp. 71–81, 2018.
- [2] Howson, W.P.; Williams, F.W.: Natural frequencies of frames with axially loaded Timoshenko members. *Journal of Sound and Vibration*, Vol. 26, pp. 503–515, 1973.
- [3] Howson, W.P.; Banerjee, J.R.; Williams, F.W.: Concise equations and program for exact eigensolutions of plane frames including member shear. *Advances in Engineering Software*, Vol. 5, pp. 137-141, 1983.



## Accurate Free Vibration Analysis of Rectangular Mindlin Plates with Arbitrary Boundary Conditions by the Superposition Method

Shudong Yu

Department of Mechanical and Industrial Engineering, Ryerson University  
 Toronto, Ontario, Canada M5B 2K3; Email: [syu@ryerson.ca](mailto:syu@ryerson.ca)

Xuewen Yin

China Ship Scientific Research Center,  
 222 Shanshui East Road, Wuxi, China, 214072; Email: [x.w.yin@cssrc.com.cn](mailto:x.w.yin@cssrc.com.cn)

### Summary

**Introduction.** For thick plates, it is necessary to include the effects of transverse shear and rotary inertia. In this paper, Gorman's superposition method (Gorman 1982) is extended in connection with Mindlin's first order shear deformation plate theory to obtain a general analytical solution for free flexural vibration of moderately thick isotropic rectangular plates with arbitrary boundary conditions (BCs) by means of a two building block scheme.

**Background and Motivation.** The proposed scheme overcomes the deficiencies of the traditional superposition method in that there is one unified set of general solution for rectangular plates having arbitrary BCs on all four edges. This eliminates the need for constructing ad-hoc BCs-dependent building blocks. Only the unknown coefficients in the general analytical solution need to be determined for the desired BCs. The scheme has been successfully employed by Yu and Yin (2019) to obtain a general analytical solution for free vibration of thin rectangular plates and plate assemblies with arbitrary classical BC's.

**Governing Equations.** The governing differential equations for flexural vibration of a moderately thick plate may be written in the Cartesian coordinates as

$$\begin{aligned}
 D_{11} \frac{\partial^2 \Psi_x}{\partial x^2} + D_{66} \frac{\partial^2 \Psi_x}{\partial y^2} + (D_{12} + D_{66}) \frac{\partial^2 \Psi_y}{\partial x \partial y} - A_{55} \left( \Psi_x + h \frac{\partial W}{\partial x} \right) + \frac{1}{12} \rho h^3 \omega^2 \Psi_x &= 0 \\
 (D_{12} + D_{66}) \frac{\partial^2 \Psi_x}{\partial x \partial y} + D_{66} \frac{\partial^2 \Psi_y}{\partial x^2} + D_{22} \frac{\partial^2 \Psi_y}{\partial y^2} - A_{44} \left( \Psi_y + h \frac{\partial W}{\partial y} \right) + \frac{1}{12} \rho h^3 \omega^2 \Psi_y &= 0 \quad (1) \\
 A_{55} \frac{\partial}{\partial x} \left( \Psi_x + L_0 \frac{\partial W}{\partial x} \right) + A_{44} \frac{\partial}{\partial y} \left( \Psi_y + h \frac{\partial W}{\partial y} \right) + \rho h \omega^2 W &= 0
 \end{aligned}$$

where  $W$  is the lateral displacement amplitude of a material point  $(x, y)$  on the plate midplane;  $\Psi_x$  and  $\Psi_y$  are the amplitudes of bending angles;  $h$  is the plate thickness;  $\rho$  is the plate density;  $D_{ij}$  are the plate flexural rigidity parameters;  $A_{kk}$  are the plate extensional rigidity parameter;  $\omega$  is the natural frequency of flexural vibration;  $\kappa^2$  is the shear correction factor.

**Mathematical Formulations.** The basis of the success in accomplishing the task lies in that (i) the availability of the Levy solution for rectangular plates having a pair of edges subjected to roller-supports, (ii) any continuous function can be expanded into orthogonal half-cosine

series in a closed interval along a rectilinear edge. The solution for free vibration of a rectangular plate with arbitrary BCs on its four edges is the superposition of the solutions for the two building blocks (BBs) shown in Fig. 1.

The first BB is subjected to the guided roller support on edges  $\eta = 0, 1$ . The second BB is subjected to the guided roller support on edges  $\xi = 0, 1$ . Along an R edge  $\eta = \text{const.}$ , the following three quantities vanish  $(\Psi_y, M_{yx}, Q_y)$ . Along an R-edge  $\xi = \text{const.}$ ,  $(\Psi_x, M_{xy}, Q_x)$  vanish. The Levy solutions for the two BBs are

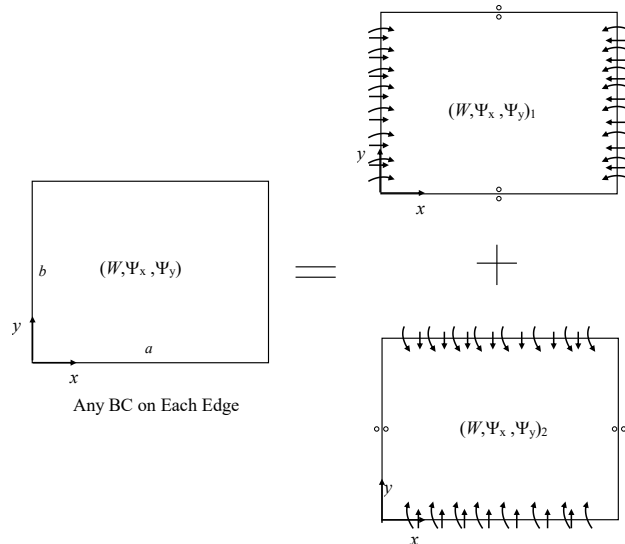


Fig. 1 Illustration of solution scheme for free vibration of a rectangular plate

$$\begin{Bmatrix} \Psi_x(\xi, \eta) \\ \Psi_y(\xi, \eta) \\ W(\xi, \eta) \end{Bmatrix}_I = \begin{Bmatrix} X_0(\xi) \\ 0 \\ Z_0(\xi) \end{Bmatrix} + \sum_{n=1}^{K_n} \begin{Bmatrix} X_n(\xi) \cos n\pi\eta \\ Y_n(\xi) \sin n\pi\eta \\ Z_n(\xi) \cos n\pi\eta \end{Bmatrix} \quad (2)$$

$$\begin{Bmatrix} \Psi_x(\xi, \eta) \\ \Psi_y(\xi, \eta) \\ W(\xi, \eta) \end{Bmatrix}_{II} = \begin{Bmatrix} 0 \\ \hat{Y}_0(\eta) \\ \hat{Z}_0(\eta) \end{Bmatrix} + \sum_{m=1}^{K_m} \begin{Bmatrix} \hat{X}_m(\eta) \sin m\pi\xi \\ \hat{Y}_m(\eta) \cos m\pi\xi \\ \hat{Z}_m(\eta) \cos m\pi\xi \end{Bmatrix} \quad (3)$$

Substituting Eq. (2) into Eq. (1), we obtain four sets of ordinary differential equations (ODEs) for  $(X_0, Z_0)$ ,  $(X_n, Y_n, Z_n)$ ,  $(\hat{Y}_0, \hat{Z}_0)$ , and  $(\hat{X}_m, \hat{Y}_m, \hat{Z}_m)$ . Solving these ODEs, a unified analytical solution may be written as

$$\begin{Bmatrix} \Psi_x(\xi, \eta) \\ \Psi_y(\xi, \eta) \\ W(\xi, \eta) \end{Bmatrix}_I = [\Gamma(\eta)] [\Phi(\xi)] \{G\}_I, \quad \begin{Bmatrix} \Psi_x(\xi, \eta) \\ \Psi_y(\xi, \eta) \\ W(\xi, \eta) \end{Bmatrix}_{II} = [\hat{\Gamma}(\xi)] [\hat{\Phi}(\eta)] \{\hat{G}\}_{II} \quad (4)$$

where

$$[\Gamma(\eta)] = \text{diag}[[\Gamma(\eta)]_0 \quad [\Gamma(\eta)]_I \quad \Lambda \quad [\Gamma(\eta)]_{K_n}], \quad [\Phi(\xi)] = [[\Phi(\xi)]_0 \quad [\Phi(\xi)]_I \quad \Lambda \quad [\Phi(\xi)]_{K_n}]$$

$$[\Gamma(\eta)]_k = \text{diag}[\cos k\pi\eta \quad \sin k\pi\eta \quad \cos k\pi\eta], \quad k = 0, 1, \dots, K_n$$

$$[\hat{\Gamma}(\xi)] = \text{diag}[[\hat{\Gamma}(\xi)]_0 \quad [\hat{\Gamma}(\xi)]_I \quad \Lambda \quad [\hat{\Gamma}(\xi)]_{K_m}], \quad [\hat{\Phi}(\eta)] = [[\hat{\Phi}(\eta)]_0 \quad [\hat{\Phi}(\eta)]_I \quad \Lambda \quad [\hat{\Phi}(\eta)]_{K_n}]$$

$[\hat{\Gamma}(\xi)]_k = \text{diag}[\sin \hat{k}\pi\xi \quad \cos \hat{k}\pi\xi \quad \cos \hat{k}\pi\xi], \quad \hat{k} = 0, 1, \dots, K_m$ ; and  $\{G\}_I$  is a vector containing  $6K_n + 2$  unknown constants;  $\{\hat{G}\}_{II}$  is a vector containing  $6K_m + 2$  unknowns.

The unknown constants are to be determined by enforcing the boundary conditions (BCs) on the four edges. The enforcement of the BC's lead to a set of homogeneous algebraic equations from which the eigenvalues and eigenvectors can be extracted.

**Numerical Results.** The proposed scheme is applied to obtain natural frequencies or non-dimensional eigenvalues of a fully clamped plate. Eigenvalues of the first ten modes were

determined using different terms in the Levy solutions and are shown in Table 1.

Table 1 Eigenvalues  $\lambda_G^2$  of a fully clamped moderately thick rectangular plate

Modes	This paper $K_n = K_m = K$ $h = 0.1$ m			This paper $K_n = K_m = K$ $h = 0.08$ m			CPT (Gorman 1982)
	$K = 6$	$K = 8$	$K = 10$	$K = 6$	$K = 8$	$K = 10$	
1	6.242	6.242	6.242	6.409	6.409	6.409	6.736 (SS-1)
2	9.394	9.394	9.394	9.720	9.720	9.720	10.43 (AS-1)
3	14.207	14.207	14.207	14.915	14.915	14.915	16.53 (SA-1)
4	14.429	14.429	14.429	15.097	15.097	15.097	16.63 (SS-2)
5	16.816	16.817	16.817	17.738	17.739	17.739	19.95 (AA-1)
6	20.869	20.873	20.874	22.121	21.202	22.124	25.20 (AS-2)
7	21.102	21.104	21.104	22.423	22.124	22.425	25.78 (SA-2)
8	24.790	24.791	24.791	26.604	22.425	26.604	31.32 (SS-3)
9	27.015	27.021	27.022	28.739	26.604	28.769	34.02 (AA-2)
10	28.350	28.355	28.355	29.081	28.767	29.087	34.66 (AS-3)
<p>- Geo-material properties: <math>a = 1</math> m, <math>b = 1.5</math> m, <math>E = 201</math>GPa, <math>\nu = 0.3</math>, <math>\rho = 7800</math> kg/m<sup>3</sup></p> <p>- The shear correction factor used <math>\kappa^2 = 0.8601</math></p> <p>- For direct comparison, eigenvalue <math>\lambda^2 = \omega a^2 \sqrt{\rho/E} / h</math> of the current paper is related to that of Gorman (1982), <math>\lambda_G^2 = \omega a^2 \sqrt{\rho h/D}</math>, for a one-quarter plate model by <math>\lambda_G^2 = \lambda^2 \sqrt{12(1-\nu^2)} / 4</math>.</p>							

**Conclusion.** The proposed analytical method is general and rapidly convergent. The classical plate theory (CPT) over-predicts the natural frequencies appreciably because of the neglect of the transverse shear and rotary inertia. This hopefully will help attract the use of the powerful analytical method pioneered by Gorman.

### References

- D. J. Gorman, 1982, Free Vibration Analysis of Rectangular Plates. New York: Elsevier, North-Holland.
- S. D. Yu and X. W. Yin, 2019, "A generalized superposition method for accurate free vibration analysis of rectangular plates and assemblies", Journal of American Society of Acoustics, 145 (1), 185-203.



## Bio-sketch

<p>Prof. Haim Abramovich Faculty of Aerospace Engineering Technion, I.I.T., 32000, Haifa, ISRAEL. Email: <a href="mailto:haim@technion.ac.il">haim@technion.ac.il</a>; <a href="mailto:abramovich.haim@gmail.com">abramovich.haim@gmail.com</a> Tel : +972 544 696566</p>	
---	--

Obtained his B.Sc., M.Sc. and Ph.D. degrees from the Faculty of Aerospace Engineering, Technion, in 1975, 1979 and 1983, respectively.

His Ph.D. thesis was entitled “The behavior of the Blade of a Darrieus Wind Turbine”, while his M.Sc. thesis title was “Correlation between Vibrations and Buckling of Stiffened Shells with Realistic Boundary Conditions and Combined Loading”.

He has been with the Technion since 1987, and currently he is the head of the Aerospace Structures Laboratory.

He spent three years with the Israeli industry and between 1996-1998 he was Guest Professor at ETH Zurich Institut für Leichtbau und Seilbahntechnik, Switzerland, while from March-September 2018, he was at the Faculty of Aerospace Engineering, TU Delft, the Netherlands.

His main fields of interest are: static and dynamic stability of thin walled structures, piezoelectric materials, laminated composite structures, dynamic buckling of thin walled structures, smart structures technologies, structural mechanics and energy harvesting using piezoelectric and pyroelectric materials .

He has published more than 107 papers in well-known international journals on these quoted subjects. He is the author of 10 patents on piezoelectric harvesting devices. He is also the author of two new books with another one in progress:

1. H. Abramovich, *Intelligent Materials and Structures*, © 2016 Walter de Gruyter GmbH, Berlin/Boston, 386 p.
2. H. Abramovich, *Stability and Vibrations of Thin Walled Composite Structures*, © 2017 Woodhead Publishing Limited, 540 p.
3. H. Abramovich, *Advanced Aerospace Materials – Aluminum-based and Composite Materials*, in progress, to be published by Walter de Gruyter GmbH, Berlin/Boston.

Since 2017, Editor-in-Chief of The Open Aerospace Engineering Journal, Bentham Open.  
Since 2013, editorial board member of the International Journal of Composite Materials  
Since 2014, editorial board member for International Journal of Aeronautical Science & Aerospace Research (IJASAR).  
Since 2018, editorial board member for Actuators, MDPI.

## **Professor Ranjan Banerjee**

After receiving his Bachelor's and Master's Degree in Mechanical Engineering from the University of Calcutta and the Indian Institute of Technology, Kharagpur, respectively, Ranjan Banerjee joined the Structural Engineering Division of the Indian Space Research Organisation, Trivandrum in 1971 and worked there for four years, first as a Structural Engineer and then as a Senior Structural Engineer. He was involved in the dynamic analysis of multistage solid propellant rocket structures using the finite element method. He also carried out research on the response of rocket structures to acoustic loads. Later in the year 1975 he was awarded a Commonwealth Scholarship to study for a PhD degree at Cranfield University where he conducted research within the technical areas of structural dynamics and aeroelasticity. He received his PhD in 1978. An important spin-off from his PhD was the development of an aeroelastic package in Fortran, called CALFUN (CALculation of Flutter speed Using Normal modes) which was originally written for metallic aircraft, but later extended to composite aircraft. CALFUN has been extensively used as a teaching and research tool in aeroelastic studies. After completing his PhD, he joined the Structural Engineering Division of the University of Cardiff in 1979 and worked there for six years first as a Research Associate and then as a Senior Research Associate to investigate the free vibration and buckling characteristics of space structures using the dynamic stiffness method. During this period he worked in close collaboration with NASA, Langley Research Center, and he was principally involved in the development of the well-established computer program BUNVIS (BUckling or Natural Vibration of Space Frames) which was later used by NASA and other organizations to analyse spacecraft structures. He joined City University London in 1985 as a Lecturer in Aircraft Structures and he was promoted to Senior Lecturer and Reader in 1994 and 1998 respectively. In March 2003 he was promoted to a Personal Chair in Structural Dynamics. His main research interests include dynamic stiffness formulation, aeroelasticity, unsteady aerodynamics, composite structures, functionally graded materials, aircraft design, symbolic computation, free vibration and buckling analysis of structures and associated problems in elastodynamics. He has been responsible for supervising various research contracts as Principal Investigator, involving EPSRC, American Air Force Base, Embraer Aircraft Company, amongst others. To date he has published 115 journal papers and 100 conference papers from his research. He serves in the Editorial Boards of a number of international journals and established conferences and he has been a member of the EPSRC Peer Review College since its inception. He is a Fellow of both the Royal Aeronautical Society and the Institution of Structural Engineers in the UK and an Associate Fellow of the American Institute of Aeronautics and Astronautics. He taught the subjects of mechanics, strength of materials, aircraft structures, composite materials, computational structural mechanics and aeroelasticity, and he acted as external examiner in five British universities for their undergraduate and postgraduate programmes in aeronautical and aerospace engineering. He has supervised 15 PhD students and acted as external examiner for PhD candidates on 25 occasions. He was awarded the degree of Doctor of Science by City, University of London in 2016. Professor Banerjee retired in February 2017 and currently he is Professor Emeritus of Structural Dynamics.



Dipartimento Ingegneria Civile e  
Architettura

Università degli Studi di Catania, Italy

Salvatore  
Caddemi, Ph.D.

Prof. Salvatore Caddemi is native of Noto (Siracusa), Italy, on 29th of November 1960. He received his master degree in Civil Engineering in 1984, served as Officer in the Italian Navy until 1986 and obtained his Ph.D. in Structural Engineering in 1990, from the University of Palermo.

His research activity in the period 1988-1991 has been developed at the "FRD/UCT Centre for Research in Computational and Applied Mechanics" of the University of Cape Town, South Africa, as "Visiting Researcher" and "Postdoctoral Research Fellow" contributing to theoretical advances in the integration of nonlinear plastic constitutive laws and formulating iterative procedures for the relevant incremental analysis.

Prof. Caddemi was appointed Researcher of Mechanics of Materials in July 1991 at the Department of Structural and Geotechnical Engineering of the University of Palermo and was "Visiting Researcher" within the program HCM network of the European Community at the Department of Structural Engineering and Materials of the Technical University of Denmark in 1996.

In November 1998 he became associate professor of "Strength of Materials" at the Institute of Structural Engineering of the Engineering Faculty of the University of Catania and since 1 October 2001 he is full professor at the Department of Civil and Architectural Engineering of the University of Catania where he is currently conducting his teaching and research activity.

His research interest has been oriented to deterministic analysis of elastic-plastic and no-tension material structures, stochastic dynamic structural analysis, structural and damage identification, static and dynamic analysis of structures with singularities, seismic vulnerability assessment of masonry structures.

Prof. Caddemi is currently involved in the use of generalised functions for the solution of direct and inverse problems of beam-like and frame structure in presence of strong discontinuities and singularities.



Dipartimento Ingegneria Civile e Architettura,  
*Università degli Studi di Catania, Viale Andrea Doria 6, 95128, Catania, Italy*



**DIPARTIMENTO INGEGNERIA CIVILE E  
ARCHITETTURA  
UNIVERSITÀ DEGLI STUDI DI CATANIA**

**Ivo Calio is Full professor of Dynamics of Structures, joined at the University of Catania as researcher in 1997. Since his PhD, he has extensively worked on nonlinear analysis methods for structural dynamic problems. Since 2004 he introduced a new modelling strategy for masonry buildings based on a simplified macro-element approach. Currently he coordinates a research group for developing alternative macro-element numerical strategies, suitable both for practical engineering purposes and academic investigations. The main results of these researches have been implemented in two structural analysis computer codes: 3DMacro, for masonry and mixed reinforced concrete and masonry buildings and HiStrA (Historical Structures Analysis) focused on the Structural Assessment of Historical Monumental Structures and Masonry Bridges.**

**In the field of continuous systems, he is involved in structural and damage identification, static and dynamic analysis of structures with singularities. To this purpose, generalised functions are employed for the solution of direct and inverse problems of beam-like and frame structure in presence of strong discontinuities and singularities.**

**Dipartimento Ingegneria Civile e Architettura, Università degli Studi di Catania, Viale Andrea Doria 6, 95128, Catania, Italy**



**DIPARTIMENTO INGEGNERIA CIVILE E  
ARCHITETTURA  
UNIVERSITÀ DEGLI STUDI DI CATANIA**

**Francesco Cannizzaro is native of Caltagirone (Catania), Italy, on 1st of September 1981. He received his master degree in Civil Engineering in 2007, and obtained his Ph.D. in Structural Engineering in 2011, from the University of Catania. His research activity was at first devoted to computational models of historical masonry constructions contributing with the introduction of a new element for modelling masonry vaults aiming at the enrichment of a modelling strategy based on a discrete macro-element approach. He spent part of his postdoc at the University of Minho at the Institute for Sustainability and Innovation in Structural Engineering (ISISE) as “Visiting Researcher”, developing a strategy to numerically simulate the nonlinear behaviour of fiber-reinforced masonry structures. Among the other interests, he has been providing several contributions in the field of statics, stability and dynamics of discontinuous straight and curved beams as well as frames; in particular, exact closed form solutions have been proposed by making use of generalised functions to treat the discontinuities. Since May 2018 he is researcher at the University of Catania in “Mechanics of Structures”.**

**Dipartimento Ingegneria Civile e Architettura, Università degli Studi di Catania, Viale Andrea Doria 6, 95128, Catania, Italy**

Dr. Erasmo Carrera



Erasmo Carrera is Professor of Aerospace Structures and Aeroelasticity at Politecnico di Torino, Italy. He graduated in Aeronautics in 1986 and Space Engineering in 1988 at the Politecnico di Torino. He obtained a Ph.D. in Aerospace Engineering in 1991. He became Assistant Professor in 1992, Associate Professor (2000) and Full Professor (2010) at the Politecnico di Torino. Carrera has introduced the Reissner Mixed Variational Theorem, RMVT, as a natural extension of the Principle of Virtual Displacement to layered structure analysis. He introduced the Unified Formulation, or CUF (Carrera Unified Formulation), as a tool to establish a new framework in which to develop linear and nonlinear theories of beams, plates and shells for metallic and composite multilayered structures loaded by mechanical, thermal electrical and magnetic loadings. Carrera has been author and coauthor of about 800 papers on the above topics, most of which have been published in first rate international journals, including a few recent books.

Professor Carrera is founder and leader of the MUL2 group at the Politecnico di Torino. The MUL2 group has acquired a significant international reputation in the field of multilayered structures subjected to multifield loadings, see also [www.mul2.com](http://www.mul2.com).

Professor Carrera has been recognized as Highly Cited Researchers (Top 100 Scientist) by Thompson Reuters in the two Sections: Engineering and Materials (2013) and Engineering (2015). He currently acts as President of AIDAA (Associazione Italiana di Aeronautica ed Astronautica).



**Weiqiu Chen** is a Professor of the Department of Engineering Mechanics, Zhejiang University. He received his BS and PhD degrees from Zhejiang University in 1990 and 1996, respectively. He had been working as a postdoctoral research associate at The University of Tokyo (1997-1999). He was promoted as an associate professor in 1999 and a full professor in 2000. He has engaged himself in mechanics of soft materials and structures, mechanics of smart materials/structures, and vibration/waves in structures for over twenty five years. He has co-authored over 350 peer-reviewed journal articles and three English books on elasticity of transversely isotropic elastic materials, piezoelectricity, and Green's functions, respectively. His H-index is 44. He now serves as the editorial member (or associate editor-in-chief) of 14 academic journals including Mechanics of Advanced Materials and Structures, Composite Structures, International Journal of Mechanical Sciences, Theoretical and Applied Mechanics Letters, Journal of Thermal Stresses, and Applied Mathematics and Mechanics (English Edition).

## Noise and Vibration Mitigations for Aeronautical and Aerospace Applications

**Li Cheng**

*Chair Professor of Mechanical Engineering*

*Department of Mechanical Engineering, Hong Kong Polytechnic University*



### **Bio-sketch**

Dr. Li Cheng is currently a Chair Professor and the Director of Consortium for Sound and Vibration Research (CSV) at the Hong Kong Polytechnic University. He received his BSc degree from Xi'an Jiaotong University, DEA and Ph.D. degrees from the Institut National des Sciences Appliquées de Lyon (INSA-Lyon), France. After two years in Sherbrooke University, he started his academic career at Laval University, Canada in 1992, rising from an assistant professor to Associate/Full Professor, before coming to Hong Kong in 2000, where he was promoted to Chair Professor in 2005 and was the Head of Department from 2011 to 2014. Dr. Cheng published extensively in the field of sound and vibration, structural health monitoring, smart structure and fluid-structure interaction. He is an elected fellow of the Acoustical Society of America, Acoustical Society of China, IMechE, Hong Kong Institution of Engineers and Hong Kong Institute of Acoustics. He currently serves as Deputy Editor-in-Chief and Receiving Editor of *Journal of Sound and Vibration*, Associate Editor for the *Journal of Acoustical Society of America*, Associate Editor of *Structural Health Monitoring: An International Journal* and editorial board member of 6 other journals. Dr. Cheng also been a Plenary/Keynote Speaker at conferences in the USA, UK, France, Japan, Greece, India, South Korea, Poland, Bangladesh and China, including some of the most prestigious conferences in his field such as 47<sup>th</sup> Inter-noise, 23<sup>rd</sup> ICSV, 13<sup>th</sup> RASD, 15<sup>th</sup> APVC and 12<sup>th</sup> ICOVP. He also served as the general Chair of the 46th International Congress on Noise Control Engineering (Inter-noise) and the Chair of 14<sup>th</sup> and 17th Asia Pacific Vibration Conference (APVC). Dr. Cheng was the President of the Hong Kong Society of Theoretical and Applied Mechanics. He is also a board director of both IIAV (International Institutes of Acoustics and Vibration) and I-INCE (International Institutes of Noise Control Engineering).

## Piotr Cupiał

I graduated in 1987 in the field of applied and computational mechanics. In 1997 I obtained my PhD from the Cracow University of Technology, in the field of the application of damping polymers in the vibration suppression of composite structures. Since March 2011 I hold a professorship at the Faculty of Mechanical Engineering and Robotics of the AGH University of Science and Technology in Krakow.

My scientific interests have always lied in the field of the vibration of continuous systems. During different periods of my academic life I have been involved in research on: the optimal design of plates subjected to non-conservative loading, vibration suppression of plates through the use of polymeric damping treatments, the dynamics of structures made of composite materials, the modelling of continua subjected to electromagnetic and thermal loading, and the analysis of piezoelectric structures and their use as smart materials.

During the years 1998-2001 I worked at the European Organization for Nuclear Research (CERN) in Geneva. At CERN I performed numerical analyses and dynamic measurements related to the design of the Large Hadron Collider (LHC). I am still in touch with the high-energy physics community. I am in charge of one of the work packages of the H2020 project “Feasibility study for employing the uniquely powerful ESS linear accelerator to generate an intense neutrino beam for leptonic CP violation discovery and measurement” (<https://essnusb.eu/site/>), supervising the design of the target station. The work addresses very interesting vibration issues too, including the study of the stress levels and estimation of the fatigue life of elements subjected to short duration pulses of microsecond duration, mainly of electromagnetic and thermal origin.

For many years now I have served on the editorial board of the Journal of Sound and Vibration, I am a member of the editorial board of the Journal of Theoretical and Applied Mechanics and editor-in-chief of the journal Mechanics and Control.

I am married to Gabriela and we have one son. I have always enjoyed the mountains, hiking in the summer and skiing during winter.

## Biographical sketch of Dr. Anirvan DasGupta

Dr. Anirvan DasGupta obtained his PhD from IIT Kanpur, India, in 1999. Thereafter, he joined IIT Kharagpur as a faculty in the Department of Mechanical Engineering, where is currently a Professor. His research interests include mechanics of inflatable structures, vibrations and waves in continuous systems, vibration induced transport, rail vehicle dynamics, and kinematics of flows. He has published on these topics and also co-authored a book (*Vibrations and Waves in Continuous Mechanical Systems* with Peter Hagedorn). He has been a Monbusho Research Fellow at the University of Tokyo, Japan, and an Alexander von Humboldt Research Fellow at TU Darmstadt, Germany.



SERGIO DE ROSA



My parents, in the summer of 1970, gave me a small airplane with turning wings. It went up into the sky with a wire, like a kite. I am that child.

I turned 28, about 28 years ago. I spent the most important part of my life with Antonella: we still walk together and have two wonderful sons. Passionate about movies, comics, shooting pictures and listening music.

I teach at the Università di Napoli Federico II where I got my degree in aeronautical engineering in 1988. In the same year I became researcher at the Italian Aerospace Research Centre, CIRA, where I have continued studying the themes belonging to the vibroacoustics. All the research activity was and still are in the engineering fields concerning the structural dynamics and the fluid-structure interaction in large sense: fascinating and even challenging topics.

In 1992, I was appointed as junior researcher at University of Naples Federico II at the Department (now named) Industrial Engineering - Aerospace Section. During the last days of 2014, I was appointed as Full Professor.

I am still studying the propagation of fluid and elastic waves aimed at understanding the vibration and interior noise distributions as well as the fluid loading conditions for high speed transportation systems. Actual themes are:

- models for the structural dynamics and interior acoustics;
  - definition of ASMA, asymptotical scaled modal analysis;
  - definition of SAMSARA, similitudes and asymptotical modelling for structural acoustics researches and applications;
- stochastic response of structural and fluid-structural systems under random and convective excitations;
- convective effect on the acoustic radiated power by structural components;
- influence of the uncertainties on the dynamic system response;
- enhancements of the wave and finite element approach;
- use of machine learning for the identification of vibroacoustic systems and the assistance in the numerical predictions and experimental data analyses.

I was one of the founders of the FLINOVIA community, symposia and books: [www.flinovia.org](http://www.flinovia.org).

I have co-authored more than 150 papers, 50 of them in peer reviewed Journals and belong to the following boards:

- **Associate Editor:**
  - Advances in Aircraft and Spacecraft Science, **An International Journal** (TECHNOPRESS).
  - Proc. of the Inst. of Mech. Eng., Part C, Journal of Mechanical Engineering Science (SAGE).
  - Aerotecnica Missili & Spazio, The Journal of Aerospace Science, Technology and Systems (SPRINGER).
- **Editor:** Mechanical Systems and Signal Processing (ELSEVIER).

## Lorenzo Dozio

*Department of Aerospace Science and Technology, Politecnico di Milano, Italy*

Lorenzo Dozio was born near Milan, Italy, on 1972. He received a M.S. degree in Aerospace Engineering in 1998 and a Ph.D. in Aerospace Engineering in 2002, both at the Politecnico di Milano. After two years as a post-doc, he won a position as Assistant Professor at the same University in 2004. In June 2015 he became Associate Professor at Department of Aerospace Science and Technology, Politecnico di Milano. He is now Chair of the BSc and MSc Programs on Aerospace Engineering.

Since 2002 he has been involved in teaching activities concerning servosystems for aerospace applications, introduction to engineering experimentation, dynamics and control of aerospace structures and fundamentals of aeroelasticity.

His main research interests are vibration of structures, composite and smart materials, active and shunt piezoelectric control, coupled structural-acoustic and real-time control systems. He has been involved in many research projects in collaboration with industries on active noise reduction inside helicopter cabins, active control of instabilities in combustion chambers and design and implementation of real-time operating systems. He is currently working on refined computational and analytical models for bending, vibration and buckling analysis of multilayered plates and shells.

He has co-authored more than 40 papers in international journals and over 50 conference papers. He has advised more than 30 graduate students at Politecnico of Milano. He served as a reviewer for, among others, Journal of Sound and Vibration, Journal of Vibration and Acoustics, Composite Structures and International Journal of Mechanical Sciences.

He is married to Letizia, and they have four children, two sons Paolo (17) and Tommaso (15), and two twin daughters Anna and Matilde (11). In his spare time, he loves playing acoustic and electric guitar.

Technion - Israel Inst. of Technology Faculty of Civil Engineering

## Moshe Eisenberger

June 2019

### Degrees

B.Sc.	Civil Engineering, Technion, Haifa	1977
M.Sc.	Civil Engineering, Stanford University, USA	1978
Engineer	Civil Engineering, Stanford University, USA	1979
Ph.D.	Civil Engineering, Stanford University, USA	1980

### Academic Appointments

Lecturer	Civil Engineering, Technion, Haifa	1980
Senior Lecturer	Civil Engineering, Technion, Haifa	1985
Tenure Senior Lecturer	Civil Engineering, Technion, Haifa	1987
Associate Professor	Civil Engineering, Technion, Haifa	1993
Professor	Civil Engineering, Technion, Haifa	2003

### Publications and Supervision of Graduate Students

Published over 80 Journal papers and 80 Conference papers  
Supervised 30 Ph.D. and MSc. Students

### Research Interests

Main area are applied and computational mechanics including static, dynamic, and stability analysis of structures. In the last 10 years I have been working on Dynamic Stiffness Analysis of various elements. Recent years were devoted to the exact solution for plates.

### Personal Interests

I am an active cyclist both road and mountain, and hiker. Last year I was on sabbatical leave in Argentina and loved it! Next semester I shall spend in Brazil.

## **Peter Hagedorn**

Peter Hagedorn was born in Berlin, Germany. He grew up in Brazil, where he graduated (Engineer's degree) in mechanical engineering in 1964 at EPUSP and in 1966 earned his doctoral degree at the same University. He then worked as a research assistant and later as 'dozent' (similar to lecturer) at the University of Karlsruhe, Germany. In 1971 he got his 'habilitation' (similar to Dr. Sc.) at Karlsruhe. From 1973 to 1974 he was a visiting Research Fellow at the Department of Aeronautics and Astronautics, Stanford University. Since October 1974 he is full professor of mechanics at the Technische Universität Darmstadt and head of the Dynamics and Vibrations group. He also has served as visiting professor at Rio de Janeiro (Brazil), Berkeley, Paris, Irbid (Jordan) and Christchurch (New Zealand), where he also holds an Adjunct Professorship at UCC. He has served as Head of Department and Vice-President to his home University in Darmstadt and he is serving in a number of professional and editorial committees. He is author of over 200 papers and several books on a variety of topics in the general field of dynamics and vibrations and analytical mechanics. He is officially retired since 2009 but still quite active and heads the Dynamics and Vibrations Group, presently affiliated to the chair of professor Michael Schäfer, at the graduate school of computational engineering of TU Darmstadt.

## BIOGRAPHICAL SKETCH

Dr. Paul R. Heyliger was awarded a B.S degree in Civil Engineering from Colorado State University in 1981, and also received his M.S. degree from CSU in the Structural Engineering and Solid Mechanics Program in 1983. He also holds a Ph.D. degree in Engineering Mechanics from Virginia Polytechnic Institute and State University in 1986.

Following his doctoral studies, Dr. Heyliger was awarded a two-year post-doctoral research position in the Fracture and Deformation Division of the National Bureau of Standards (now the National Institute of Standards and Technology) in Boulder, Colorado. Dr. Heyliger accepted a position of Assistant Professor in the Structural Engineering and Solid Mechanics program at Colorado State University in the Fall of 1988 and was promoted to Full Professor in 1999. He has taught courses in dynamics, mechanics of solids, structural analysis, mechanics of composite materials, the finite element method, advanced structural analysis, vibrations, boundary element methods, and advanced solid mechanics. He has been honored with numerous teaching awards, including the Golden Key award for teaching excellence by the Chi Epsilon Honor Society and the Best Professor Award by the Engineering Legislature at CSU. He has been a visiting researcher at NASA-Lewis Research Center, the University of California at Santa Barbara, the University of Stuttgart, and the University of Hamburg-Harburg. He has published over 100 articles in refereed journals, and has completed scientific studies for NASA, NIST, USDA, NSF, ARO, and the Advanced Materials Institute. Dr. Heyliger holds membership in the American Society of Civil Engineers (ASCE).

**Shinya Honda**  
**Hokkaido University, Sapporo, Japan**

I am an associate professor of the Department of Human Mechanical Systems & Design in Faculty of Engineering, Hokkaido University. I graduated the Department of Mechanical Engineering in 2005, and obtained Master of Engineering in 2007 from Hokkaido University. In 2009, I also obtained a PhD from Hokkaido University in the area of optimization of composite plates under supervision of Prof. Yoshihiro Narita. The title of my doctor thesis is “Study on vibration design of fibrous composite plates with locally anisotropic structure”.

From 2009 to 2013, I worked with Prof. Narita as an assistant professor in the same laboratory.

From 2013 to 2014, I was a visiting researcher of ETH Zurich and worked with Dr. Gerald Kress and Prof. Paolo Ermanni about corrugate laminate shell structures. During stay in Switzerland, I promoted to the associate professor.

From 2017, after retirement of Prof. Narita, I am working with Prof. Katsuhiko Sasaki who is also my sub-supervisor and associate prof. Ryo Takeda.

I have still an interest in a research field of optimization of composite structures. Recently I am taking part in the Cross-ministerial Strategic Innovation Promotion Program (SIP) by Japan cabinet office, and we are trying to develop a new design approach of aerospace structures with other research groups. Some other collaborative works with companies and research institute ranging from smart phone structures to concrete buildings are in progress.

I was born and had grown up in Sapporo where I live in now with my wife and two sons who are seven and two years old.

Sinniah Ilanko, The University of Waikato/Te Whare Wananga o Waikato

Ilanko was born in the north of Sri Lanka (Jaffna), and according to the common Tamil practice, he does not have/use a family name. Ilanko is his given name and Sinniah is his late father's given name and conveniently remains informal.

He graduated from the University of Manchester (U.K) with a BSc in civil engineering and also obtained an MSc from the same university under the supervision of late Dr S.C. Tillman, investigating the effect of initial imperfections on in-plane loaded rectangular plates. He commenced doctoral studies at the University of Western Ontario under the supervision of Professor S.M. Dickinson, continuing on the same topic. Soon after completing his PhD, he worked as a postdoctoral fellow at the UWO briefly before joining the University of Canterbury (NZ) in 1986. He continued his academic career at Canterbury for nearly 20 years, in various positions, as lecturer, senior lecturer and associate professor until he joined the University of Waikato in 2006. In 2012 he became a full professor. He has served as the Chairperson and later the Head of School of Engineering from January 2013 to December 2015. He has also previously served as the Head of Mechanical Engineering Department at Canterbury (2001-2202).

His research areas include vibration and stability of continuous systems, numerical modelling and adaptive mechanisms. His most recent research projects include active control for adaptive stiffness foundations for earthquake isolation and crack detection using frequency measurements in structures with roving test bodies possessing rotary inertia. He has published 43 journal papers and in 2014 authored a book "The Rayleigh-Ritz Method for Structural Analysis" jointly with Dr Luis Monterrubio and Dr Yusuke Mochida. Since January 2009, he is serving as the Subject Editor for Journal of Sound and Vibration, for analytical methods for linear vibration. He has secured two major grants, a [Marsden grant](#) for research into vibration analysis of complex structures and more recently a [grant](#) by the New Zealand government's Ministry of Business Innovation and Employment (Category Smart Ideas) to conduct research on the development of an omnidirectional base isolator.

His current research topics include adaptive vibration isolation from vertical seismic excitation and crack detection. He is also interested in computer-aided learning and has developed and used several interactive lectures and tutorials for teaching Mechanics of Materials and Vibration, as well as computer based tutorials and games for learning/teaching Tamil language.

He is married to Krshnanandi and they have two daughters, Kavitha and Tehnuka.

## Short Curriculum Vitae

### *Dr. ir. Eelco Jansen*

Gottfried Wilhelm Leibniz Universität Hannover, Institute of Structural Analysis  
Appelstrasse 9A, 30167 Hannover, Germany

Dr. ir. Eelco Jansen is a senior faculty member, head of the Section “Composites” at the Institute of Structural Analysis of Leibniz Universität Hannover since 2009. Formerly (2000 – 2009) he was an assistant professor at Delft University of Technology, Faculty of Aerospace Engineering, Aerospace Structures Group, where he also obtained his PhD in 2001. He coordinates a wide range of research topics in the area of composite and layered structures and has a specific expertise and long-time experience in the field of nonlinear stability and dynamic analysis of thin-walled structures.

#### **Professional career**

From November 2009:	Senior faculty member (head of section “Composites”) at Leibniz Universität Hannover (Germany), Faculty of Civil Engineering and Geodetic Science, Institute of Structural Analysis
2000 – 2009:	Assistant professor at Delft University of Technology (Netherlands), Faculty of Aerospace Engineering, Aerospace Structures Group
December 2001:	PhD from Delft University of Technology (Netherlands), on the topic of nonlinear shell vibrations (supervisor: Prof. Dr. J. Arbocz)
1998 – 2000:	Research associate at Delft University of Technology (Netherlands), Faculty of Aerospace Engineering, Aerospace Materials Group

#### **Functions in university, foundations and in associations**

- Member of Editorial Board of journal “Composite Structures”, since 2016
- Reviewer for various international journals (International Journal of Nonlinear Mechanics, Nonlinear Dynamics)
- Member of European Cooperation for Space Standardization (ECSS) Working Group E-HB-32-24 Buckling Handbook, 2005 – 2009

#### **Selected publications**

- T. Rahman and E.L. Jansen. Computational aspects for stability and vibrations of thin-walled composite structures. In *Stability and Vibrations of Thin Walled Composite Structures*, pp. 693–734. H. Abramovich, ed., Woodhead Publishing, 2017.
- T. Rahman, E.L. Jansen, and Z. Gürdal: Dynamic buckling analysis of composite cylindrical shells using a finite element based perturbation method. *Nonlinear Dynamics*; 66(3): pp. 389-401, 2011.
- E.L. Jansen: A perturbation method for nonlinear vibrations of imperfect structures: Application to cylindrical shell vibrations. *International Journal of Solids and Structures*; 45(3): pp. 1124-1145, 2008.
- E.L. Jansen: Dynamic stability problems of anisotropic cylindrical shells via a simplified analysis. *Nonlinear Dynamics*; 39(4): pp. 349-367, 2005.
- E.L. Jansen: Non-stationary flexural vibration behaviour of a cylindrical shell. *International Journal of Non-Linear Mechanics*; 37(4-5-37): pp. 937-949, 2002.

**David Kennedy**  
**Professor of Structural Engineering**  
**School of Engineering, Cardiff University, United Kingdom**

David Kennedy obtained a First Class Honours degree at the University of Cambridge in 1978 and a PhD in the area of efficient transcendental eigenvalue computation from the University of Wales, Cardiff in 1994.

From 1978 to 1983 he was employed as an Analyst/Programmer for the computer services company Scicon Ltd, where he worked on the development of the Mathematical Programming software SCICONIC/VM. In 1981 he was awarded a 2-year BP Venture Research Fellowship in Non-linear Optimization, supervised by the late Professor Martin Beale.

In 1983 he was appointed as a Research Associate in the University of Wales Institute of Science and Technology, which was merged into Cardiff University in 1988. Working under the supervision of Professor Fred Williams and funded under a collaborative agreement with NASA, he co-ordinated the development of the space frame analysis software BUNVIS-RG which was released by NASA to US users in 1986/87. Further collaboration with NASA and British Aerospace (now BAE Systems) led to the development and successive releases, starting in 1990/91, of VICONOPT, a buckling and vibration analysis and optimum design program for prismatic plate assemblies. Both of these programs use analysis methods based on the Wittrick-Williams algorithm.

He was appointed to a Lectureship in the School of Engineering in 1991, promoted to Senior Lecturer in 2000, Reader in 2005 and Professor in 2009. He has continued to manage the collaborative development of VICONOPT, successfully supervising 20 PhD students and holding Research Council grants on parallel computing, aerospace panel optimization, local postbuckling and mode finding. He has visited NASA Langley Research Center several times, and in 2007 he undertook a 6-month secondment to Airbus UK, funded by a Royal Society Industry Fellowship. A former Deputy Head of the School of Engineering with responsibility for staff matters, he now co-chairs the School's Equality, Diversity and Inclusivity Committee.

Through the Cardiff Advanced Chinese Engineering Centre, Professor Kennedy has participated for over 25 years in collaborative research projects with leading Chinese universities, including Tsinghua University, Dalian University of Technology and Shanghai Jiao Tong University.

Professor Kennedy is the author of over 200 publications of which approximately 50% are in refereed journals of international standing.

He lives with his wife Helen in a village near Cardiff, where he plays the church organ and sings in a community choir. In 2017 he walked the length of Hadrian's Wall and an ambition for retirement is to complete the Pennine Way in northern England.

## **Xiang Liu, PhD**

Dr Xiang Liu, is now working as a Professor in High-speed Train Research Center, School of Traffic & Transportation Engineering at Central South University, China. His research interests include elastodynamics, vibro-acoustics, structural instabilities, aeroelasticity, composite structures.

XL received his Bachelor's and Master's degrees with First Class in Civil and Geotechnical Engineering respectively. Then he joined University of Glasgow in 2010 to work for his PhD in Applied Mathematics working on surface instabilities of membranes, plates and solids. After completing his PhD, XL joined City, University of London in 2013. He worked as a Research Fellow with Prof. J. Ranjan Banerjee. To this end, a novel method called the spectral dynamic stiffness method (SDSM) has been proposed for exact free vibration analysis of isotropic and anisotropic plate assemblies with arbitrary boundary conditions (BCs). A set of novel related techniques have been developed so that the new SDSM becomes unconditionally stable with remarkable accuracy and computational efficiency. This theory has broadened the applicability of the SDSM for real life structures.

In February 2017, XL received a specially-appointed professorship from Central South University (China). Now the main theme of his theoretical research is to remove the limitations of analytical methods and applied them to real engineering problems. And the main goal of his industrial research is to make the transportation systems more quiet and comfortable.

## **Brian Mace**

I am currently Professor of Mechatronics in the Department of Mechanical Engineering at the University of Auckland, which I re-joined in 2011. Prior to that I was Professor of Structural Dynamics at the Institute of Sound and Vibration Research (ISVR), University of Southampton.

I graduated MA (Hons) in Engineering Science and subsequently DPhil (1977) from the University of Oxford. Following that I was Research Fellow at the ISVR (1977-1980), Lecturer in the Department of Civil and Structural Engineering, University College, Cardiff, Wales (1980-1983) and then moved to the University of Auckland, returning in 2000 to the ISVR.

My general research interests concern structural dynamics, vibrations, acoustics, smart structures and dynamics. More specifically they include uncertainty modelling and wave-based approaches, particularly regarding noise and vibration behaviour at higher frequencies. A strong interest concerns wave motion in structures. A significant amount of current work concerns a hybrid wave and finite element (WFE) method for structural dynamic and acoustic analysis and a hybrid FE/WFE method for prediction of transmission through joints. Applications include noise and vibration in buildings, tyre noise and vibration, composites, rail vehicles etc. Recent activity also includes vibrations of complex, built-up structures such as cars, aircraft etc., when data uncertainty and product variability become important. Modelling the uncertainty is an important part of the virtual design process, but computational cost etc. is a real problem. My research concerns energy approaches and methods based on component mode synthesis. Other interests include smart structures for noise and vibration control, periodic structures and acoustic metamaterials and active noise and vibration control.

Interests outside work include fishing, bridge, golf, walking and doing what my wife Gwyneth tells me to do in the garden.

Shinichi Maruyama  
Gunma University

Shinichi Maruyama is an associate professor of the Division of Mechanical Science and Technology, Graduate School of Science and Technology, Gunma University, Japan.

He was born in Takamatsu and had been lived in Chiba, suburb area of Tokyo, until he graduated university. He obtained Master of Engineering and Doctor of Engineering in 1999 and 2002, both from Keio University. Since 2002, he has been taking an academic position in Gunma University and working with Professor Ken-ichi Nagai.

His research interests include nonlinear and chaotic vibrations of mechanical systems, and analyses and experiments on dynamics of thin elastic structures.

He is a member of the Japan Society of Mechanical Engineers. Since 2010, He was the former chair of the Technical Section on Basic Theory of Vibration in the Division of Dynamics, Measurement and Control in JSME.

# **YUSUKE MOCHIDA**

**University of Waikato**  
**Te Whare Wananga o Waikato**  
**Hamilton, New Zealand**  
yusuke@waikato.ac.nz

I am currently working at the University of Waikato in New Zealand. The overall aim of my current research is to develop a vibration isolator for earthquake protection. The method under consideration includes the use of the concept of pseudo-zero/negative stiffness mechanism.

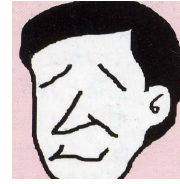
I was born and grew up in Japan. After I graduated with a B.E. in Mechanical Engineering from the Tokyo Metropolitan University (Japan) I worked for a while in Japan and went to New Zealand as a working holiday maker to travel around and work. Actually I was away from the engineering field for several years. This made me miss engineering and so after learning English, I enrolled in a Postgraduate Diploma programme at the University of Canterbury (New Zealand). During my postgraduate study I became interested in vibration and decided to continue towards an M.E. under the supervision of Professor Ilanko, who had at this time relocated to the University of Waikato. I completed my M.E. and then continued working towards a Ph.D at the same university. Since commencing my M.E. studies I have developed several codes based on the Superposition Method, the Rayleigh-Ritz Method and the Finite Difference Method to solve free vibration problems of plates and shells using MATLAB. I was also involved in research on the development of analytical procedure for vibration analysis of complex structures using the concept of negative structures, and structural health monitoring using frequency measurement. In addition to my research experience, I have been lecturing in Dynamics and Mechanisms, Vibration, Mechanics and Finite Element Analysis classes.

Through my career, I hope I can contribute to the development of research relationships between New Zealand and other countries, especially Japan, and the advancement of research in New Zealand.

Personally, I am also interested in snowboarding, golf, playing drums, Shorinji Kempo (Japanese martial arts), foreign exchange, personal development and cooking.

# NARITA Yoshihiro

ynarita@eng.hokudai.ac.jp



Current position (till December 2019)

JICA, Expert (Academic Advisor) at Higher Education project

Hasanuddin University, Makassar, South Sulawesi 92171, INDONESIA

\*\*\*\*\*

1980: Dr.Eng., Hokkaido University

1980-2004: Hokkaido Institute of Technology

2004-2017: Hokkaido University, Professor Emeritus

2017-present: Hasanuddin University

I have attended First ISVCS (1997) through Tenth ISVCS (2015), but I missed 11-th ISVCS in UK. I am very happy to come back.



I started my research on vibration of continuous systems when I was a PhD student under advisor Prof.Irie of HU in 1976, and had a chance to study one year in 1978-1979 under Prof.Leissa at the Ohio State University. The research outcomes under both advisors were summarized into my PhD dissertation in 1980 with the title “Free Vibration of Elastic Plates with Various Shapes and Boundary Conditions”. Even after 39 years, it is downloaded more than 22000 internationally from HUSCAP website: <http://eprints.lib.hokudai.ac.jp/dspace/handle/2115/32630>.

I still make computer programs and write papers.

*Let's enjoy research!*

## **Alfonso Pagani**

Alfonso Pagani is professor assistant at the Department of Mechanical and Aerospace Engineering, Politecnico di Torino. He earned a Ph.D. in Aerospace Engineering at City University of London in 2016 and, earlier, a Ph.D. in Fluid-dynamics at Politecnico di Torino. He gained an MSc and a BSc in Aerospace Engineering at Politecnico di Torino in December 2011 and October 2009, respectively.

In 2018, Alfonso joined California Institute of Technology as visiting associate to work on acoustics of meta-materials. Also, he spent research periods at Purdue University in 2016, where he worked on micro-mechanics of fibre-reinforced composites with Prof. W. Yu; RMIT Melbourne in 2014, where he developed models for flutter analysis and gust response of composite lifting surfaces with Prof. E. Carrera and M. Petrolo; at Universidade do Porto in 2013, where he carried out investigations on the use of RBFs for the solution of equations of motion of higher-order beam models with Prof. A.J.M. Ferreira; at London City University in 2012, where he formulated exact, DSM-based models for metallic and composite structures with Prof. R. Banerjee.

Alfonso Pagani is the co-author of more than 100 publications, including 65 articles in International Journals, which have collected more than 800 citations (h-index 17, source: Scopus). He acts as a reviewer for more than 20 International journals and serves as assistant editor for *Advances in Aircraft and Spacecraft Structures*, an Int'l Journal edited by Techno-Press.

Department of Mechanical and Aerospace Engineering  
Corso Duca degli Abruzzi, 24  
10129, Torino, Italy  
Tel: +39 - 011 090 6870  
Fax: +39 - 011 090 6899  
e-mail: [alfonso.pagani@polito.it](mailto:alfonso.pagani@polito.it)  
website: [www.mul2.com](http://www.mul2.com)

## **Biography of Francesco Pellicano**

Francesco Pellicano is Aeronautical Engineering and Ph.D. in Theoretical and Applied, he is currently Full Professor, vice-Head of the Centre Intermech MoRe and committee president of 2 BsC and 2 MsC programmes. He was coordinator of EU Regional projects: METaGEAR (Gears, Materials, Robotics), INDGEAR (condition monitoring) and HPGA Fortissimo (applications of high performance computing); he was coordinator of several international and national projects. He published 2 Books, about 60 Journal papers and more than 100 conference papers. Bibliometry: h-index 27, more than 2000 citations. His research activities are: gear stress and vibration modelling and testing; nonlinear vibrations of structures; vibration control; shell dynamics and stability; thermal effects, fluid-structure interaction; vibration of carbon nanotubes; non-smooth dynamics; Chaos; axially moving systems; devices for Parkinson disease mitigation.

## **Wolfgang Seemann**

Wolfgang Seemann was born on 31 March, 1961 in Kelttern (Germany, Baden-Württemberg). After studying mechanical engineering at the University of Karlsruhe from 1980 to 1985 and after civil service (1985-1987) he worked as a PhD-student at the Institute of Applied Mechanics at the University of Karlsruhe (now Karlsruhe Institute of Technology). The PhD under the supervision of Prof. Jörg Wauer was finished in 1991 with a thesis on 'Wave propagation in rotating or pre-stressed cylinders'. In 1992 he joined the group of Peter Hagedorn at Darmstadt University of Technology to work in a post-doc position until 1998 when he got a professorship on machine dynamics in Kaiserslautern. In 2003 he got an offer to go back to the University of Karlsruhe on the chair of Applied Mechanics.

His previous and current research interests are in fluid bearings, ultrasonic motors, nonlinear vibration, multibody dynamics, vibration of continuous systems, active materials, nonlinear phenomena in piezoelectric materials, humanoid robots, dynamics of human motion, mechatronic systems, road-vehicle interaction, rotor dynamics and wave propagation.

Besides his duties in teaching and research he is responsible for the French-German cooperations of the KIT.

## **Silvio Sorrentino**

Master Degree in Mechanical Engineering at the *Politecnico di Torino* (I). PhD in Mechanics of Machines at the *Politecnico di Torino*. Research Associate at the *University of Sheffield*, at the *Georgia Institute of Technology*, Atlanta (USA), and at the *University of Bologna* (2003-2010). Associate Professor in Mechanics of Machines at the *University of Modena and Reggio Emilia*, Department of Engineering *Enzo Ferrari* (present).

Research topics: identification methods from vibration data (output-only methods, subspace stochastic methods); vibration analysis of viscoelastic models (general damping distributions, fractional derivative models with analytical developments and experimental validation); dynamics of oleohydraulic systems coupled with mechanical systems (non-newtonian fluids); dynamic behaviour of structures with travelling loads (deterministic, stochastic); wave propagation in solid structures (catenary-pantograph problem); dynamic analysis of plates (coordinate mapping, homogenization of periodic lattices); rotor-dynamics (distributed parameter and finite element modelling, stability analysis); vehicle dynamics (motorcycle stability, self-excited oscillation analysis).

### **Selected papers on dynamics of continuous systems.**

S. Sorrentino, S. Marchesiello, B.A.D. Piombo, *A new analytical technique for vibration analysis of non-proportionally damped beams*. *Journal of Sound and Vibration* 265 (2003), pp. 765-782.

S. Sorrentino, A. Fasana, *Finite element analysis of linear systems with fractional derivative damping models*. *Journal of Sound and Vibration* 299 (4-5) (2007), pp. 839-853.

S. Sorrentino, A. Fasana, S. Marchesiello, *Analysis of non-homogeneous Timoshenko beams with generalized damping distributions*. *Journal of Sound and Vibration* 304 (3-5) (2007), pp. 779-792.

G. Catania, S. Sorrentino, *Spectral modeling of vibrating plates with general shape and general boundary conditions*. *Journal of Vibration and Control* 2012 18 (11), pp. 1607-1623.

S. Sorrentino, D. Anastasio, A. Fasana, S. Marchesiello, *Distributed parameter and finite element models for wave propagation in railway contact lines*. *Journal of Sound and Vibration* 410 (2017), pp. 1-18 (published online 29 August 2017).

S. Sorrentino, *Power spectral density response of bridge-like structures loaded by stochastic moving forces*. *Shock and Vibration* 2019 (2019), pp. 1-10.

## **Professor Ji Wang, Ningbo University, China**

**Professor Ji Wang** has been a Qianjiang Fellow Professor of Zhejiang Province at Ningbo University since 2002. He also served as Associate Dean for Research and Graduate, School of Mechanical Engineering and Mechanics, Ningbo University, from 2013 to 2019. Professor Ji Wang is the founding director of the Piezoelectric Device Laboratory, which is a designated Key Laboratory of City of Ningbo. Professor Ji Wang was employed at SaRonix, Menlo Park, CA, as a senior engineer from 2001 to 2002; NetFront Communications, Sunnyvale, CA, as senior engineer and manager from 1999 to 2001; Epson Palo Alto Laboratory, Palo Alto, CA, as Senior Member of Technical Staff from 1995 to 1999. Professor Ji Wang also held visiting positions at Chiba University, University of Nebraska-Lincoln, and Argonne National Laboratory. He received his PhD and Master degrees from Princeton University in 1996 and 1993 and bachelor from Gansu University of Technology in 1983.



Professor Wang has been working on acoustic waves and high frequency vibrations of elastic and piezoelectric solids for resonator design and analysis with several US and Chinese patents, over 120 journal papers, and frequent invited, keynote, and plenary presentations in major conferences around world. He has been board members, advisors, and consultants to many leading companies in acoustic wave device industry. Professor Wang has been a member of many international conference committees and currently serving the IEEE UFFC Technical Program Committees of the Frequency Control and Ultrasonics Symposia, the IEEE MTT-S, and the IEC TC-49. He is also the funding chair of Committee on Mechanics of Electronic and Magnetic Devices, CSTAM, and the SPAWDA. From 2015, Profess Wang is the editor-in-chief of *Structural Longevity* and members of the editorial boards of several international journals.

**Andrew Watson**  
**Lecturer of Aerospace Structures**  
**Department of Aeronautical and Automotive Engineering**  
**Loughborough University, United Kingdom**

Andrew obtained his undergraduate and higher degrees from Cardiff University. His PhD looked at the stability analysis and optimisation of light weight structures. After two post-doctoral appointments at Cardiff Andrew joined Loughborough University as a member of academic staff in 2004.

His research includes buckling and postbuckling of aerospace panels and vibration of Timoshenko beams. Buckling and vibration problems can be approached by using the Dynamic Stiffness Method along with the Wittrick-Williams algorithm. Vibrating structures can be modelled as quantum graphs and Andrew is currently researching higher order graphs to obtain the spectral results of tree shaped graphs all using the DSM.

Outside of this research Andrew has been looking at fossil fuels and other finite resources. To facilitate this he is developing analytical methods to optimise structures where the objective function can be mass, energy costs or environmental degradation. He is the co-investigator of an externally funded research programme with Jaguar Land Rover researching the development of a hybrid car that produces smaller quantities of carbon dioxide compared to the non hybrid versions.

In his spare time he likes to keep up with current affairs and enjoys walking and sailing.

## **Autobiographical Sketch**

Dr. Xuewen Yin is currently a senior research engineer in China Ship Scientific Research Center. His research activities are mainly engaged to acoustic design of ships and underwater vehicles, which is an increasingly tough requirement so as to ensure more silent, more comfortable, or more endurable products. He has made persistent and efficient endeavors to address novel analytical and numerical methods, especially for the dynamics and acoustics of plate and shell structures. Also, as an engineer, he laid more focus on digging the fundamentals, mechanisms, and insights to better understand a plenty of phenomena relating to structure-borne, airborne, and underwater sound. Due to his excellence, Dr. Yin has participated in drafting the blueprints of several national research funds, especially in the subject of vibration and vibration control.

Dr. Xuewen Yin has published nearly 30 papers in leading scientific journals, 10 presentations in international conferences. Among these works, one of highlighted contributions lies in the dynamic stiffness method on the dynamics of built-up ship structures, which makes it possible to address the vibration and acoustics of real ship hulls at varied design period in very wide frequency range up to 10, 000 Hz. Stemming from this work, novel design strategies associated with vibration isolation, ship hull optimization, and even machinery selection are contrived in a straightforward but efficient way. Other remarkable contributions can be found that are dedicated to: acoustic radiation from composite and stiffened cylindrical shells using wavenumber transformation method, immersed boundary-LBM method and its application to microscopic biologic medium, and etc.

He is an Engineering Consultant to China Ship Research Foundation, senior member of China Shipbuilding Association, member of China Mechanical Engineering Association, member of Canadian Machinery Vibration Association. He is not only a great attendant, but an active contributor. He has reviewed more than 10 papers for one conference in response to the assignments from the organizing committee.

He works closely with the ship and ocean equipment industries, and as a team leader, he is currently conducting nearly 10 research projects ranging from computational and experimental methods, innovative ship design, development of novel vibration isolator, and etc.

He and his team won many awards from our fund sponsors and even China provincial or ministry government.

## **Shudong Yu**

Shudong Yu received his bachelor's degree 1982 from Jiangxi University of Technology (Mechanical Engineering), master's degree in 1984 from Northeastern University (Applied Mechanics), and PhD degree in 1995 from University of Toronto (Mechanical Engineering). He worked as a nuclear fuel design engineer for Atomic Energy of Canada Limited (AECL) during 1994-1997. He joined Ryerson University (Mechanical Engineering) in 1997, and held assistant professorship (1997-2004), associate professorship (2004-2009), and full professorship (2009-present).

Dr. Yu's research areas include flow induced vibration, structural dynamics, chaos and bifurcations. He has published over 62 papers in recognized scientific and technical journals, and presented 87 papers at national and international conferences. He also authored and co-authored 47 technical reports, resulted from various industrial projects.

Dr. Yu is a fellow of Canadian Society for Mechanical Engineering (CSME). He served as a Vice President for CSME Ontario during 2002-09. He is an associate editor, Journal of Vibration Testing and Dynamics (2018-present).